

**UCSF**

**UC San Francisco Electronic Theses and Dissertations**

**Title**

Catalysis dependent destruction of cytochrome P-450

**Permalink**

<https://escholarship.org/uc/item/7vs2x202>

**Author**

Kunze, Kent Luvern

**Publication Date**

1981

Peer reviewed|Thesis/dissertation

CATALYSIS DEPENDENT DESTRUCTION OF CYTOCHROME P-450:  
CHARACTERIZATION OF THE N-ALKYLATED PROSTHETIC HEME ADDUCTS

by

KENT LUVERN KUNZE

DISSERTATION

Submitted in partial satisfaction of the requirements for the degree of

DOCTOR OF PHILOSOPHY

in

PHARMACEUTICAL CHEMISTRY

in the

GRADUATE DIVISION

of the

UNIVERSITY OF CALIFORNIA

San Francisco



Date

University Librarian

Degree Conferred: . . . . . SEP 23 1981 . . . . .

## Acknowledgements

It is with the deepest appreciation that I acknowledge the support, guidance, and encouragement given to me by Professor Paul Ortiz de Montellano. His ability to critically examine my research and enthusiasm for discussion and speculation have made my graduate career a most positive and fulfilling experience.

I would like to thank Professors Neal Castagnoli, Jr. and Manfred Wolff for their review of this dissertation.

I am indebted to Professor A. L. Burlingame for providing generous access to the field desorption mass spectrometer and Dr. Ken Straub and Fred Walls for their patience and help when things went wrong.

I would like to acknowledge the friendship and collaboration of Doctors Hal Beilan, Bruce Mico, Almira Correia, Geoff Farrell, Gary Yost, and Peter Mirau.

Many thanks to Professor William Trager, Dr. Lance Pohl, and Dr. William Porter who devoted many hours to the development of a neophyte undergraduate student interested in research.

Thanks also go to my roommates at the Hotel Hugo, Peter Kennedy and Karen Rodriguez for gracefully allowing me to shirk my responsibilities during the final push.

Finally, I wish to express my continuing appreciation to soon-to-be Dr. Kathryn Prickett (the white-out woman) for her invaluable aid in the preparation of this manuscript.

To:

my parents, LuVern and Elsie Kunze

my brother, Don Kunze

my sisters, Linda and Kathy Kunze

and to Kathryn Prickett.

with love and gratitude.

CATALYSIS DEPENDENT DESTRUCTION OF CYTOCHROME P-450:  
CHARACTERIZATION OF THE N-ALKYLATED PROSTHETIC HEME ADDUCTS

Abstract

Hepatic cytochrome P-450 is destroyed during catalysis-dependent oxidation of substrates containing terminal acetylene functional groups. The destructive effect of these compounds is due to the covalent attachment of a reactive intermediate, formed during oxidative transformation of the triple bond, to the heme prosthetic group of the enzyme. The alkylated derivatives of protoporphyrin IX (purified as the iron-free dimethyl esterified porphyrins) display highly similar electronic absorption spectra. Field desorption mass spectral studies performed on nine of these adducts demonstrate that they are stoichiometrically composed of the elements of protoporphyrin IX dimethyl ester plus the destructive agent plus atomic oxygen. The structure of the propyne adduct, established by proton NMR studies, is the isomer of N-(2-oxopropyl)-protoporphyrin IX dimethyl ester bearing the N-alkyl group on pyrrole ring A. Thus, the destructive event involves addition of the terminal unsaturated carbon of the substrate to one of the four pyrrole nitrogens of prosthetic heme. The propyne adduct is optically active indicating that the alkylation sequence is selective for one of the two faces of heme. These results suggest a destructive sequence initiated by enzyme-catalyzed oxidation of the triple bond to a reactive intermediate, and terminated by a

regio- and stereo-selective alkylation of prosthetic heme. Cytochrome P-450 catalyzed oxidation of biphenylacetylene to biphenylacetic acid proceeds through oxidation of the acetylene pi bond to the substituted oxirene and/or ketocarbene which is followed by rearrangement, via a 1,2 hydride shift, to give the ketene precursor to the arylacetic acid. The manifold of reactive intermediates exposed by these studies are presented, and mechanistic alternatives for the destructive process are suggested.

The cytochrome P-450 prosthetic heme adducts formed during catalytic processing of ethylene, propene, propyne, and the 4-alkyl dihydropyridines, 3,5-dicarbethoxy-1,4-dihydrocollidine (DDC) and 3,5-dicarbethoxy-2,6-dimethyl-4-ethyl-1,4-dihydropyridine (DDEP), are characterized by 360 MHz NMR studies. The structure and isomer assignment of these N-alkylated derivatives of dimethyl-esterified protoporphyrin IX is made by a combination of spin-lattice relaxation, proton-proton nuclear Overhauser effect, and spin-decoupling experiments.

## TABLE OF CONTENTS

### CHAPTER I HEPATIC CYTOCHROME P-450

1.1	Introduction . . . . .	1
1.2	Distribution and Heterogenous Nature . . . . .	4
1.3	Oxygen Activation and Transfer to Substrates . . . . .	10
1.31	Binding of Substrate . . . . .	12
1.32	Transfer of the First Electron . . . . .	14
1.33	Dioxygen Binding . . . . .	16
1.34	Generation of Activated Oxygen . . . . .	16
1.35	Insertion of Oxygen into Carbon Hydrogen Bonds . . . . .	21
1.36	Pi Bond Oxidation Reactions . . . . .	25
1.40	Catalysis Dependent Destruction of Cytochrome P-450 by Xenobiotics . . . . .	30
1.41	Apoprotein Degredation and Enzyme Inactivation . . . . .	32
1.42	Heme Degradation . . . . .	35

### CHAPTER II

#### DESTRUCTION OF CYTOCHROME P-450 BY ACETYLENES

2.0	Introduction . . . . .	42
2.1	Destruction of Cytochrome P-450 by Norethisterone: Covalent Attachment of the Sterol to Prosthetic Heme . . . . .	46
2.2	<u>In Vitro</u> Destruction of Hepatic Cytochrome P-450 by Acetylenes . . . . .	53
2.3	Characterization of the Terminal Acetylene-Prosthetic Heme Adducts . . . . .	65

2.31	Green Pigment Formation and Purification: A Study of Fourteen Acetylenes . . . . .	66
2.32	Electronic Absorption Spectra . . . . .	69
2.33	Field Desorption Mass Spectr . . . . .	71
2.34	Proton Nuclear Magnetic Resonance Studies . . . . .	79
2.35	Circular Dichroism Spectra of the Propyne Adduct: The Two Faces of Heme . . . . .	91
2.36	Potential Mechanisms for Terminal Acetylene Mediated Destruction of Cytochrome P-450 . . . . .	94
2.4	Oxidation of the Triple Bond by Cytochrome P-450: The UC Shift . . . . .	101

### CHAPTER III

#### SYNTHESIS AND IDENTIFICATION OF N-ALKYLATED DERIVATIVES OF PROTOPORPHYRIN IX

3.0	Introduction . . . . .	113
3.1	The Four Isomers of N-Methyl Protoporphyrin IX Dimethyl Ester . . . . .	115
3.11	Synthesis and Separation of the Four N-Methyl Isomers . . . . .	116
	Synthesis of Meso-Deuterated Isomers of N-Methyl Protoporphyrin IX Dimethyl Ester: Assignment of the Alpha and Gamma Meso Protons . . . . .	126
	Spin-Lattice Relaxation Time Measurement: Assignment of the Ester Methyl Proton Signals . . . . .	129
	Proton-Proton Nuclear Overhauser Effects: The Missing Link . . . . .	133
	Isomer Assignments . . . . .	139
3.12	N-Methyl Protoporphyrin IX Dimethyl Esters: The Porphyrins Isolated from Rats Treated with 3,5-Diethoxycarbonyl-1,4-dihydrocollidine . . . . .	143



3.2	Synthesis and Characterization of the Four Isomers of N-Ethyl Protoporphyrin IX Dimethyl Ester: The Porphyrins Isolated From Rats Treated with 3,5-Dicarbethoxy-2,6-dimethyl-4-ethyl-1,4-dihydropyridine	145
3.21	Synthesis and Separation of the Four Isomers	146
	Strategy of Peripheral Proton Assignments	155
	Gamma Meso Proton Signal	155
	Ester Methyl Proton Signals	156
	Delta Meso Proton Signal	156
	1, 3, 8 Methyl Proton Signals	156
	Alpha and Beta Meso and 5 Methyl Proton Signals	157
	Isomer Assignment and Chemical Shift Correlations	162
3.22	Conclusions and Applications	164
3.3	Structure of the Green Pigments Isolated from Rats Treated with Ethylene and Propene	166
	The Ethylene Adduct	166
	The Propene Adduct	178
3.4	Structure of the Propyne Adduct	187

## CHAPTER IV

### EXPERIMENTAL

4.0	Instrumentation	196
4.10	Biological Experiments	197
4.11	Preparation of Liver Microsomes	197
4.12	Assay for Cytochrome P-450 Destruction In Vitro	199
4.13	Isolation and Purification of Hepatic Green Pigments Generated In Vivo	200
4.14	Demetalation of Zinc-Complexed Pigments	203

4.3	Synthesis . . . . .	203
4.31	Meso-Desuterated Protoporphyrin IX Dimethyl Ester . . . . .	203
4.32	N-Methyl Protoporphyrin IX Dimethyl Ester (4 Isomers) . . . . .	205
4.33	N-Ethyl Protoporphyrin IX Dimethyl Ester (4 Isomers) . . . . .	206
4.34	1- <sup>2</sup> H-2-Biphenylacetylene . . . . .	208
4.35	Methyl-2- <sup>2</sup> H-2-Biphenylacetate from 1- <sup>2</sup> H-2-Biphenyl- acetylene . . . . .	208
4.36	Methyl-2- <sup>2</sup> H-2-Biphenylacetate from 1- <sup>2</sup> H-2-Biphenyl- acetylene by Microsomal Oxidation . . . . .	209
4.37	1- <sup>13</sup> C-1-Biphenylacetylene from Biphenyl . . . . .	210
4.4	NMR Studies . . . . .	211
	References . . . . .	213

## LIST OF FIGURES

Figure		Page
1	One of the Possible Arrangements of Cytochrome P-450 and Cytochrome P-450 Reductase on the Endoplasmic Reticulum . . . . .	7
2	The Catalytic Cycle of Cytochrome P-450 . . . . .	11
3	The Role of Iodosobenzene in the Monooxygenation of Substrates catalyzed by Cytochrome P-450 . . . . .	18
4	The Metabolism of Bromobenzene . . . . .	27
5	Electronic Absorption Spectra of the Norethisterone Pigment . . . . .	49
6	HPLC Analysis of the Pigments Isolated from Rats Treated with 9,11- <sup>3</sup> H-Norethisterone . . . . .	51
7	HPLC Analysis of the Pigment Isolated from Rats Treated with 3-Phenoxy-propyne . . . . .	70
8	Electronic Absorption Spectra of the 3-Phenyl-1-propyne and Acetylene Pigments . . . . .	72
9	Field Desorption Mass Spectra of the Metal-Free and Zinc-Complexed Ethynyl Cyclohexanol Adduct . . . . .	75
10	NMR Spectrum of the Chloro-Zinc Complex of the Propyne Pigment . . . . .	81
11	Structure of the Metal-Free Propyne Adduct . . . . .	81
12	NMR Spectrum of Chloro-Zinc Complexed Pigments Isolated from Acetylene-Treated Rats . . . . .	86
13	Field Desorption Mass Spectrum of the Metal-Free Fluorene Adduct . . . . .	89
14	Circular Dichroism Spectra of the Metal-Free and Zinc-Complexed Propyne Adduct . . . . .	92
15	Destruction of Cytochrome P-450 by Propyne: Potential Alkylating Species . . . . .	96
16	Reaction of Carbenes with Iron Tetraphenylporphyrin . . . . .	99

17	Alternative Pathways for Cytochrome P-450 Catalyzed Oxidation of the Triple Bond of Biphenylacetylene . . . . .	103
18	NMR and EIMS Spectra of Methyl Biphenylacetate Obtained from Chemical and Microsomal Oxidation of 1- <sup>2</sup> H-2-Biphenylacetylene . . . . .	106
19	The 1,2 Shift During Triple Bond Oxidation: Aryl versus Hydride . . . . .	109
20	Electron Impact Mass Spectra of Methyl-Biphenylacetate Obtained by Chemical and Microsomal Oxidation of 1- <sup>13</sup> C-1-Biphenylacetylene . . . . .	110
21	Electronic Absorption Spectra of Metal-Free and Zinc-Complexed N-Methyl Protoporphyrin IX Dimethyl Ester . . . . .	118
22	Field Desorption Mass Spectrum of a Mixture of the N-Methyl Protoporphyrin IX Dimethyl Ester Isomers . . . . .	119
23	HPLC Separation of the Four Isomers of N-Methyl Protoporphyrin IX Dimethyl Ester . . . . .	121
24	360 MHz NMR Spectra of the Chloro-Zinc Complexed Isomers of N-Methyl Protoporphyrin IX Dimethyl Ester . . . . .	122
25	Meso Regions of the NMR Spectra of Partially-Deuterated N-Methyl Isomers I-III and Protoporphyrin IX Dimethyl Ester . . . . .	127
26	NMR Spectra of the Methyl Proton Region of the N-Methyl Isomers I-IV . . . . .	131
27	Nuclear Overhauser Effect Enhancement of the Meso Proton Signals of Isomers I-IV . . . . .	136
28	Separation by HPLC of the Four Isomers of N-Ethyl Protoporphyrin IX Dimethyl Ester . . . . .	148
29	Field Desorption Mass Spectrum of a Mixture of the N-Ethyl Protoporphyrin IX Dimethyl Ester Isomers . . . . .	149
30	360 MHz NMR Spectra of the Chloro-Zinc Complexed Isomers of N-Ethyl Protoporphyrin IX Dimethyl Ester . . . . .	150
31	N-Ethyl Protoporphyrin IX Dimethyl Ester Isomers I and III: NOE Enhancement of the Meso Signals and Methyl to Vinyl Proton Coupling . . . . .	158
32	360 MHz NMR Spectrum of the Zinc-Complexed Ethylene Adduct . . . . .	167

33	Spin Decoupling of the N-2-Hydroxyethyl Protons in the Ethylene Adduct . . . . .	170
34	Spin Decoupling of the Methylene Protons in the Ethylene Adduct . . . . .	171
35	The Ethylene Adduct: NOE Enhancement of the Meso Proton Signals . . . . .	174
36	The Ethylene Adduct: Sharpening of the Internal Vinyl Proton Signals Due to Spin Decoupling of the Methyl Group Protons . . . . .	175
37	360 MHz NMR Spectrum of the Zinc-Complexed Propene Adduct . . . . .	180
38	Spin Decoupling of the N-(2-Hydroxypropyl) Methine Proton . . . . .	182
39	The Propene Adduct: NOE Enhancement fo the Meso Proton Signals . . . . .	185
40	Analysis of the Propyne Adduct by HPLC . . . . .	188
41	Electronic Absorption Spectra of the Zinc-Complexed and Metal-Free Propyne Adduct . . . . .	189
42	NMR Spectrum of the Chloro-Zinc Complex of the Propyne Pigment . . . . .	191
43	The Propyne Adduct: NOE Enhancement of the Meso Proton Signals . . . . .	193

## LIST OF TABLES

Table		Page
1	Destruction of Cytochrome P-450 by Norethisterone In Vitro: Cofactor Requirements and the Effect of Inducing Agents (White and Muller-Eberhard, 1977)	44
2	In Vitro Destruction of Cytochrome P-450 by Acetylenes . . . . .	57
3	Analysis of the Terminal Acetylene Adducts by Field Desorption Mass Spectrometry . . . . .	77
4	Chemical Shift and Relaxation Time Values for the Methyl and Meso Protons in the Four Isomers of N-Methyl Protoporphyrin IX Dimethyl Ester . . . . .	132
5	Upfield Shift of the Ring Methyl Groups When Present on the N-Alkylated Ring or on the Ring Opposite to It . . . . .	142
6	Chemical Shift and Relaxation Time Values for the Meso and Methyl Protons in the Four N-Ethyl Protoporphyrin IX Dimethyl Ester Isomers . . . . .	161
7	Upfield Shift of the Ring Methyl Group Signals when Present on the N-Alkylated Ring or on the Ring Opposite to It . . . . .	163
8	Chemical Shift and Relaxation Time Values for the Meso and Methyl Protons of the Ethylene Adduct . . . . .	176
9	Chemical Shift and Relaxation Time Values for the Methyl and Meso Protons of the Propene Adduct . . . . .	186
10	Chemical Shift and Relaxation Time Values for the Meso and Methyl Protons of the Propyne Adduct . . . . .	194

## CHAPTER ONE

## HEPATIC CYTOCHROME P-450

1.1 INTRODUCTION

The cytochrome P-450 enzymes are members of a large family of hemoproteins which perform functions crucial to the existence of virtually every organism on earth. Dominant among these processes are electron transport and oxygen transport and metabolism. The type of chemistry carried out by a particular hemoprotein is conducted by the heme but orchestrated by the protein. The environmental matrix supplied by the protein dictates the reaction course by regulating the oxidation and spin states of the iron, via ligation at the axial sites of heme, and access to the catalytic center by electrons, oxygen and substrates. Cytochrome P-450 utilizes both functions of hemoproteins, oxygen binding and electron transport, to generate a highly reactive, iron-bound oxygen species capable of donating atomic oxygen to a wide variety of substrates.

The stoichiometry of cytochrome P-450 catalyzed reactions is given in the following equation.



In this reaction the substrate (generalized as RH) undergoes a two electron oxidation. During the reaction sequence, oxygen is reductively cleaved (formally a 4 electron process) into water and oxidized substrate and a pyridine nucleotide (NADPH) is oxidized via an associated flavoprotein. The dual requirement of molecular oxygen and reducing equivalents characterizes the overall process as a mixed-function oxidation (Mason, 1957).

Cytochrome P-450 is ubiquitous in nature being found in such diverse organisms as bacteria, plants and animals. Mammalian cytochrome P-450 enzymes participate in monooxygenation reactions with two classes of substrates. Certain forms of the enzyme are involved with the synthesis and degradation of endogenous compounds. For example, the synthesis of steroid hormones in the adrenal gland is mediated by a series of cytochrome P-450 catalyzed reactions at specific  $sp^3$  carbon centers. These transformations include the conversion of cholesterol to pregnenolone, as well as stereospecific hydroxylations at the 11-beta, 17-alpha, and 21-methyl positions (Walsh, 1979). A form of cytochrome P-450 catalyzes the rate-limiting 7-alpha hydroxylation step in the breakdown of cholesterol to the bile acids (Myrant and Mitropoulos, 1977). The utilization of cytochrome P-450 enzymes to perform these and other highly specific reactions on endogenous compounds is in sharp contrast to the role they play in the elimination of absorbed, exogenous com-



pounds.

The hallmark of this second function of the cytochrome P-450 enzymes is low substrate specificity as witnessed by the fact that almost any lipophilic compound is a likely substrate for the enzyme. Without general mechanisms for transformation of otherwise non-biodegradable lipophilic substances such as drugs, environmental contaminants, and food constituents the organism would rapidly accumulate toxic concentrations of these compounds. Cytochrome P-450 enzymes enhance the clearance of lipophilic compounds admitted into the body by oxidatively transforming them into more polar, and therefore more rapidly eliminated, substances. Cytochrome P-450 enzymes are located in membranes into which lipophilic compounds partition. Moreover, particularly high concentrations of the enzyme are found in highly perfused organs such as the liver, lung, and kidney. This strategic distribution facilitates access of the enzyme to absorbed compounds.

The cytochrome P-450 enzymes are not alone in their ability to transform foreign compounds. Rather they belong to a much larger family of enzymes that are characterized by broad substrate specificities, low turnover rates and poor substrate affinities. The glutathione-S-transferases, epoxide hydrolases, monoamine oxidases, esterases, and glucuronyl transferases are all involved in processing xenobiotic agents for elimination. The organism, therefore, has a

variety of weapons to choose from in its continual battle against chemical intrusion. A distinguishing characteristic of the cytochrome P-450 enzymes is the wide variety of functional groups which are susceptible to their catalytic action.

## 1.2 DISTRIBUTION AND HETEROGENOUS NATURE

Mammalian cytochrome P-450 enzymes are membrane bound and have been identified as constituents of most organs, including lung, liver, adrenal gland, skin, kidney, intestine, testis and placenta (Sato, 1978). Cytochrome P-450 is the major hepatic hemoprotein, comprising 2-3% of the total protein and up to 15% of the microsomal protein (Estabrook et al, 1971). Hepatic cytochrome P-450 is primarily distributed in the rough and smooth endoplasmic reticulum, but is also present to a lesser extent in the golgi apparatus, nuclear membrane, lysosomes, and mitochondria (Ichikawa and Mason, 1973). The endoplasmic reticulum is a tubular lipoprotein matrix which extends through the cytoplasm. The critical function of the rough endoplasmic reticulum in protein synthesis is well known. This organelle is usually isolated by differential centrifugation of disrupted liver cells and is found in what is termed the microsomal fraction. The microsomal fraction consists of particles which remain suspended at 10,000xg but sediment at 100,000xg. The

preparation and characterization of disrupted liver fractions is discussed in detail elsewhere (Ichikawa and Mason, 1973; Eriksson et al, 1978). The endoplasmic reticuli isolated in this manner are mere shadows of their former selves since homogenization of liver cells shears the endoplasmic reticulum into small particles. The sheared organelles appear to pinch-off and vesiculate, forming doughnut-shaped entities that actually maintain the inside-outside arrangement present in the intact organelle (Eriksson et al, 1978). Other major enzymes associated with the microsomal fraction include NADPH-cytochrome P-450 reductase, epoxide hydrase, the glutathione-S-transferases, cytochrome b5, cytochrome b5 reductase and glucose-6-phosphatase.

Hepatic microsomal cytochrome P-450's are membrane bound, hydrophobic hemoproteins with molecular weights ranging from 48,000 to 58,000 daltons as judged by SDS polyacrylamide gel electrophoresis (see White and Coon, 1980 for references and discussion). Each enzyme unit contains one molecule of heme (iron protoporphyrin IX), 2-3 molecules of glucosamine, and 400-500 amino acid residues (Coon et al, 1977). The primary, secondary, and tertiary structures of the enzymes are unknown although some information has been obtained on the N- and C-terminal amino acid sequences.

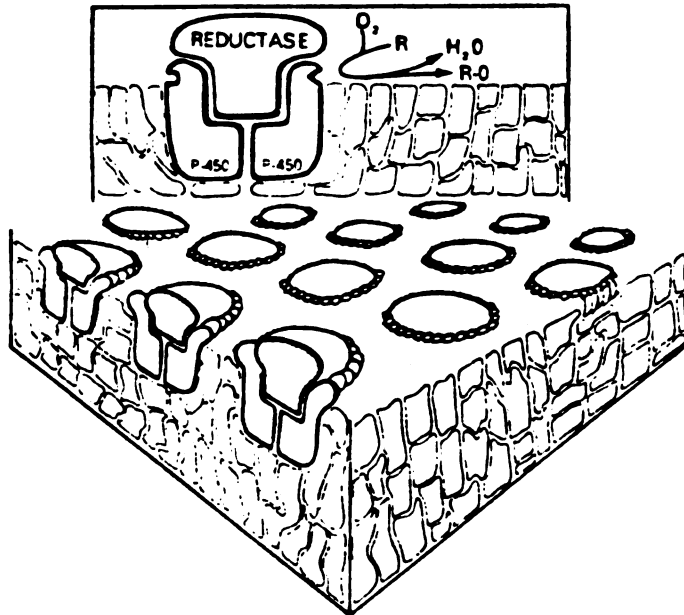
Associated with cytochrome P-450 is another membrane bound protein, NADPH cytochrome P-450 reductase (alternatively named cytochrome c reductase), which is responsible

for mediating the flow of electrons from NADPH to cytochrome P-450. NADPH cytochrome P-450 reductase has a molecular weight of 78,000 daltons and has, as its prosthetic group, one molecule each of the flavins FMN and FAD (Masters, 1980). In contrast to the multiplicity of cytochrome P-450's, it appears that only one form of the reductase is present in a given tissue (Masters, 1980).

Studies concerning the interaction of reductase and cytochrome P-450 have raised a number of interesting points. In intact microsomes the ratio of reductase to cytochrome P-450 varies considerably with induction state (values ranging from 1:10 to 1:30 have been reported) yet electron transfer is not normally rate-limiting for catalysis (Estabrook and Werringloer, 1979). The inevitable conclusion that one reductase services a manifold-higher number of cytochrome P-450 molecules places some intriguing constraints on the microsomal membrane architecture (see Estabrook and Werringloer, 1978; Omura, 1978; Nebert et al, 1981). Catalytic turnover of cytochrome P-450 requires the delivery of two reducing equivalents. Reconstitution experiments have established that the reductase can supply both electrons. However, evidence exists which suggests that reduced cytochrome b5 may also contribute reducing equivalents in intact microsomal systems (Omura, 1978). The movement of electrons through potential gradients between these proteins is currently an area of active investigation.

FIGURE 1

ONE OF THE POSSIBLE ARRANGEMENTS  
CYTOCHROME P-450 AND CYTOCHROME P-450 REDUCTASE  
ON THE ENDOPLASMIC RETICULUM



Taken from Nebert et al (1981)

Among the many fascinating problems confronting the experimentalist in the area of cytochrome P-450 research is the question of isozymes. How many are there and how do they differ? It is now clear that different forms of the enzyme populate the liver as well as other organs. Thus techniques have to be developed to separate and characterize the different forms. This problem is further compounded by the fact that the levels of the different forms are exquisitely sensitive to the presence of lipophilic compounds. Exposure of animals to agents such as 3-methylcholanthrene (3MC), phenobarbital (PB), pregnenolone-16-alpha-carbonitrile (PCN), mixtures of polychlorinated aromatics such as Arachlor 1254, or benzonaphoflavone (BNF) induces the levels of certain forms of cytochrome P-450 potentiating and altering metabolic rates as well as causing morphological changes. It is generally believed that there is a finite number of cytochrome P-450 isozymes (five to seven) in rat liver microsomes (Lu and West, 1980). However it has been argued that hundreds of distinct forms may actually be present which display overlapping substrate specificities and nearly homologous amino acid sequences (Nebert et al, 1981).

At least four forms of cytochrome P-450 have been demonstrated to be present in uninduced rat liver (Agosin et al, 1979; Warner and Neims, 1979). Treatment of animals with inducing agents such as PB, 3MC and PCN differentially

stimulates cytochrome P-450 dependent drug oxidation reactions (Conney et al, 1973). The alterations in rate and specificity of xenobiotic metabolism reflect complex changes engendered by inducing agents. These changes are primarily attributable to altered rates of de novo enzyme synthesis (Nebert et al, 1981; Conney, 1967; Gelboin and Whitlock, 1979; Kuntzman et al, 1969; Omura, 1979). A reduction in enzyme degradation rates may also play a minor role in the induction process (Gelboin, 1971). Induction by some agents, such as the barbiturate phenobarbital, not only increases and alters cytochrome P-450 isozyme content, but also increases total liver weight, NADPH cytochrome P-450 reductase, glucuronyl transferase and phospholipid and causes a general proliferation of the endoplasmic reticulum (Orrenius et al, 1969). Induction by 3MC, on the other hand, appears to affect primarily the distribution of isozymes without changing the total enzyme content. Interestingly enough, induction with 3MC is not marked by pronounced changes in liver weight, phospholipid content or reductase levels (Parke, 1979). Cytochrome P-450 is inducible by many xenobiotics including drugs, environmental contaminants, and carcinogens.

The existence of multiple forms of cytochrome P-450 has been confirmed by substrate selectivity studies (Trager, 1977) as well as by purification to apparent homogeneity. The purified forms of the enzyme have been reconstituted

with the reductase in phospholipid vesicles and shown to be catalytically competent. The purified isozymes have also been shown to be different by SDS polyacrylamide gel electrophoresis, spectral properties, catalytic activities, immunological properties, N-and C-terminal amino acid sequences and proteolytic peptide maps (see review by Lu and West, 1980 and references therein).

### 1.3 OXYGEN ACTIVATION AND TRANSFER TO SUBSTRATES

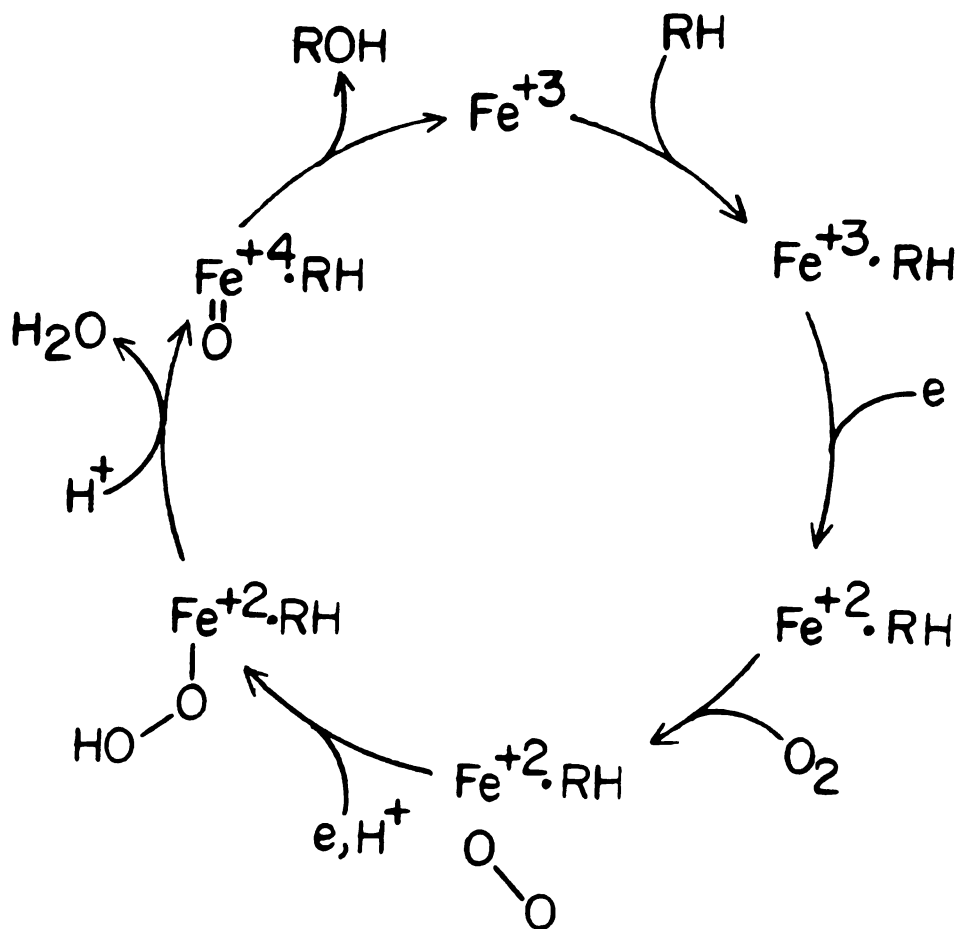
Substrate oxidation by cytochrome P-450 may be viewed most economically as the result of a chemical reaction between an electrophilic six-electron oxygen atom and a relatively electron-rich molecular orbital of a substrate molecule. Since the activated oxygen species is bound to the iron of heme which is, in turn, imbedded in a lipid-bound protein matrix, the observable consequences of the reaction are governed by steric as well as electronic factors. This discussion will be concerned with the biochemical machinery required for the bioactivation of oxygen, and the mechanisms by which it is formed and transferred to substrate.

The cytochrome P-450 enzymes catalyze the monooxygenation of an overwhelming number of xenobiotics, including polycyclic aromatic hydrocarbons, halogenated hydrocarbons, aliphatic hydrocarbons, amines, most drugs, and a host of



FIGURE 2

THE CATALYTIC CYCLE OF CYTOCHROME P-450\*



\* A number of the intermediates depicted in this scheme have not been firmly established. See text for discussion

other compounds. The major documented biotransformation reactions include epoxidation, hydroxylation, N-oxidation, S-oxidation, and N- and O-dealkylation. A number of excellent reviews have been published on these subjects (White and Coon, 1980; Ishimura, 1978; Wislocki et al, 1980; Low and Castagnoli, 1980; Trager, 1980).

The catalytic cycle of cytochrome P-450 is portrayed in Figure 2. The identity of the actual intermediate species involved at each step in the cycle is, in some cases, still a matter of active controversy. Especially tentative are the intermediates formed following the introduction of the second electron.

### 1.31 BINDING OF SUBSTRATE

The resting state of the enzyme finds the prosthetic heme iron in the ferric state. The four equatorial ligand positions of the hexacoordinate iron are occupied by the porphyrin pyrrole nitrogens leaving the two axial positions available for ligation. Occupancy of the fifth ligand position, for years a matter of controversy, is now believed to be held by thiolate, presumably part of a cysteine residue of the apoprotein (Cramer et al, 1978). The identity of the sixth ligand is uncertain since reasonable evidence exists for either imidazole (Sligar and Gunsalus, 1979; Chevion et al, 1977) or water (Ebel et al, 1977; Philson et al, 1979).

Whatever this ligand is, it is neutral, exchangeable with water (Philson et al, 1979; Griffin and Peterson, 1975), and easily replaced by a number of substrates (Peterson et al, 1976).

Electronic absorption spectra of cytochrome P-450 preparations reflect the spin and ligation state of the heme prosthetic group. Most forms of the cytochrome contain a sixth ligand of sufficient strength to favor the low spin (spin 1/2) configuration in which the iron is in the plane of the porphyrin ring. The corresponding visible spectrum displays a Soret band (the dominant  $\pi$  to  $\pi^*$  transition of porphyrins) at 418 nanometers and well defined alpha and beta bands (quasi-allowed  $\pi$  to  $\pi^*$ ) of lesser intensity at 568 and 535 nanometers respectively. Purified cytochrome P-450 LM4, the predominant isozyme induced by 3-methylcholanthrene, contains no sixth ligand or, at best, one with weak ligation abilities. The heme in this form of cytochrome P-450 is in the high spin (spin 5/2) state and has a Soret absorbance at much shorter wavelengths (394 nanometers) and a broad absorbance at 545 nanometers with no well defined alpha and beta bands. Addition of butanol to a purified preparation of cytochrome P-450 LM4 results in the appearance of a normal low spin cytochrome spectrum (White and Coon, 1980).

Substrate binding to cytochrome P-450 may be conveniently monitored in a spectrophotometer equipped to han-

dle turbid solutions. The binding of apolar, hydrophobic compounds at the active site displaces the endogenous sixth ligand with a substrate which is of insufficient strength to maintain the heme iron in the low spin state. This binding interaction is reversible although the equilibrium normally favors the substrate-bound complex. This interaction, known as Type I, lowers the ratio of absorbances at 418 and 394 nanometers to favor the latter. Thus Type I substrates bind to give pentacoordinate, high spin heme. A substrate bearing a strongly ligating functional group such as an amine shifts the spin state equilibrium to the low spin hexacoordinate cytochrome which absorbs light at 420-425 nanometers (Type II). The binding of substrates with less strongly ligating functional groups such as butanol also shift the spin state equilibrium to the low spin form (Soret 416-418 nanometers) and are called reverse Type I substrates. Under saturating conditions substrate binding is not rate-limiting to catalysis (Bjorkhem, 1977).

### 1.32 TRANSFER OF THE FIRST ELECTRON

Two reducing equivalents are required for substrate turnover by cytochrome P-450. The first of these sequentially transferred electrons simply reduces the heme iron from the ferric to the ferrous state. The ferrous form of the enzyme readily binds carbon monoxide at the sixth ligand

position in a manner similar to ferrous hemoglobin or myoglobin. The resulting hexacoordinate, ferrous carbonyl complex absorbs light at 450 nanometers (Klingenberg, 1958) which is an abnormally low-energy Soret transition for hemoproteins (most hemoproteins which form ferrous carbonyl complexes exhibit Soret transitions in the range of 400-420 nanometers). This abnormally high wavelength transition is the basis on which the enzyme is named (Omura and Sato, 1964). This value is now known to vary from 446 to 452 nanometers depending on the specific isozyme employed for the measurement.

Single electron, cytochrome P-450 reductase mediated, reduction of cytochrome P-450 by NADPH exhibits biphasic kinetics in both intact microsomal preparations (Peterson et al, 1976) and reconstituted systems (Iyanagi et al, 1978; Oprian et al, 1979). The rate of reduction depends on the isozyme of cytochrome P-450 examined as well as on the presence and type of substrate. These differences are presumably due to modulation of the heme spin-state equilibria by substrates and the active site environment (Iyanagi et al, 1978; Oprian et al, 1979; White and Coon, 1980). Chemical reduction of the cytochrome with sodium dithionite, while slower than the reductase-mediated process, indicates that only about 50% of microsomal cytochrome P-450 is available for enzymatic reduction (Klingenberg, 1957; Sligar et al, 1979). Whether this in vitro observation has any relevance

for the in vivo situation is unknown.

### 1.33 DIOXYGEN BINDING

Binding of dioxygen to pentacoordinate, high-spin cytochrome P-450 ferrous heme (spin 2) has been observed spectrophotometrically in microsomes from phenobarbital-treated rats during steady state oxidation (Baron et al, 1973). Stopped-flow (Guengerich et al, 1976) and low temperature (Bonfils et al, 1979) experiments with purified preparations have confirmed the presence of the species which readily decomposes to ferric heme and superoxide anion as well as ferrous heme and dioxygen. Presumably, dioxygen is bound end-on in a manner similar to oxygenated hemoglobin or myoglobin.

### 1.34 GENERATION OF ACTIVATED OXYGEN

The generation of water and oxidized substrate from the one electron reduced, iron-dioxygen complex is one of the most mystifying and fascinating aspects of cytochrome P-450 catalysis. The reaction stoichiometry requires the addition of a second electron and two protons. The order in which this occurs, and the intermediates involved, are still matters of intense debate. It appears that substrate oxidation is preceded by reduced dioxygen cleavage and water

formation (White and Coon, 1980). If true, the tentative conclusion can be reached that the activated oxygen species is an iron-bound oxygen atom. Perhaps the most persuasive evidence supporting the existence of such a species is the ability of the single oxygen donor iodosobenzene to assume the roles of dioxygen and reducing equivalents in cytochrome P-450 mediated oxidation reactions (Rahimtula and O'Brien, 1974). The most direct interpretation of this result, that is, that a common oxidizing intermediate is generated in both pathways, is presented schematically in Figure 3. The proposed intermediate is stoichiometrically composed of enzyme-bound ferric heme and atomic oxygen, although the actual distribution of electrons among the component atoms is unclear. Viable possibilities for the structure of the reactive oxygen species include a thiolate-ferric iron-oxygen complex 1, a thiolate-perferryl iron-oxygen dianion complex 2, a thiolate-iron IV-oxygen anion complex 3, or a thiyl-ferric iron-oxygen anion complex 4 (see White and Coon, 1980 for discussion and references). Clues to the composition of

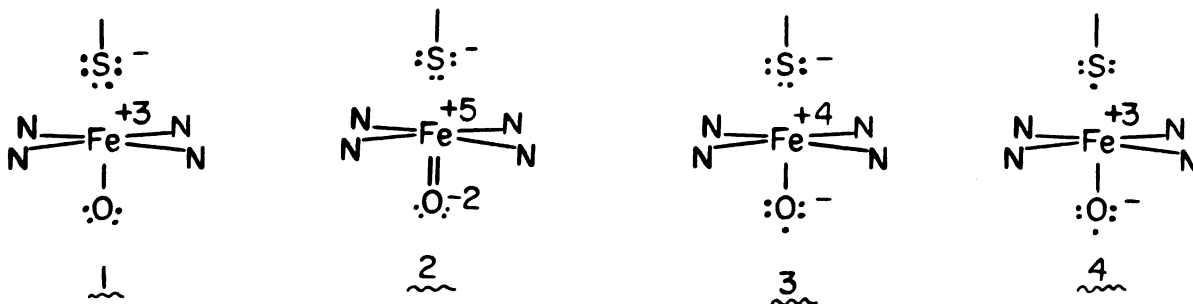
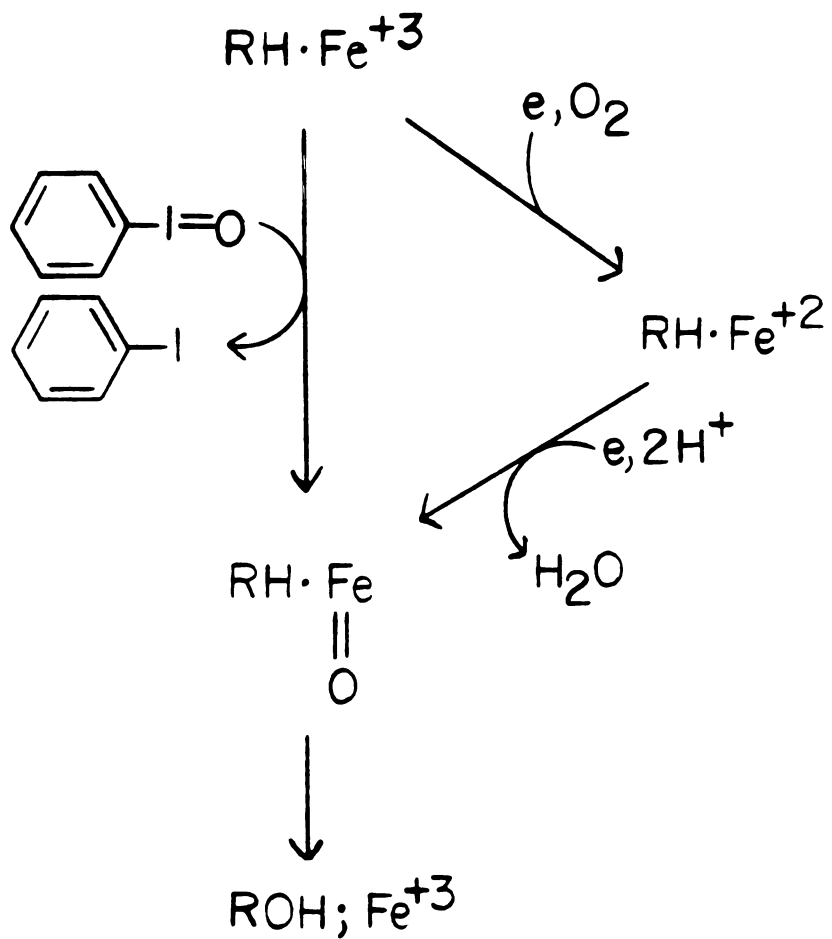


FIGURE 3

THE ROLE OF IODOBENZENE IN THE MONOOXYGENATION OF  
SUBSTRATES CATALYZED BY CYTOCHROME P-450





this intermediate have been obtained from model systems. Groves et al (1979) have shown that hemin chloride or chloro-ferri-tetraphenylporphyrin are capable of supporting both epoxidation and hydroxylation reactions in the presence of iodosobenzene. The intermediate iron-oxygen complex was unfortunately too unstable to characterize. However, in a later paper (Groves and Kruper, 1979) it was shown that a chromium III tetraphenyl porphyrin iodosobenzene system also catalyzed similar oxidation reactions. A stable chromium-oxygen complex could be generated in the absence of substrate. Spectroscopic characterization of the intermediate identified it as a chromium V oxygen complex. An identical species could be generated using meta-chloroperbenzoic acid, a compound also known to support cytochrome P-450 mediated hydroxylation reactions. The intermediate formed during oxidative turnover of cytochrome P-450, extrapolated from the chromium complex data, would be expected to be the perferryl species  $\underline{2}$ . The evidence supporting the perferryl iron oxygen complex remains circumstantial, however. Complex  $\underline{2}$  will, nevertheless, be used as a model for mechanistic discussions in this dissertation.

Iodosobenzene is not unique in its ability to circumvent the need for NADPH and oxygen during cytochrome P-450 catalysis. Indeed it is among the most recently discovered of this growing class of reagents. Many organic and inorganic peroxy compounds have been shown to be members of this

group including cumene hydroperoxide, sodium periodate, hydrogen peroxide and a number of peracids (O'Brien, 1978). Significant differences have been found among the peroxy reagents in terms of substrate selectivities and rates of substrate oxidation. Particularly disturbing is the fact that the substrate selectivities vary from reagent to reagent when the oxidation reactions are catalyzed by purified preparations of cytochrome P-450. This indicates that either a uniform iron-oxygen species is not common to the peroxy oxidants or that the molecule delivering the six-electron oxygen somehow perturbs substrate binding (White and Coon, 1980; Gustavsson, 1979). Also, cytochrome P-450 itself survives only a few turnovers before being irreversibly degraded by these artificial oxidants, presumably by oxidation of the porphyrin framework of heme (White et al, 1980).

The reactive iron-oxygen species formed during steady state oxidation undergoes reactions with substrates which are analogous to those of carbenes. These include insertion into double bonds and carbon-hydrogen bonds. This fact prompted Hamilton (1964; 1974) to describe the oxygen transfer to substrate as "oxenoid" in nature. The advantage of this interpretation is that it allows rather accurate predictions to be made concerning the susceptibility of certain sites on a molecule to monooxygenation by cytochrome P-450 (Trager, 1980). It is, however, somewhat misleading

in a mechanistic sense as will be seen in the following sections.

### 1.35 INSERTION OF OXYGEN INTO CARBON HYDROGEN BONDS

Cytochrome P-450 efficiently oxidizes  $sp^3$  carbon-hydrogen bonds to the corresponding alcohols. Hydroxylation of simple aliphatic substrates is a regioselective process (carbon hydrogen bonds adjacent to terminal methyl groups are especially vulnerable) and generally follows the decreasing order tertiary:secondary:primary (Trager, 1980). The applicability of this reactivity pattern in a predictive sense is considerably muted by steric effects as well as by the fact that inducing agents perturb both the rate and selectivity of hydroxylation reactions (Frommer et al, 1972; Ryan et al, 1978).

The carbon hydrogen-bond is particularly accessible to mechanistic experiments designed to probe the nature of the bond breaking step. For instance, if the oxygen insertion were to occur in a concerted fashion it would be expected that configuration about a carbon center of the substrate would be conserved in the product alcohol. Non-concerted insertion, on the other hand, might be expected to lead to some racemization. To the extent that cleavage of the carbon-hydrogen bond is rate limiting to the overall reaction sequence, a primary isotope effect should be observed

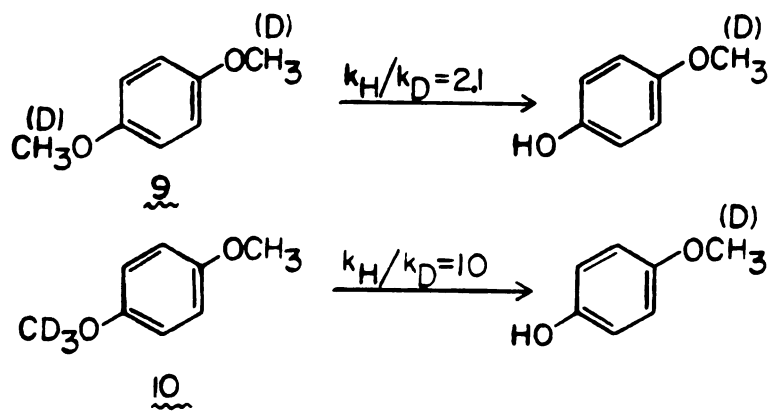
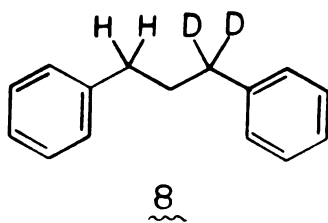
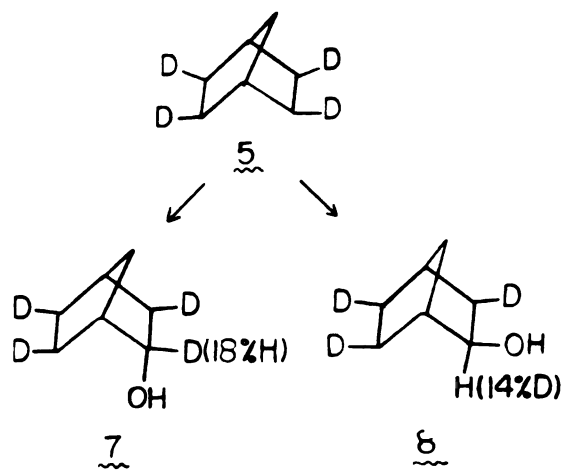
using appropriately labeled compounds. The magnitude of the isotope effect observed can provide critical information concerning the transition state involved in the bond breaking step. For instance, singlet carbene insertions into carbon-hydrogen bonds proceed with retention of configuration and low  $k_H/k_D=1.5-2.0$  deuterium isotope effects, as expected for the three-centered, two-electron transition state operative in these reactions (Kirmse, 1971).

Until recently, isotope effects of cytochrome P-450 catalyzed aliphatic hydroxylation reactions had also been observed to be low ( $k_H/k_D=1.2-2.0$ ) (Thompson and Holtzman, 1974; McMahon et al, 1969; Mitoma et al, 1971). These results, while not conclusive, suggested that oxygen insertion proceeds in a concerted fashion similar to singlet carbene insertion reactions. More recently, it has been shown that aliphatic hydroxylation can proceed with some inversion and is subject to large isotope effects. Groves et al (1978) have shown that hydroxylation of exo, exo, exo, exo, 2,3,5,6 tetradeuteronorbornane (5) by reconstituted cytochrome P-450 LM2 proceeds with a large ( $k_H/k_D=11.5$ ) isotope effect to give the exo alcohol 6 with 14% inversion. Endo hydroxylation occurred with 18% inversion to give 7. These results, and the lack of any carbon skeleton rearrangement products typical of norbornyl cations, led to the proposal that the hydroxylation proceeded via initial hydrogen atom abstraction to give a carbon radical of sufficient longevity

to epimerize before recombination with the iron-bound hydroxyl radical.

Large isotope effects have also been observed during the microsomal oxidation of 1,3-diphenylpropane-1,1-<sup>2</sup>H (8) (Hjelmeland et al, 1977). Hydroxylation at the symmetrically-arranged benzylic position was found to proceed to a much greater extent at the non-deuterated carbon ( $k_H/k_D=11$ ). The isotope effect measured in this study represents an intramolecular effect and has the distinct advantage of circumventing contributions from other potentially rate limiting steps in the reaction sequence.

A striking example illustrating the power of this methodology has been provided by Foster et al (1974) in their studies on the microsomal metabolism of *p*-dimethoxybenzene (9). The initial step in the production of the monomethylated phenol from *p*-dimethoxybenzene involves cytochrome P-450 dependent hydroxylation of a methyl group to the hemiacetal. Further non-enzymatic hydrolysis of the acetal leads to the formation of the observed phenol product. The rate of O-demethylation of *p*-dimethoxybenzene 9 was compared with its hexadeuterated analog by incubation of an equal mixture of the two compounds with rat liver microsomes and measurement of the ratio of the two products formed by mass spectrometry. The rate of non-deuterated phenol formation was found to be twice that of the trideuterated product. However, the intramolecular competition



experiment utilizing  $^{10}$  as the substrate gave an isotope effect, again measured as a product ratio, of 10! These apparently divergent results indicate that for cytochrome P-450, a multistep enzyme with a plurality of potentially rate limiting steps (Bjorkhem, 1977), the true isotope effect for C-H bond cleavage may be unmasked only by carefully designed experiments (Northrop, 1975).

It is evident that cytochrome P-450 hydroxylation reactions can proceed via a transition state other than the three-centered one operative in singlet carbene insertions into carbon hydrogen bonds. The enzymatic insertion is therefore not "oxenoid" in the strictest sense of the word. The results of the studies discussed here suggest that the transition state involves hydrogen radical abstraction from the substrate by activated oxygen. This highly energetic intermediate then collapses to give the product alcohol.

### 1.36 PI BOND OXIDATION REACTIONS

Cytochrome P-450 catalyzed olefin and aromatic pi bond oxidations have proven to be interesting reactions from a toxicological as well as chemical point of view. The initial product of oxygen transfer to the substrate is a three-membered ring formed by insertion of atomic oxygen into a carbon-carbon pi bond. Epoxides and arene oxides are reactive electrophiles with respect to cellular constituents

and it is now painfully clear that their binding to protein and DNA initiates necrotic, mutagenic, and carcinogenic events. For instance vinyl chloride (11) (Pessayre et al, 1979), aflatoxin B1 (12) (Miller and Miller, 1977), benzo(a)pyrene (13) (Moore et al, 1977), and bromobenzene (Jollow et al, 1974) are all activated by the mixed-function oxidase system to reactive epoxides which are proximate toxic agents.

The first line of defense against these reactive intermediates, aside from their intrinsic propensity to rearrange to less harmful compounds, is chemical or enzymatic hydrolysis to the corresponding diols and nucleophilic addition of glutathione catalyzed by the glutathione-S-transferases. These reactions are illustrated in Figure 4. Cytochrome P-450 catalyzed monooxygenation of bromobenzene occurs via epoxide formation at the 2,3 and 3,4 positions (Jollow et al, 1974) and, to a lesser degree, by direct insertion into the meta carbon-hydrogen bond. The hepatic centrilobular necrosis resulting from bromobenzene administration has been shown to be associated with covalent binding of the 3,4 epoxide to protein. The 3,4 epoxide undergoes a number of secondary reactions in addition to protein alkylation. The most famous of these is rearrangement of the epoxide via a 1,2 hydride shift, followed by tautomerization, to the para phenol. This pathway, known as the NIH shift (Guroff et al, 1967), was the first evidence that aromatic hydroxylation



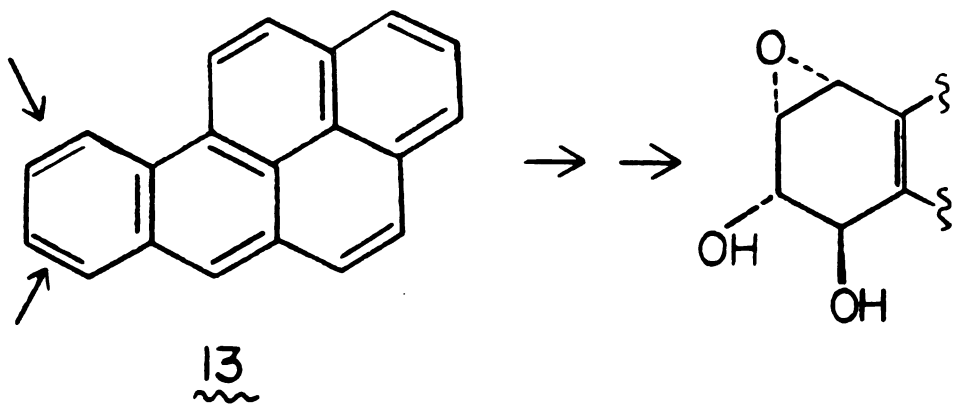
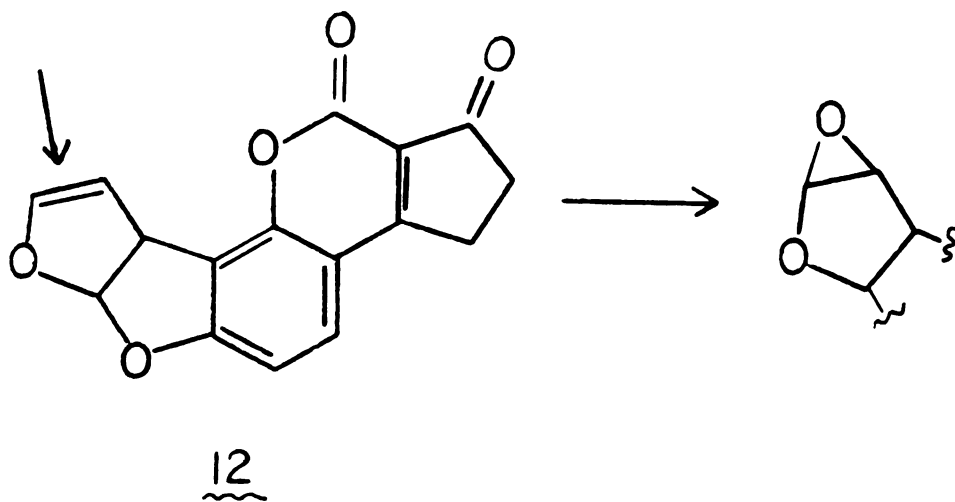
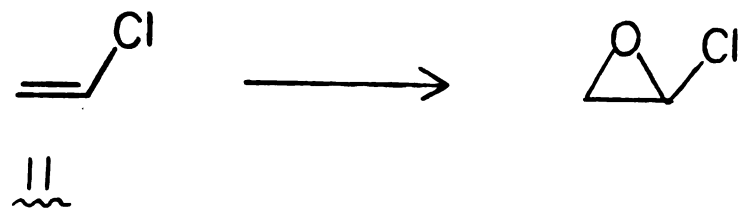
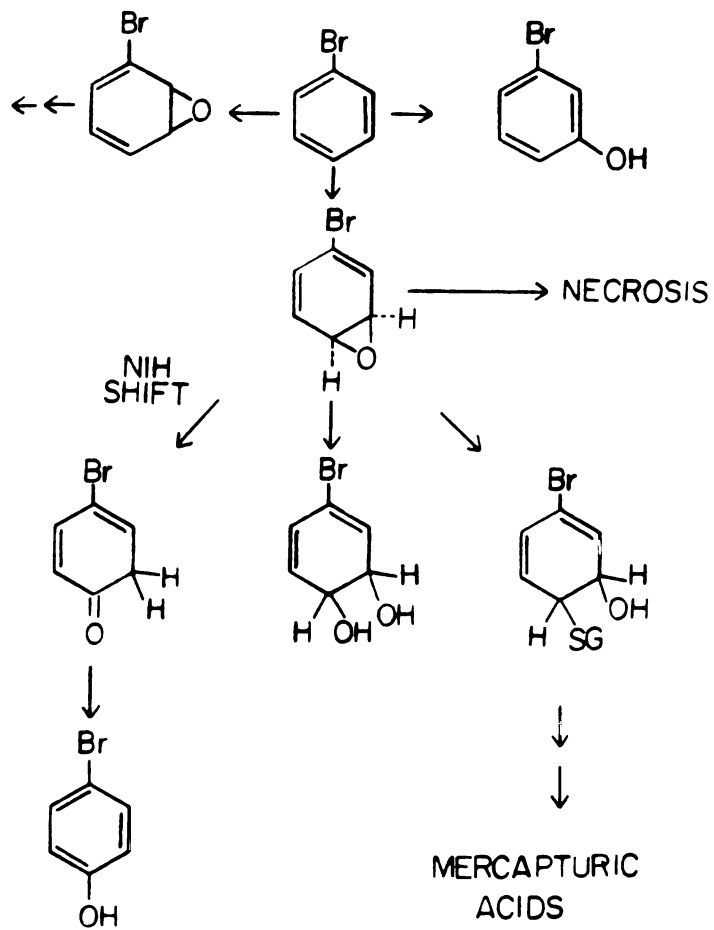


FIGURE 4

## THE METABOLISM OF BROMOBENZENE



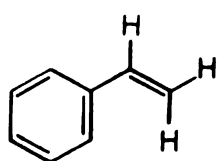
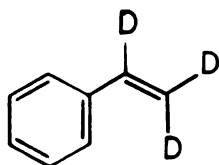
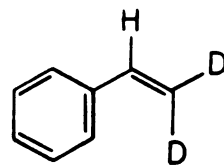
See Jollow et al (1974)

reactions involved pi bond epoxidation rather than sigma bond insertion. The 3,4 epoxide is also hydrolyzed by epoxide hydrase to the trans diol which can then be further, non-enzymatically, oxidized to the catechol. The reactive epoxide is also disarmed by the enzyme-catalyzed nucleophilic attack of glutathione to give the beta-hydroxy thioether. Dose dependent, covalent binding of the 3,4 epoxide to tissue macromolecules is, unfortunately, competitive with these pathways. The magnitude of the covalent binding and the associated necrosis is enhanced by prior depletion of hepatic glutathione levels and can be attenuated by the administration of cysteine. The enhancement of toxicity by prior depletion of glutathione levels has become a classic test for the generation of reactive electrophiles in vivo.

Monooxygenase catalyzed epoxide formation has proven to be less accessible to mechanistic studies than aliphatic hydroxylation reactions. For example, it is not known whether the formation of the two epoxide carbon-oxygen bonds occurs synchronously or asynchronously. In the case of olefins, synchronous oxygen addition would require retention of stereochemistry whereas asynchronous addition would not. Thus, loss of stereochemistry during the epoxidation process may be considered to be definite proof for non-concerted oxygen addition while retention of stereochemistry could result from either addition process. Triplet carbene

cyclopropanation of olefins provides an example of an asynchronous, three-membered ring formation which has been shown, in some cases, to proceed with retention of stereochemistry (Lowry and Richardson, 1976). To date, cytochrome P-450 olefin epoxidation reactions have all been shown to retain stereochemistry, leading to the conclusion that either oxygen addition is concerted, or that the acyclic intermediates in asynchronous addition closes to product before carbon-carbon bond rotation can occur (Watabe and Akamatsu, 1974; Maynert et al, 1970).

Epoxidation involves hybridization changes from  $sp^2$  to  $sp^3$  at the two pi bond carbon atoms. In principle, a secondary isotope effect should arise from this step. Epoxidation of 1,2,2- $^2H$ -1-phenyl ethylene (15) by rat liver microsomes

141516

proceeds with a secondary isotope effect of  $k_H/k_D=0.93$  when

compared with styrene (14), indicating that oxirane formation is at least partially rate limiting to the over all reaction sequence. Interestingly enough, no difference in the rate of epoxide formation was noted when the terminal di-deuterated olefin 16 was compared with styrene itself. Thus, expression of the secondary isotope effect required deuterium only at the benzylic vinyl carbon. These results suggest that styrene oxide formation involves two distinct carbon oxygen bond forming steps and thus provide some evidence that cytochrome P-450 epoxidation may be non-concerted, or may involve an asymmetric transition state.

#### 1.4 CATALYSIS DEPENDENT DESTRUCTION OF CYTOCHROME P-450 BY XENOBIOTICS

The oxidative metabolism of xenobiotics by cytochrome P-450 terminates in the release of a host of new substances into the biological compartment. A portion of these metabolites have pharmacological activities of their own and in many cases their formation has been associated with detrimental effects. The cytochrome P-450 dependent production of potent bioalkylating metabolites such as the arene oxides and other epoxides provides clear examples of this generally benevolent detoxifying mechanism gone astray. It is now evident that cytochrome P-450 itself is susceptible to alkylation by the products of its own metabolism and that this

covalent modification of the enzyme can bring about its inactivation. Alkylation of cytochrome P-450 can occur at two experimentally discernible sites. The first of these is the apoprotein matrix of the enzyme. Catalysis dependent covalent binding of radiolabeled substrates to the apoprotein indicates that reactive species have been formed. Correlation of the extent of label incorporation with the loss of enzyme activity provides circumstantial evidence linking the two events. This approach is limited by the fact that a precise molecular definition of the destructive event cannot be made. The other potentially labile site is the heme prosthetic group of the enzyme. A number of agents have been shown to effect both heme loss and a reduction of spectroscopically observable cytochrome P-450. Since the catalytic activity of cytochrome P-450 is absolutely dependent upon the presence of heme properly positioned in the active site, the loss of this moiety provides strong evidence for its modification and a rationale for loss of activity.

#### 1.41 APOPROTEIN DEGRADATION AND ENZYME INACTIVATION

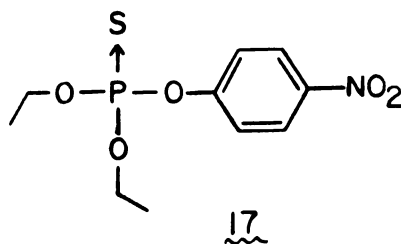
##### Carbon Disulfide and Parathion

Cytochrome P-450 dependent metabolism of carbon disulfide markedly reduces the enzymes ability to process alternate substrates both in vivo and in vitro (Dalvi et al, 1975; DeMatteis and Seawright, 1973; Bond and DeMatteis, 1969; Freundt and Dreher, 1969). Sulfur (Dalvi et al, 1974; DeMatteis, 1974; Neal et al, 1976) and, to a lesser extent, carbon (DeMatteis and Seawright, 1973) from carbon disulfide become bound to the protein component of cytochrome P-450 during the course of inactivation. The amount of enzyme capable of forming the diagnostic ferrous carbonyl complex is reduced as well, but the levels of heme are unaffected (Dalvi et al, 1975). It would appear, therefore, that covalent binding of carbon disulfide metabolites to protein interferes with ligation and retention of prosthetic heme by the enzyme.

The extent of metabolism-dependent incorporation of  $^{35}\text{S}$  into the apoprotein is greater than one to one and attempts to remove the bound sulfur from the protein by chemical means indicate the presence of more than one mode of sulfur attachment. Treatment of the labeled protein with sodium cyanide liberates 50% of the bound sulfur as thiocyanide. This observation is consistent with the hypothesis that a portion of the labeled sulfur is bound through a

hydrosulfide linkage to protein sulfhydryl groups such as those present on cysteine residues (Catignani and Neal, 1975). It has been proposed that singlet sulfur is released during the oxidative metabolism of carbon disulfide to carbon dioxide and that this reactive metabolite is readily incorporated into protein.

Parathion (17), an organophosphorothionate insecticide, inactivates cytochrome P-450 in a manner almost indistinguishable from that of carbon disulfide (see Neal et al, 1977 and references therein). Radiolabeled sulfur from parathion becomes bound<sup>d</sup> to protein during cytochrome P-450 metabolism and the extent of label incorporation is related to the loss of enzyme activity. Approximately 50% of the bound sulfur can be liberated by cyanide indicating that some of the sulfur was present in hydrosulfide linkages. The analog of parathion in which the sulfur is replaced by oxygen is inactive.



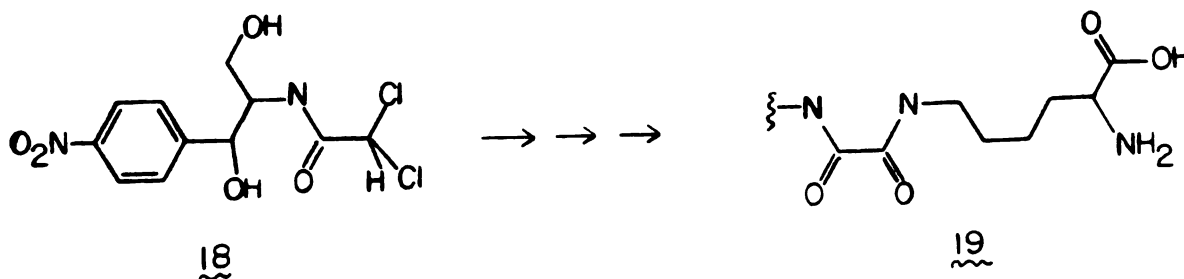
Parathion and carbon disulfide both inactivate hepatic cytochrome P-450. The loss of enzyme activity can be correlated with depletion of spectroscopically observable cyto-



chrome. Covalent binding of sulfur liberated via oxidative metabolism of these compounds into protein provides an attractive rationale for the loss of enzyme activity. However the amount of label incorporated into apocytochrome-P-450 exceeds the loss of enzyme by at least a factor of five. More than one type of protein adduct is formed during the destructive process. The nature of the lethal event is therefore unclear.

### Chloramphenicol

The antibiotic chloramphenicol (18) irreversibly inhibits monooxygenase activity in hepatic microsomes and reconstituted cytochrome P-450 preparations (Neal and Ivey, 1978; Halpert and Neal, 1980). Loss of enzyme activity is not marked by changes in heme concentration or level of spectroscopically observable cytochrome P-450. Radiolabeled chloramphenicol becomes bound to two distinct apoprotein residues during the inactivation process. The major adduct has been identified as the chloramphenicol oxamyl amide adduct 19 with an apoprotein lysine residue



by protein hydrolysis, chromatography and comparison with a synthetic standard (Halpert, 1981). Formation of this adduct to protein is suggested to occur through oxidative metabolism of the dichloroacetyl group of chloramphenicol to the oxamyl chloride which then reacts with the free amino group of a lysine residue to give the oxamide 19. Approximately 0.8 nanomoles of lysine adduct and 5 nanomoles of chloramphenicol oxamyl chloride are formed per nanomole of enzyme inactivated in the purified, reconstituted system. No conclusive evidence has been forthcoming as to whether this covalent event is involved in enzyme inactivation. The approximately one-to-one relationship of enzyme inactivation to lysine adduct formation provides good correlative support for the possibility that adduct formation is the lethal event.

#### 1.42 HEME DEGRADATION

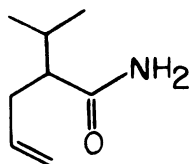
##### Carbon Tetrachloride

Carbon tetrachloride is known to produce lipid peroxidation both in vivo and in vitro and to cause hepatic centrilobular necrosis (Recknagel and Ghoshal, 1966; Rao and Recknagel, 1968). Carbon tetrachloride also causes a loss of hepatic cytochrome P-450 (Smuckler et al, 1967) and heme (Levin et al, 1972). The extensive degradation of lipid and

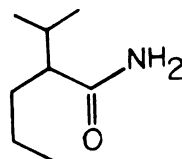
other cellular constituents due to the administration of this agent indicates an environment teeming with reactive species. The toxic effects produced by carbon tetrachloride are most likely due to the cytochrome P-450 catalyzed homolytic cleavage of the carbon-chlorine bond to give the trichloromethyl radical. The trichloromethyl radical has been detected by ESR measurements (Calligaro and Vannini, 1975) and its presence deduced by isolation of hexachloroethane (Bini et al, 1975). Labeled carbon tetrachloride is incorporated into protein and lipid (Reynolds, 1967). The extensive lipid peroxidation observed due to carbon tetrachloride administration most likely arises from the reaction of the trichloromethyl radical with unsaturated lipids. Lipid hydroperoxides are known to destroy cytochrome P-450 heme although the product of the reaction is unknown (Nerland et al, 1980). The key observation of Uehleke et al (1973) that suppression of lipid peroxidation does not attenuate label incorporation into cellular components but does eliminate the loss of spectroscopically observable cytochrome P-450 and heme strongly suggests that the loss of these components is due to lipid hydroperoxides rather than the trichloromethyl radical. In the absence of any evidence as to the heme breakdown products, confirmation of this hypothesis will be difficult.

Allylisopropylacetamide (AIA) and other olefins

Allylisopropylacetamide (2-isopropyl-4-pentenamide, AIA) (20) destroys hepatic cytochrome P-450 both in vivo and in vitro (Wada et al, 1968; DeMatteis, 1971; Levin et al, 1972) by a process which is dose dependent and which favors those forms of the enzyme induced by phenobarbital (DeMatteis, 1971; Levin et al, 1972).



20



21

AIA propagated enzyme loss in vitro requires oxygen (Ortiz de Montellano and Mico, 1981a) and NADPH, and is inhibited by SKF 525A (DeMatteis, 1971), suggesting that enzyme turnover is intimately involved in the destructive process. The destruction is marked by a reduction in cytochrome P-450, an equimolar loss of heme (DeMatteis, 1971; Bradshaw et al, 1978) and the formation of an abnormal hepatic pigment (Schwartz and Ikeda, 1955; DeMatteis, 1971).

Radiolabeling experiments have forged the link joining these observations. Prelabeling of the microsomal heme pool in vivo with radioactive ( $^{14}\text{C}$  and  $^3\text{H}$ ) delta aminolevulinic acid (DeMatteis, 1971) or  $^{57}\text{Fe}$  (DeMatteis, 1978) revealed that the heme lost during the destructive process is con-

verted into the green pigment and that the iron retained by the pigment is easily removed by treatment with mild acid. These results suggested that the terminal event in the destruction of cytochrome P-450 involved modification of the heme prosthetic group.

The role of AIA in the destructive process, for years a matter of speculation, was convincingly demonstrated by members of this laboratory who found that the green pigment is the product of covalent addition of AIA to the porphyrin framework of heme (Ortiz de Montellano et al, 1978). The critical experiment involved the administration of  $^{14}\text{C}$  labeled AIA to phenobarbital pretreated rats followed by isolation and purification of the green pigment as the iron-free, dimethyl esterified porphyrin. The incorporation was unambiguously established by extensive purification by high pressure liquid chromatography. These results were consistent with the hypothesis that catalytic processing of AIA leads to the covalent attachment of an activated form of AIA to the heme prosthetic group, and that the product of this reaction is the green pigment.

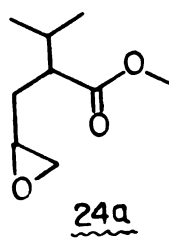
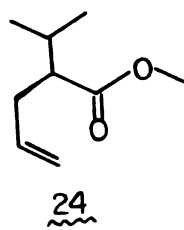
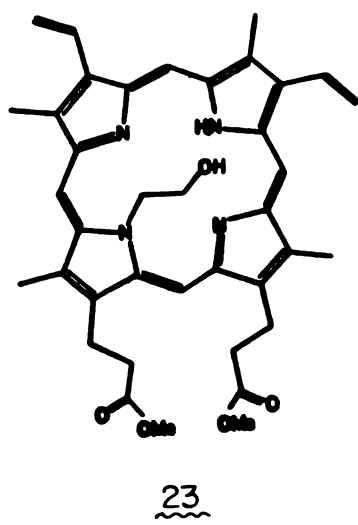
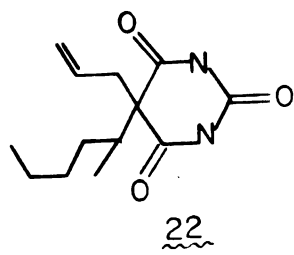
The saturated analog of AIA 21 was found to be ineffective as a destructive agent (Levin et al, 1973), suggesting that metabolism of the double bond is intimately involved in the alkylating event. A number of olefin-containing barbiturates and substituted amides, including secobarbital (22), have been shown to destroy cytochrome P-450 while their

saturated analogs were found to be inactive (Abritti and DeMatteis, 1971; Levin et al, 1972b; Levin et al, 1973). The most conclusive proof that the double bond is the sole determinant of destructive activity was provided by the finding that the simplest olefin, ethylene, is an active destructive agent (Ortiz de Montellano and Mico, 1980b). The implication that the presence of a double bond is in itself sufficient for destructive activity is not entirely correct, however. Structure activity studies indicate that only mono-substituted olefins are efficient destructive agents (Ortiz de Montellano et al, 1979a; Ortiz de Montellano and Mico, 1980b).

Green pigments isolated from animals treated with a variety of olefins share two common characteristics: (a) virtually identical visible absorption spectra and (b), in the absence of secondary chemical reactions, field desorption mass spectral protonated molecular ions equal to the sum of the molecular weights of protoporphyrin IX dimethyl ester plus the substrate plus atomic oxygen (Ortiz de Montellano et al, 1979a, 1980c; Ortiz de Montellano and Mico, 1980b). This formulation, coupled with proton nuclear magnetic resonance studies (Ortiz de Montellano et al, 1981a; section 3.3), shows the pigments to result from covalent attachment of the cytochrome P-450 activated olefin to a pyrrole nitrogen of the porphyrin framework of prosthetic heme. The N-alkylated protoporphyrin IX derivatives owe

their common visible light absorption spectra to alterations in the porphyrin electronic structure caused by N-alkylation, a phenomenon essentially independent of the alkylating functionality.

The structure of the pigment isolated from the livers of rats treated with ethylene is N-(2-hydroxyethyl)-protoporphyrin IX dimethyl ester (23) (Ortiz de Montellano et al, 1981a; section 3.3). The simplest rationale for its formation is that the epoxide metabolite is formed via oxygen transfer from iron-bound activated oxygen and that it subsequently alkylates a pyrrole nitrogen of heme. Evidence accumulated in this laboratory argues against this interpretation. It is now clear that epoxides with access to the active site of the enzyme are ineffective as destructive agents. In fact, it has been shown that the epoxide 24a of a known destructive agent (methyl-2-isopropyl-4-pentenoate) 24 actually inhibits the destruction mediated by the olefin. The destruction of cytochrome P-450 by AIA has been shown to be a suicidal process, indicating that the a short-lived, enzyme-bound intermediate is the reactive species (Ortiz de Montellano and Mico, 1981c). Thus, it appears that a reactive intermediate prior to epoxide formation is the actual destructive entity.



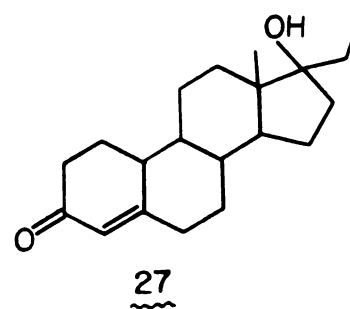
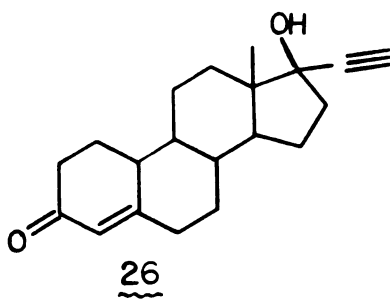
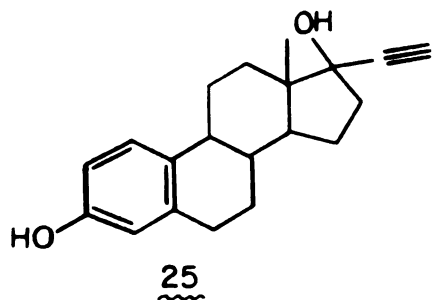


## CHAPTER II

## DESTRUCTION OF CYTOCHROME P-450 BY ACETYLENES

2.0 INTRODUCTION

The ability of 17-alpha-ethynyl-beta-hydroxy sterols to reduce hepatic cytochrome P-450 levels was first noted by Mackinnon et al (1975), who showed that administration of the oral contraceptive steroid ethynyl estradiol 25 to rats resulted in 20% loss of spectroscopically observable hepatic cytochrome P-450 as well as in a five-fold decrease in microsomal N-demethylase activity (Mackinnon and Simon, 1975; Mackinnon et al, 1978). These results were confirmed and extended by White and Muller-Eberhard (1977) in studies of the effects of the oral contraceptive sterols ethynyl estradiol 25, norethisterone 26, and norethandrolone 27 on hepatic cytochrome P-450 levels in vitro and in vivo.



Norethisterone and ethynyl estradiol were found to cause significant losses of spectroscopically observable cytochrome P-450 both in vivo and in vitro. Norethisterone was appreciably more effective in vivo than ethynyl estradiol and marginally so in vitro. Norethandrolone, the non-acetylene containing sterol, was essentially inactive in both systems. Time course experiments in vivo indicated that minimum enzyme levels were obtained within two hours when the sterols were injected intraperitoneally. By twenty-four hours cytochrome P-450 levels had returned to normal. Dramatic increases in mitochondrial ALA synthetase activity, the rate limiting step in heme biosynthesis, and total liver porphyrins, indicating an acceleration in hepatic heme biosynthesis, accompanied the decrease of cytochrome P-450. No change in the microsomal hemoprotein cytochrome b5 was observed.

The reduction of cytochrome P-450 levels in vitro, by norethisterone, was concentration dependent and required the presence of NADPH and oxygen, the two cofactors required for catalytic turnover of the enzyme. The loss of cytochrome P-450 was essentially complete in fifteen minutes at a nominal substrate concentration of 1 mM. The absence of NADPH, or its replacement by NADH in the incubation mixture resulted in no loss of cytochrome P-450 (Table 1). The destructive process also required oxygen, as evidenced by the fact that incubations under an atmosphere of nitrogen or of

TABLE 1

DESTRUCTION OF CYTOCHROME P-450 BY NORETHISTERONE IN VITRO  
 COFACTOR REQUIREMENTS AND THE EFFECT OF INDUCING AGENTS\*

<u>INDUCING AGENT</u>	<u>CONDITIONS</u>	<u>PERCENT LOSS AT 15 MIN.</u>
NONE	COMPLETE	20
3MC	COMPLETE	0
PCN	COMPLETE	15
PB	COMPLETE	31
PB	NITROGEN ATMOSPHERE	6
PB	CARBON MONOXIDE	2
PB	NO NADPH	-10**
PB	NADH NO NADPH	-7**

\* Data from White and Muller-Eberhard (1977)

\*\* No explanation is given by the authors for these high values.

80% carbon monoxide in air exhibited unchanged levels of the enzyme. These results suggest that enzyme loss occurs as a consequence of cytochrome P-450 catalyzed oxidation of norethisterone.

The fraction of cytochrome P-450 susceptible to destruction in vitro was found to be a function of pretreatment of the animals with chemical inducing agents (Table 1). Microsomes from phenobarbital induced animals are enriched in labile forms of the enzyme when compared with those isolated from untreated or pregnenolone-16-alpha-carbonitrile (PCN) treated animals. The isozymes present in 3MC treated animals were resistant to the destructive effects of the sterol. Thus only certain forms of the enzyme, especially those induced by phenobarbital pretreatment, are prone to destruction by norethisterone, a result strongly reminiscent of the selectivity of enzyme loss observed with AIA.

An even stronger link between the ethynyl sterol and olefin provoked losses is the fact that the livers of animals treated with norethisterone or ethynyl estradiol, but not norethandrolone, estradiol or progesterone, contain green pigments with visible absorption spectra almost identical to those isolated from olefin treated animals (White and Muller-Eberhard, 1977). The destructive effects of olefins and 17-alpha-ethynyl sterols are, thus, remarkably similar in a number of respects, including isozyme specificity, cofactor requirements, ALA synthetase stimulation, and

the ability to cause formation of abnormal hepatic pigments.

The similarities between olefin and ethynyl sterol mediated losses of cytochrome P-450 suggested to us that they may share similar mechanistic origins. The fact that AIA mediated cytochrome P-450 destruction involves covalent attachment of the destructive agent to prosthetic heme had recently been established by members of this laboratory (Ortiz de Montellano et al, 1978). The critical experiment involved the demonstration that radiolabeled AIA becomes covalently bound to prosthetic heme to form the green pigments. The observation that the ethynyl sterols norethisterone and ethynyl estradiol also cause the formation of green pigments was consistent with their activation to a species which alkylates prosthetic heme. If this hypothesis is correct elements of the offending sterols should be incorporated into the green pigments resulting from their administration. This possibility has been examined by radioactive assay of the green pigments isolated from rats treated with radiolabeled norethisterone.

### 2.1 DESTRUCTION OF CYTOCHROME P-450 BY NORETHISTERONE: COVALENT ATTACHMENT OF THE STEROL TO PROSTHETIC HEME

The generation and purification of pigments from norethisterone treated animals was achieved by modification of procedures developed in this (Ortiz de Montellano et al,

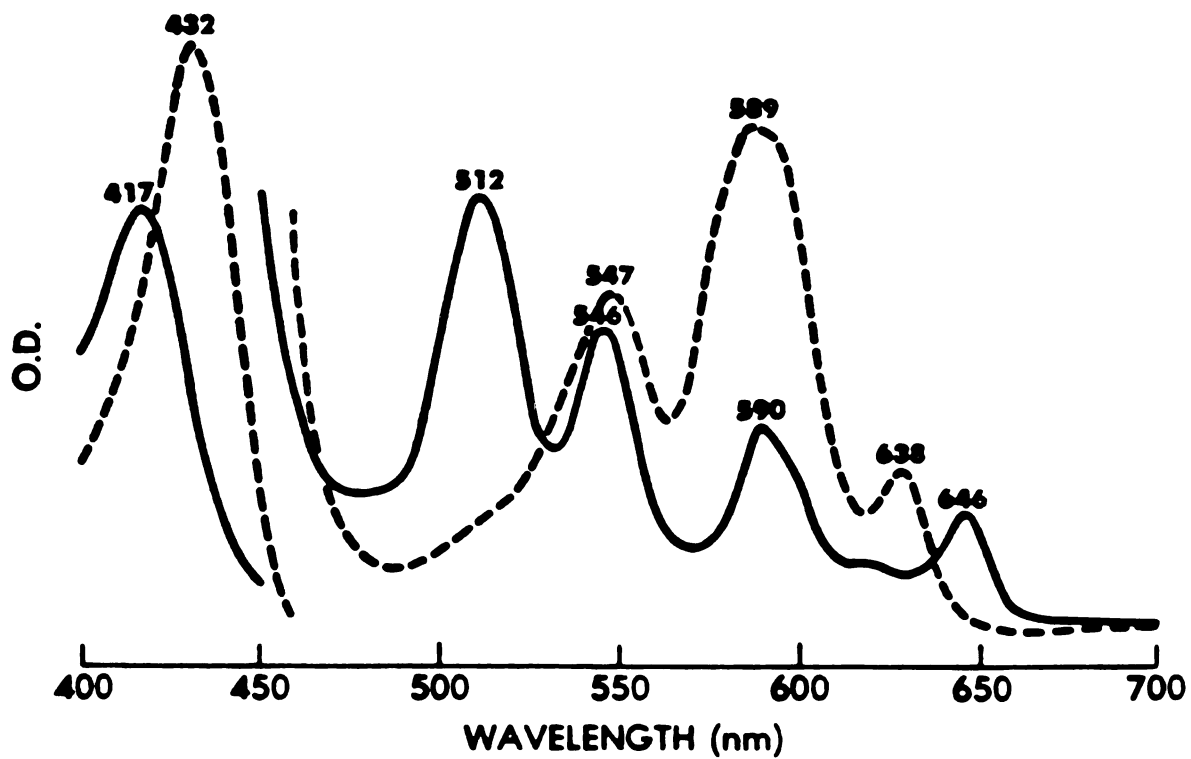
1978) and other laboratories (White and Muller-Eberhard, 1977; Unseld and DeMatteis, 1976). Male Sprague-Dawley rats induced with phenobarbital were treated with norethisterone (100 mg/kg) by intraperitoneal injection of the agent in trioctanoin. Four hours after administration of the sterol the animals were sacrificed and their livers perfused in situ with cold isotonic saline. No visible alteration in color of the perfused livers was observed due to this treatment. The livers were homogenized in acidic methanol and left overnight at 4°C in the dark. This procedure converts the pigments to the metal-free dimethyl esterified porphyrins (Ortiz de Montellano et al, 1978). The porphyrins were extracted into chloroform by addition of equal volumes of water and chloroform to the filtered methanol solution. The chloroform layer was washed with additional volumes of water until the aqueous layer was neutral. The organic layer was dried with anhydrous sodium sulfate, filtered, and stripped of solvent. The brown residue was applied to preparative silica plates and chromatographed in a 2:1 mixture of chloroform and acetone. The desired pigments ( $R_f=0.4-0.6$ ) were readily identified on the plate by their characteristic red fluorescence under 365 nm light and green color under normal light. The pigments were eluted from the silica with acetone. Due to adventitious complexation of metals from the thin layer plates an acidic methanol method, based on a literature procedure (With et al, 1976), was developed to remove these chelated contaminants (section 4.24). The

ready incorporation of metals into the green pigments, once understood, proved to be advantageous in the purification of these porphyrins.

The pigments were purified by normal phase high pressure liquid chromatography. The metal-free pigment was resolved into two component peaks by this technique. The electronic absorption spectra in chloroform of the two, presumably isomeric, porphyrins were found to be identical. Figure 5 (solid line) shows the spectra of a mixture of the two metal-free porphyrins. The zinc complexes were readily generated by the addition of a small amount of a saturated solution of zinc acetate in chloroform/methanol. The visible absorption spectra of the two zinc-complexed porphyrins were identical (see Figure 5, dashed line, for a representative spectrum). Once the two metal-free porphyrins were eluted from the column, the mobile phase (hexane/THF/methanol, 10:3:1) was changed to a more polar system (methanol/THF, 4:1) and another porphyrin eluted which exhibited a visible absorption spectrum identical to that of the zinc-complexed pigment. This tentative identification, confirmed by chromatographic comparison with authentic zinc-complexed pigment, indicated the unwelcome presence of zinc on the column, presumably due to contamination by previous samples. The two metal free porphyrins were converted to the zinc forms and found to co-elute on the HPLC system. Finally, each of the two zinc-complexed por-

FIGURE 5

## ELECTRONIC ABSORPTION SPECTRA OF THE NORETHISTERONE PIGMENT



Electronic absorption spectra of the metal-free (solid line) and zinc-complexed (dotted line) norethisterone adduct in chloroform. The longwavelength region has been amplified ten-fold.



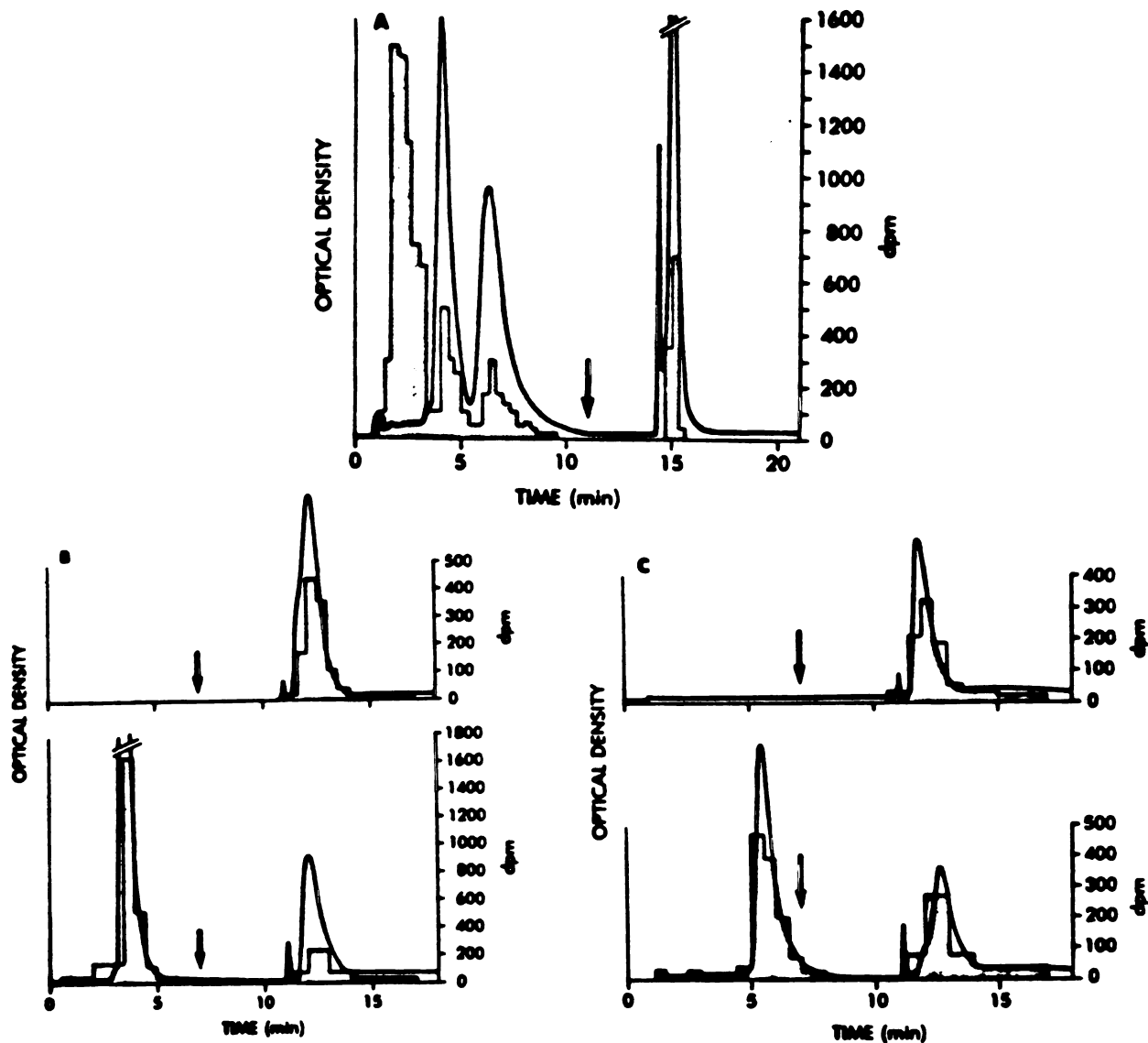
phyrins was demetalated in acidic methanol and rechromatographed to show that the two metal-free porphyrins were non-interconvertible in the acidic conditions used for pigment isolation and demetalation.

#### Incorporation of Radiolabeled Norethisterone into the Green Pigments

Specifically labeled (9,11-<sup>3</sup>H) norethisterone was administered to phenobarbital induced rats and the pigments isolated as previously detailed. The tritiated norethisterone, a gift from Syntex, was purified by thin layer chromatography and diluted with cold sterol to a final specific activity of 0.220 mCi/mmol before use. The 9 and 11 positions are known to be stable to exchange reactions (Kappus and Bolt, 1976; Hanasono and Fisher, 1974).

Figure 6 (panel A) shows the HPLC elution pattern of radioactivity and pigments from the sample first purified by thin layer chromatography. Four chromophoric (detector set at 417 nm) compounds, the two metal-free pigments and the two unresolved zinc complexes, were eluted from the column. The eluent was collected in small fractions and assayed for radioactivity content by liquid scintillation counting in Aquasol. The amount of radioactivity present in each fraction is depicted by the shaded regions (Figure 6). The first radioactive peak contained norethisterone, which is transparent to visible light. The two metal-free pigments

HPLC ANALYSIS OF THE PIGMENTS ISOLATED  
FROM RATS TREATED WITH 9,11-<sup>3</sup>H - NORESTHISTERONE



The pigments were chromatographed on a Whatman Partisil 10-PAC column eluted first with hexane/THF/methanol 10:3:1, followed by (arrow) methanol/THF, 4:1. The curve is the absorbance at 417 nm; the bars indicate the eluted radioactivity in dpm. (A) Crude methylated pigment after prepurification by thin-layer chromatography and demetalation. (B) Reanalysis of the first chromophoric peak (from A), before (lower) and after (upper) addition of zinc acetate. (C) Reanalysis of the second chromophoric peak from A before (lower) and after (upper) addition of zinc acetate.

were both found to contain significant amounts of tritium. Aliquots of the two purified metal-free pigments were treated with zinc acetate and injected onto the column. The shift in retention time due to zinc complexation was coincident with the shift in radioactivity (Figure 6; panel B, top and panel C, top). The two zinc complexes were demetalated and the metal-free porphyrins chromatographed and assayed for radioactivity to confirm the covalent association of pigment and sterol (Figure 6; panels B and C, bottom).

These results establish that elements of norethisterone are incorporated into the hepatic green pigments resulting from its administration to rats. Furthermore, it is now evident that two chromatographically distinct porphyrins are formed during the destructive process. The presence of additional isomers cannot be excluded. The amount of radioactivity associated with each metal-free and zinc-complexed porphyrin was found to be proportional to the total absorbance of the sample. Since the specific activity of the norethisterone used is known (0.220 mCi/mmol) an extinction coefficient for the green pigments may be calculated if one assumes that one molecule of norethisterone is bound to each pigment molecule. The Soret transition (432 nm) extinction coefficient of the zinc-complexed pigments has thus been calculated and found to be between of 123,000 to 125,000 liter mole<sup>-1</sup> cm<sup>-1</sup>. The extinction coefficient of

the metal-free porphyrin Soret transition (417 nm) is 116,000 to 118,000 liter mole<sup>-1</sup> cm<sup>-1</sup>.

The relative intensities and positions of the visible transitions observed in the electronic absorption spectra of the metal-free and zinc-complexed porphyrins are essentially identical to those in the corresponding spectra of the AIA adduct (Ortiz de Montellano et al, 1978). The AIA adduct has been explicitly shown to result from covalent attachment of elements of AIA to the heme prosthetic group of cytochrome P-450 (see section 1.42 for discussion and references). Destruction of cytochrome P-450 by AIA and norethisterone has been shown to require catalytic processing of the substrate by the enzyme. The fact that glutathione does not attenuate the destructive process (White and Muller-Eberhard, 1977) indicates that a short-lived reactive intermediate generated during oxidation of these two compounds is responsible for the destructive interaction. The close analogy between sterol- and AIA-mediated destruction and pigment formation provides strong evidence that the norethisterone pigments also originate from the prosthetic heme.

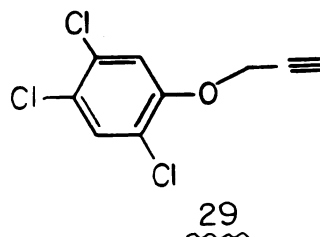
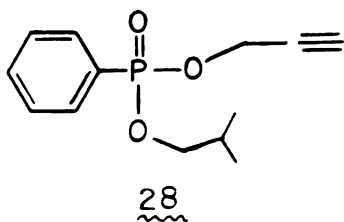
## 2.2 IN VITRO DESTRUCTION OF HEPATIC CYTOCHROME P-450 BY ACETYLENES

Norethisterone reduces hepatic cytochrome P-450 levels in vitro by a process which requires catalytic turnover of

the enzyme and which favors those forms of the enzyme induced by phenobarbital (White and Muller-Eberhard, 1977). We have shown that the green pigments formed during the destructive process are composed of elements of norethisterone and heme, the latter almost surely contributed by the enzyme itself (Ortiz de Montellano et al, 1979b). Destruction of the enzyme and green pigment formation are therefore inextricably linked since they both reflect the same event.

What portion of the sterol structure is required for enzyme destruction to occur? The results of White and Muller-Eberhard (1977) suggested that the sterol D ring 17-alpha-ethynyl-17-beta-hydroxy structure is the offending functionality since only the sterols containing this assembly were effective destructive agents. Oxidative metabolism at this position has been demonstrated for norethisterone (Palmer et al, 1969), norgestrel (Sisenwine et al, 1973;1974;1979) and ethynyl estradiol (Williams and Williams, 1975; Abdel Aziz and Williams, 1969) although the complicity of cytochrome P-450 in these reactions has not been established. Additional evidence localizing the destructive potential of the

sterols at the propargylic functionality has been provided by Skrinjaric-Spoljar et al (1971), who found that 2-propynyl phenyl phosphonate (28) and 2-(2,4,5-trichlorophenyl)- propynyl ether (29) cause measurable loss of hepatic cytochrome P-450 when administered to mice.



In order to more precisely define the structural requirements of the sterol mediated destruction process a series of acetylene containing compounds were examined for their ability to reduce hepatic cytochrome P-450 present in microsomes isolated from phenobarbital induced male Sprague-Dawley rats. This model system was used since the participation of cytochrome P-450 in its own destruction is easily determined by addition or deletion of the cofactors required for catalytic turnover of the enzyme.

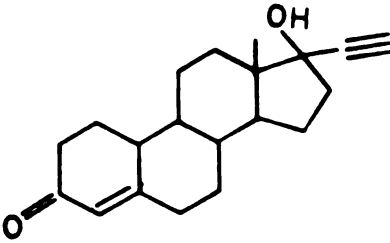
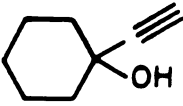
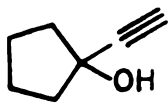
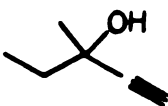
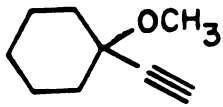
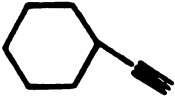
The assay for NADPH and substrate dependent destruction of cytochrome P-450 was developed in this laboratory and is described in detail in the experimental section. The dependent variable in these experiments was the concentration of cytochrome P-450 measured spectrophotometrically at 450

nanometers as the ferrous carbonyl complex. The assay solutions consisted of microsomal protein (1 mg/ml), EDTA (1.5 mM), and potassium chloride (150 mM) all in 0.1M phosphate buffer (pH 7.4). Each substrate was examined for its ability to decrease spectroscopically observable cytochrome P-450 in the presence and in the absence of 1mM NADPH. All substrates, except propyne, were added to the incubation mixture as the neat liquid or solid and were preincubated for 10 minutes at 37°C prior to initiation of the reaction with NADPH. Aliquots of the incubation mixtures were removed at specified time points and their cytochrome P-450 content measured by difference spectroscopy on an Aminco DW-2 spectrophotometer. The reference cuvette contained the carbon monoxide-saturated microsomal solution plus substrate. The sample cuvette held the NADPH-containing, carbon monoxide saturated, dithionite reduced solution. The substrate concentration was nominally 1mM although complete dissolution of the substrates in the microsomal solutions was not always possible. Agents which were ineffective at a concentration of 1 mM were also tested at 10 mM. Control experiments were also conducted to insure that no NADPH dependent losses of cytochrome P-450 occurred in the absence of substrate.

A total of twenty acetylenic compounds were tested for their ability to destroy microsomal cytochrome P-450 in this in vitro assay system. The results of these studies are

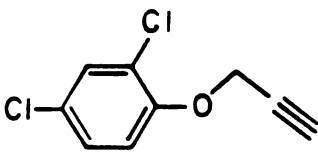
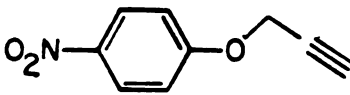
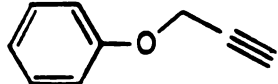
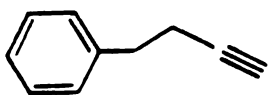
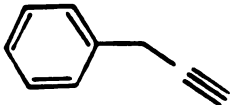
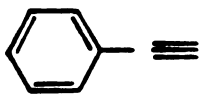
TABLE 2

IN VITRO DESTRUCTION OF CYTOCHROME P-450 BY ACETYLENES

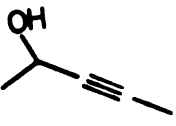
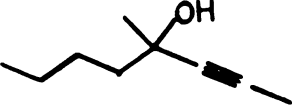
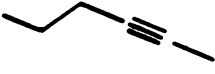
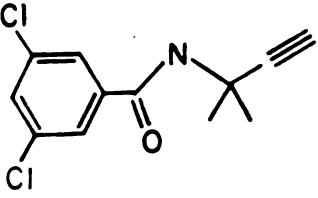
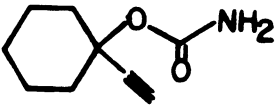
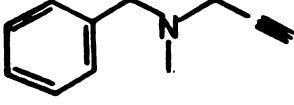
<u>SUBSTRATE</u>	<u>PERCENT LOSS OF CYTOCHROME P-450</u>		
	<u>10 min.</u>	<u>20 min.</u>	<u>30 min.</u>
 <u>26</u> *	20±5	25±2	27±3
 <u>30</u> *	18±6	22±6	26±6
 <u>31</u> *	18±3	22±4	29±3
 <u>32</u>	17	24	34
 <u>33</u>	22±5	29±6	30±6
 <u>34</u>	19±2	23±4	23±4



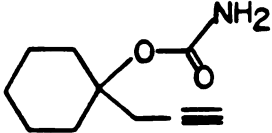

IN VITRO DESTRUCTION OF CYTOCHROME P-450 BY ACETYLENES

<u>SUBSTRATE</u>	<u>PERCENT LOSS OF CYTOCHROME P-450</u>		
	<u>10 min.</u>	<u>20 min.</u>	<u>30 min.</u>
 <u>35</u> *	21±6	23±4	24±3
 <u>36</u> *	19±10	23±11	30±4
 <u>37</u> *	25±3	31±4	34±2
 <u>38</u> *	29±3	49±4	52±3
 <u>39</u> *	12±6	24±7	34±1
 <u>40</u> *	18±3	25±2	27±2

IN VITRO DESTRUCTION OF CYTOCHROME P-450 BY ACETYLENES

<u>SUBSTRATE</u>	<u>PERCENT LOSS OF CYTOCHROME P-450</u>		
	<u>10 min.</u>	<u>20 min.</u>	<u>30 min.</u>
 <chem>CC(O)C#C</chem>	24±7	33±10	35±8
<u>41</u>			
 <chem>CCCC(C)(O)C#C</chem>	35±4	45±3	47±1
<u>42</u> **			
 <chem>CCCC#C</chem>	27±3	34±5	36±5
<u>43</u> **			
 <chem>CC(C)(C#C)N(C(=O)c1cc(Cl)cc(Cl)c1)C(=O)N</chem>	19±5	30±2	32±3
<u>44</u>			
 <chem>NC(=O)OC1(C#C)CCCC1</chem>	3±4	6±4	6±5
<u>45</u>			
 <chem>NC(=O)OC1(C#C)CCCC1</chem>	0±2	2±2	3±5
<u>46</u>			

IN VITRO DESTRUCTION OF CYTOCHROME P-450 BY ACETYLENES

<u>SUBSTRATE</u>	<u>PERCENT LOSS OF CYTOCHROME P-450</u>	
	<u>15 min.</u>	<u>30 min.</u>
 <chem>NC(=O)OC1CCCCC1</chem>	28±4	29±4
<u>47</u>		
 <chem>C#C</chem>	48±2	56±2
<u>48</u> *		

The substrate concentrations were nominally 1 mM except for 40 (10 mM), 44 (10 mM), and 48 (passed over the incubation mixture at a concentration of 10% in air). The values given are the averages of at least three determinations (standard deviations given in parenthesis) with the exception of 32 which was tested only once.

\* These compounds, when administered to rats, caused the accumulation of hepatic green pigments.

\*\* These compounds were found not to cause accumulation of green pigments in vivo.

presented in Table 2. Norethisterone (26) was found to destroy approximately 27% of the cytochrome P-450 found in the microsomes of phenobarbital pretreated rats. No loss of cytochrome P-450 was observed when the steroid was incubated with microsomes in the absence of NADPH. This result is in agreement with the finding of White and Muller-Eberhard (1977) and indicates that the sterol-mediated destruction requires catalytic turnover of the enzyme. White and Muller-Eberhard also found that maximal destruction was observed at a sterol concentration of 0.75 mM even though the sterol was incompletely dissolved at a nominal concentration of 0.1mM. In our hands, increasing the nominal concentrations of the sterol to as much as 10 mM did not increase the amount of destruction, indicating that sufficient concentrations of the sterol were available to the enzyme when a preincubation time of 10 minutes was used. Maximal destruction of the enzyme was obtained within 30 minutes. Addition of more NADPH did not increase the amount of destruction, indicating that reducing equivalent availability was not limiting the overall amount of destruction.

Ethynyl cyclohexanol (30) and ethynyl cyclopentanol (31) were found to destroy the enzyme to the same extent as the sterol 26. These results indicate that the steroid assembly is not necessary for destructive activity. Studies presented in the next section show that both of these compounds initiated hepatic green pigment accumulation in vivo.

The acyclic propargylic alcohol 3-methyl-1-pentyn-3-ol (31) was also found to destroy the enzyme. This confined the destructive potential of the sterol to the propargylic alcohol portion of the D ring. The methyl ether of ethynyl cyclohexanol 33 was then tested and was also found to deplete the enzyme. Destruction thus does not require a free hydroxyl group, nor does it require, as witnessed by the destructive ability of 34, the presence of an oxygen at all. Exposure of the microsomes to propyne gas, furthermore, also resulted in NADPH dependent destruction of the enzyme. A similar finding by White (1979) for acetylene gas terminated our search for the minimal structural requirement for destructive activity.

The series of terminal acetylenes examined in this study were all active destructive agents in vitro. In an effort to further define the destructive potential of the acetylene triple bond, three disubstituted acetylenes, 3-pentyn-2-ol (41), 4-methyl-2-octyne-4-ol (42), and 2-hexyne (43) were evaluated in the microsomal system and found to be effective destructive agents. Thus the acetylenic hydrogen present in the terminal acetylenes is not required for destruction.

The three phenyl propargyl ethers 3-phenoxy-1-propyne (37), 3-(2,4-dichlorophenoxy)-1-propyne (35), and 3-(4-nitrophenoxy)-1-propyne (36) belong to a class of compounds known to potentiate the effects of drugs and insecticides

(Fellig et al, 1970; Sacher et al, 1968). In particular, Skrinjaric et al (1971) showed that 3-(2,4,5-trichlorophenoxy)-1-propyne (29) causes an in vivo decrease in mouse hepatic cytochrome P-450. The fact that the three aryl-propargyl ethers tested in this study decrease cytochrome P-450 levels in vitro by a process requiring catalytic turnover of the enzyme suggests a common mechanism for the synergistic effects of acetylenic agents such as the propargyl phosphonates (Casida, 1970), alkynyl phthalimides (Neumeyer and Incho, 1969) and propargyl oximes (Casida, 1970).

4-Phenyl-1-butyne (38) and 3-phenyl-1-propyne (39) were found to reduce microsomal cytochrome P-450 levels when present at nominal 1mM concentrations. Phenyl acetylene (40), on the other hand, was only marginally active (10% loss) at this concentration. However, increasing the concentration of phenyl acetylene to 10 mM resulted in an increased amount of NADPH dependent destruction (27% in 30 minutes). The reduced amount of destruction at 1mM concentrations of this agent was found not to be due to depletion of NADPH.

The three drugs other than norethisterone examined in this study were ethinamate (45) and hexapropymate (47), both sedative hypnotic agents, and pargyline (46), a mono-amine oxidase inhibitor. Ethinamate and pargyline were both ineffective destructive agents even at 10 mM concentrations.

These two compounds have the distinction of being the only two acetylenic agents tested which were ineffective destructive agents in our assay system. Similar results have recently been reported for pargyline (White, 1980). Since metabolism of the triple bond would appear to be involved in the destructive process, it is conceivable that these agents are ineffective due to the fact that alternative sites are processed by the monooxygenase system instead of the triple bond. Pargyline has been shown to undergo monooxygenase catalyzed N-dealkylation to give propionaldehyde (Shirota, 1979). Ethinamate is known to be hydroxylated on the cyclohexyl ring (McMahon, 1958) and to undergo slight hydrolysis of the amide linkage (Murata, 1964) in vivo. Amide hydrolysis of ethinamate would give the destructive agent ethynyl cyclohexanol. No evidence is known to us which demonstrates that either pargyline or ethinamate undergoes cytochrome P-450 dependent metabolism of the triple bond. The closely related homolog of ethinamate, hexapropymate (47) was found to cause significant (30%) destruction of cytochrome p-450. Hexapropymate and ethinamate differ in structure by a single methylene unit. How such a small difference in structure could so drastically affect the relative potencies of these two compounds is unclear at this time.

Eighteen of the twenty acetylenic agents examined in this study have been shown to cause a time dependent loss of

the cytochrome P-450 isozymes present in microsomes isolated from phenobarbital induced rats. The loss of cytochrome P-450 is only observed when NADPH is present in the incubation mixture, indicating that catalytic turnover of the enzyme is required for destruction. These results suggest that a compound containing an acetylene group will, in all probability, destroy a portion of hepatic cytochrome P-450 when administered to rats. In the absence of more data it is not possible to extrapolate these results to other mammalian systems. The results of White and Muller Eberhard (1977) suggest that destruction of cytochrome P-450 does occur in untreated animals, leading to the possibility that the constitutive isozyme population in uninduced liver is also susceptible to the effects of norethisterone. Separate studies conducted in this laboratory have shown that the forms of cytochrome P-450 present in 3-MC induced rat liver are resistant to the destructive effects of ethynyl cyclopentanol (Ortiz de Montellano et al, 1981f).

### 2.3 CHARACTERIZATION OF THE TERMINAL ACETYLENE-PROSTHETIC HEME ADDUCTS

The destruction of cytochrome P-450 by norethisterone has been shown to result in the formation of at least two green pigments. These pigments are the products of an alkylative sequence in which the metabolically-activated



sterol becomes bound to the prosthetic heme group of the enzyme (Section 2.1; Ortiz de Montellano et al, 1979b). The fact that eighteen acetylene-containing compounds destroy cytochrome P-450 in vitro by a process which requires catalytic turnover of the enzyme indicates that metabolism of the triple bond is somehow involved in the destructive event. White (1979) has shown that acetylene itself depletes cytochrome P-450 levels in vivo and in vitro and that the loss of cytochrome P-450 in vivo is marked by an equimolar loss of microsomal heme and by the accumulation of green pigments. Since elements of norethisterone are incorporated into the green pigments formed in vivo it is reasonable to postulate that portions of other destructive agents also become bound to prosthetic heme. This hypothesis, if true, leads to the conclusion that the structures of the green pigments must, in some manner, bear the imprint of the alkylating event. The following studies outline the methods we have developed to further characterize the green pigments and the results of these studies.

### 2.31 GREEN PIGMENT FORMATION AND PURIFICATION: A STUDY OF FOURTEEN ACETYLENES

Fourteen of the acetylenes known to destroy cytochrome P-450 in vitro were examined for their ability to cause the formation of green pigments in vivo. The compounds tested in these studies are identified in Table 3. Green pigments

were found to accumulate in the livers of animals treated with each of the terminal acetylenes studied. No pigments, however, could be found in the livers of animals treated with the internal acetylenes 2-hexyne (43) and 4-methyl-2-octyn-4-ol (42) even though appreciable losses of cytochrome P-450 were observed in vitro. Similar results have been obtained from studies of three allenes which were found to destroy equal amounts of heme and cytochrome P-450 in vitro but not to cause the formation of green pigments in vivo. (Ortiz de Montellano and Kunze, 1980d). The remaining internal acetylene, 4-hydroxy-2-pentyne (41), proved to be toxic to the animals, producing almost immediate convulsions and death even at low (20 mg/kg) doses.

Purification of the hepatic pigments present in the terminal acetylene-treated animals included a minimum of three chromatographic steps. The livers of treated animals, after perfusion with isotonic sodium chloride and homogenization, were treated with acidic methanol to denature the protein, to esterify the porphyrin carboxyl groups, and to remove the iron from the pigments. The pigments were then extracted into chloroform, converted to the zinc complexes, and applied to silica plates. Insertion of zinc into the porphyrins prior to thin layer chromatography was found to circumvent the problem of complexation of trace metals from the plates. The zinc-complexed porphyrins were further purified by high pressure liquid chromatography. The puri-

fied metal complexes were treated with acidic methanol to remove the zinc and the resulting free-base porphyrins subjected to a second purification step by high pressure liquid chromatography (HPLC). The zinc-complexed porphyrins were found to be retained much more avidly by the column than the metal-free pigments. The purification of the zinc-complexed porphyrins efficiently removed from the sample those contaminants co-chromatographing with the free base porphyrins. Conversion of the purified metal complexes to the metal-free forms followed by a second purification on the HPLC column removed the remaining contaminants. With the exception of the acetylene adducts, which became irreversibly bound to the HPLC column in the metal-free state, all of the porphyrins were purified in this manner. Due to the low amounts of pigments obtained (10 to 50 micrograms), trace contaminants introduced by glassware and solvent impurities were always a problem.

Pigments isolated from ethynyl cyclohexanol (30) or ethynyl cyclopentanol (31) treated animals were resolved into two component porphyrins during chromatography of the metal-free porphyrins. In each case the two presumably isomeric porphyrins were obtained in approximately equal amounts and were found to be non-interconvertible upon treatment with acidic methanol. The zinc-complexed pigments could not be separated. It should be noted that the separation of the metal-free ethynyl cyclopentanol pigments could

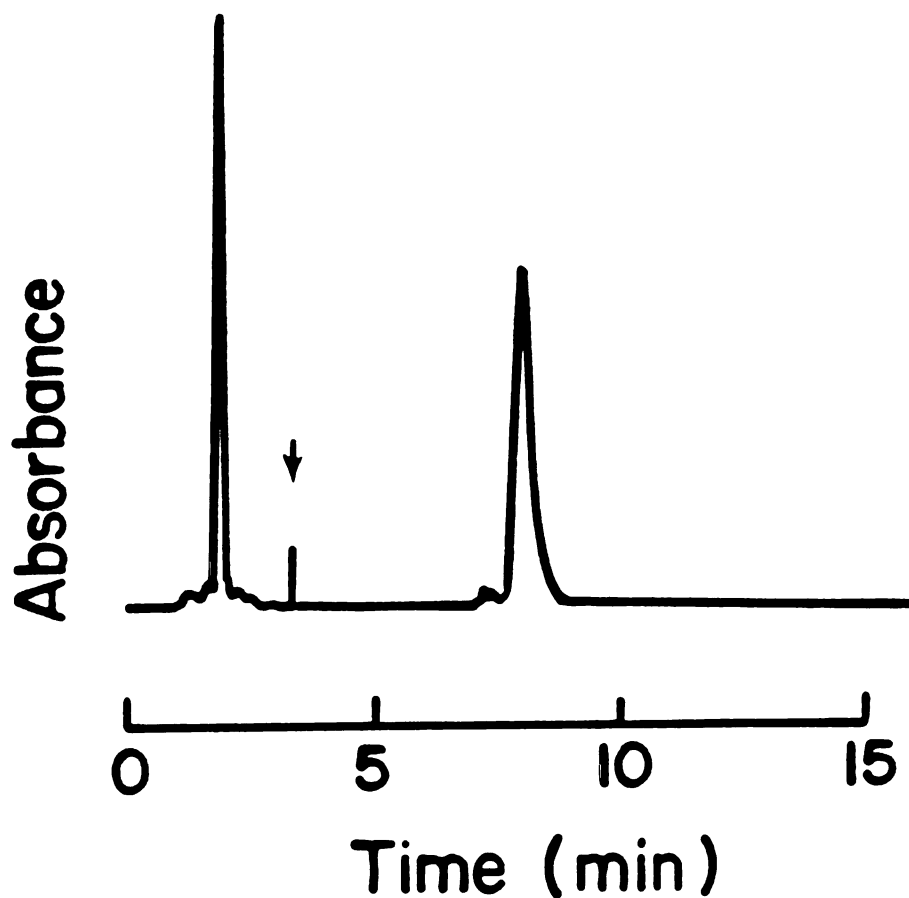
not be duplicated at a later time. Presumably the column had lost its ability to resolve the isomers. It is possible that isomeric porphyrins were also formed by other acetylenic agents. The fact that a pigment is observed as a single chromatographic peak does not provide firm evidence for its identification as a single isomer. As will become evident in later discussions, isomeric porphyrins from a single agent are possible (section 2.42). The pigments isolated from rats treated with the remaining acetylenes were each found to chromatograph as a single peak. The chromatographic profile of a mixture of the metal-free and zinc-complexed pigment isolated from rats treated with 3-phenoxy-1-propyne is shown in Figure 7.

### 2.32 ELECTRONIC ABSORPTION SPECTRA

The electronic absorption spectra of the two norethisterone pigments were found to be identical in both the metal-free and zinc-complexed forms (section 2.1; Figure 5). Moreover, they were indistinguishable from the spectra of the pigment isolated from animals treated with 2-isopropyl-4-pentenamide (AIA). To our astonishment, this similarity was found to extend to the porphyrins isolated from animals treated with each of the acetylenes examined in this study. Representative spectra are provided in Figure 8. Each metal free pigment (the acetylene pigment excepting) exhibited

FIGURE 7

HPLC ANALYSIS OF THE PIGMENT ISOLATED  
FROM RATS TREATED WITH 3-PHENOXY-1-PROPYLENE



A mixture of the metal-free and zinc-complexed pigment was chromatographed on a Whatman 10-PAC column eluted first with hexane/THF/methanol 10:3:1 followed by (arrow) methanol/THF 4:1. The pigments were detected in the eluent by absorbance at 417 nm. The first peak is the metal-free pigment, the second peak is the zinc-complexed pigment.

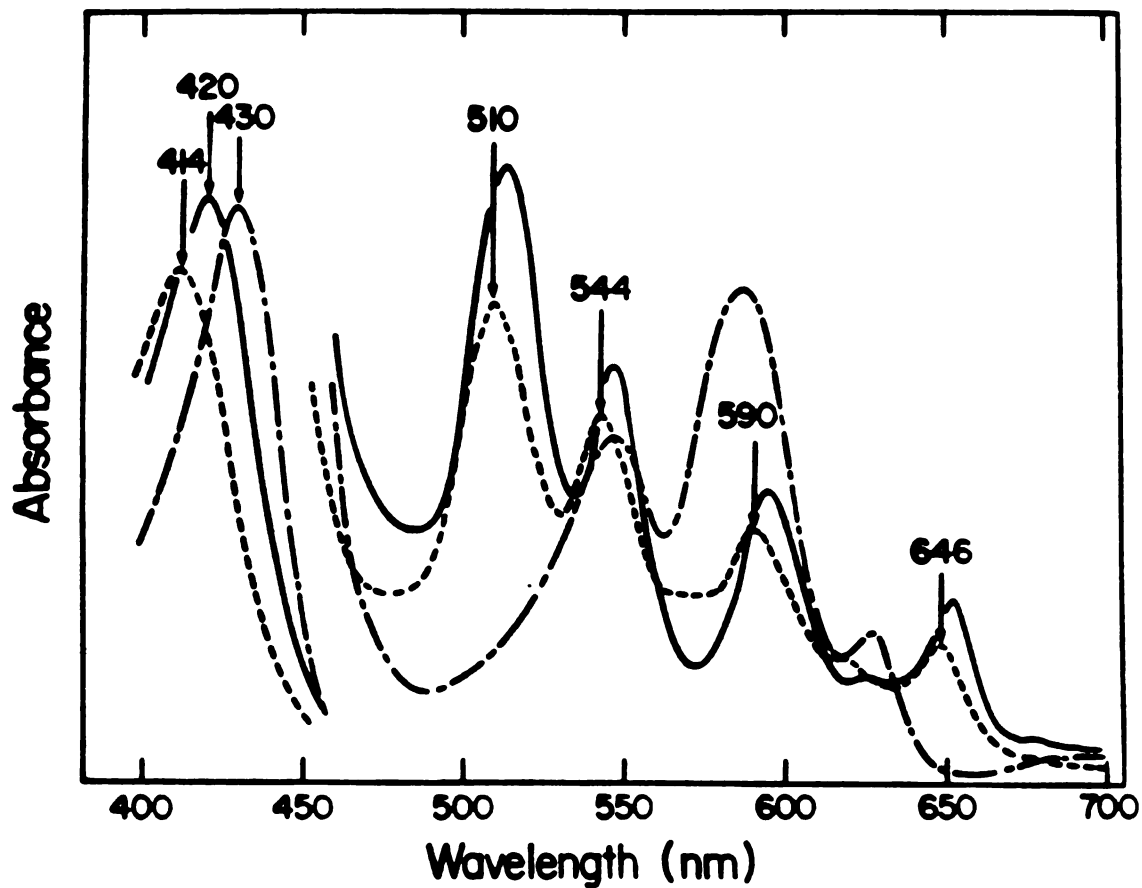
typical etio-type porphyrin spectrum in chloroform solution. These spectra were marked by a Soret absorbance at 418 (+/- 2) nanometers followed by an order of magnitude less intense peaks at 511, 545, 590 and 648 nanometers. The acetylene pigment Soret transition was found at 414 nanometers and is shown in Figure 8. The pattern of absorbances was highly similar to that of protoporphyrin IX dimethyl ester except that each pigment band was red-shifted 10-15 nanometers. The zinc-complexed pigment spectra were again highly similar, exhibiting a Soret absorbance at 430 nanometers and a trio of less intense transitions at 546, 589, and 629 nanometers (Figure 8). The spectrum of the zinc-complexed acetylene pigment was indistinguishable from those of the other pigments. A slight long-wavelength shoulder on the Soret band of the zinc-complexed pigments isolated from rats treated with propyne, phenyl acetylene, 3-phenyl-propyne, and 4-phenyl butyne was also observed.

### 2.33 FIELD DESORPTION MASS SPECTRA

Experiments with radiolabeled norethisterone have established that the pigments isolated from rats treated with this sterol are composed of an alkylated form of protoporphyrin IX plus elements of the destructive agent. The fact that a number of terminal acetylenes, including acetylene itself, are destructive agents in vitro and cause pigment

FIGURE 8

ELECTRONIC ABSORPTION SPECTRA OF  
THE 3-PHENYL-1-PROPYNE AND ACETYLENE PIGMENTS



Electronic absorption spectra in chloroform of (a) the metal-free 3-phenyl-1-propyne pigment (solid line); (b) the metal-free acetylene pigment (dashed line); and (c) the zinc-complexed 3-phenyl-1-propyne pigment. The Soret bands are attenuated ten-fold.

formation in vivo localizes the destructive potential of these compounds on the triple bond. Efforts to further define the structure of the pigments by electron impact and chemical ionization mass spectrometry were unsuccessful, leading only to pyrolysis of the samples. Field desorption mass spectrometry, however, proved equal to the task of getting the pigments airborne and provided a much-needed key to the structural elucidation of the green pigments.

The theory of field desorption mass spectrometry (FDMS) has been reviewed (Beckey and Schulten, 1979) and will not be discussed. This technique provides an important addition to the more traditional methods of sample vaporization and ion generation used in electron impact and chemical ionization mass spectrometry in that it allows the detection of structurally significant ions generated from thermally labile or non-volatile compounds. The application of FDMS to a number of such compounds has been reviewed (Beckey and Schulten, 1979; Burlingame et al, 1980; Schulten, 1979).

Pigments isolated from animals treated with nine terminal acetylenes have been characterized by FDMS studies (Table 3). Each of the metal-free porphyrins desorped from the emitter surface as a variable mixture of the protonated and non-protonated forms. Very little fragmentation was observed, as is often the case in FDMS spectra. The distribution of monoprotinated and non-protonated ions was found to vary with the purity of the sample and the temperature of



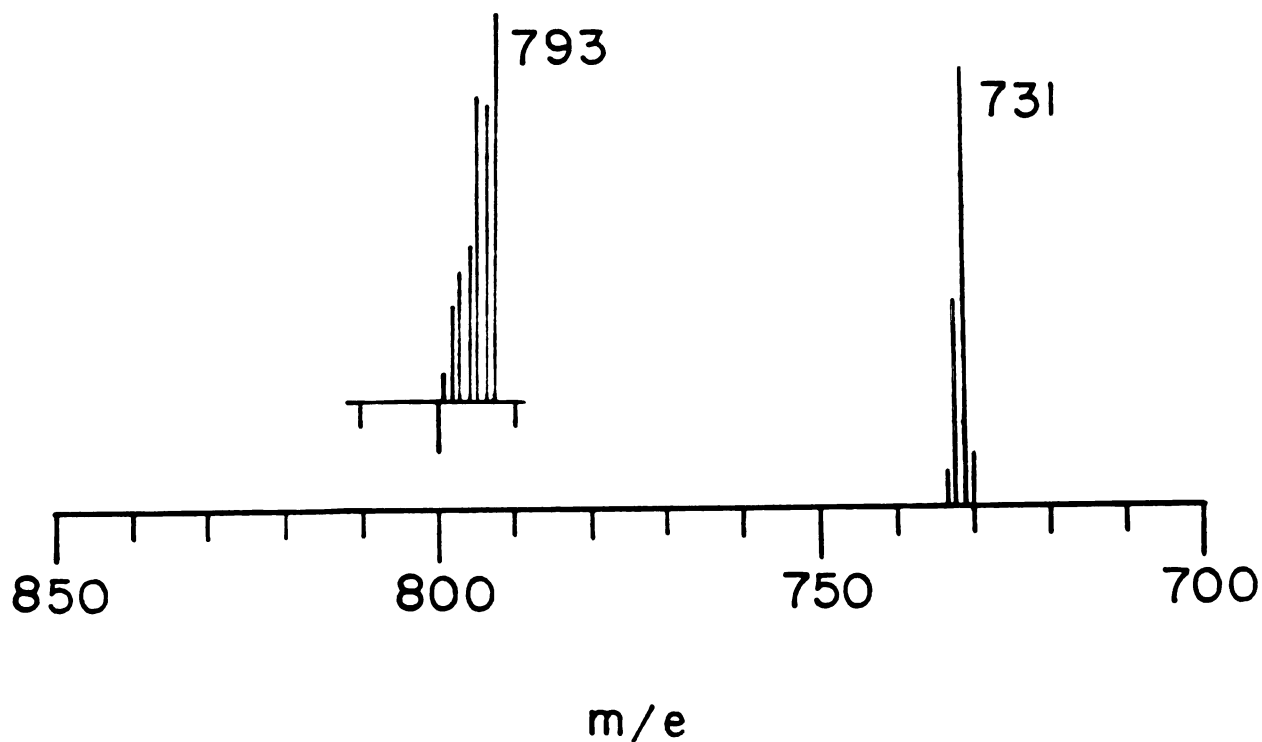
the emitter surface. Preferential formation of the protonated forms was favored by high emitter temperatures and low sample purities. In general, the monoprotonated molecular ion was found to dominate the ion current. Monoprotonated molecular ions are frequently produced by this technique (Derrick, 1977) and have been observed for other porphyrins (Jackson, 1979).

A rendition of the galvanometer tracing of the FDMS spectrum obtained from one of the ethynyl cyclohexanol pigments is shown in Figure 9. The distribution of non-protonated and protonated ions can be clearly seen. Occasionally respectable ion currents of the protonated molecular dimer ( $2M+H^+$ ) were also observed. Detection of these ions on a routine basis was not sought since their measurement required reducing the accelerating voltage, a change which lowers the sensitivity of the instrument, and provided no additional structural information.

FDMS spectra were also obtained from selected zinc-complexed pigments. The pattern of ions obtained from these pigments was that expected from the natural isotopic abundance of zinc ( $^{64}\text{Zn}$ , 49%;  $^{66}\text{Zn}$ , 28%;  $^{67}\text{Zn}$ , 4%;  $^{68}\text{Zn}$ , 18%). The unmistakable cluster of ions observed in the zinc-complexed pigment spectra corresponded only qualitatively to the known distribution of isotopic zinc due to the generally low ion currents obtained from these samples and the high scan to scan variability observed in the spectra, reliable,

FIGURE 9

FIELD DESORPTION MASS SPECTRA OF THE  
METAL-FREE AND ZINC-COMPLEXED ETHYNYL CYCLOHEXANOL ADDUCT



A representation of the galvanometer tracing obtained from the field desorption mass spectra of the metal-free and zinc-complexed pigments (inset) isolated from rats treated with ethynyl cyclohexanol. The remaining high-mass portion of the spectra were featureless. Spectra were obtained on a modified Kratos MS-902 operating at an accelerating voltage of 8.2 KV.

quantitative, ion distributions were not obtainable. Figure 9 shows an FDMS spectrum of the zinc-complex of the ethynyl cyclohexanol pigment.

The metal-free porphyrin molecular ion values are given in Table 3. The major ( $^{64}\text{Zn}$ ) ion mass numbers of the zinc complexed porphyrins are also reported. The two presumably isomeric porphyrins isolated from ethynyl cyclohexanol were separately analyzed and found to give the same pattern of ions. Similar results were obtained for the two pigments isolated from ethynyl cyclopentanol-treated animals. Only one of the norethisterone isomers was examined. The radiolabeling experiment with norethisterone indicated that a portion or all of the sterol is bound to the heme prosthetic group. This result is reinforced by the fact that each distinct acetylene adduct gave a different molecular ion. More precisely, the differences in substrate molecular weight are retained in the differences between the molecular ions. For instance, ethynyl cyclohexanol and ethynyl cyclopentanol differ in molecular weight by 14 mass units. This difference is also observed for the molecular ions of the metal-free and zinc-complexed adducts. The molecular weight of dimethyl-esterified protoporphyrin IX is 590. Subtraction of this value from the molecular weight of each adduct (except norethisterone) as determined from the FDMS data leaves, in each case, a number equal to the sum of the molecular weight of the destructive agent plus 16 mass

TABLE 3

ANALYSIS OF THE TERMINAL ACETYLENE ADDUCTS BY  
FIELD DESORPTION MASS SPECTROMETRY

SUBSTRATE ( $M_R$ )	PREDICTED MOLECULAR ION	MOLECULAR ION	
		METAL-FREE*	$^{64}\text{Zn}$ COMPLEX**
26 (298)	904	886 ( $\text{Na}^+$ )	
30 (124)	730	730 ( $\text{H}^+$ )	793
31 (110)	716	716 ( $\text{H}^+$ )	779
35*** (200)	806	806 ( $\text{H}^+$ )	869
37 (132)	738	738 ( $\text{H}^+$ )	801
38 (130)	736	736 ( $\text{H}^+$ )	799
39 (116)	722	722 ( $\text{H}^+$ )	785
48 (40)	646	646 ( $\text{H}^+$ )	
acetylene (26)	632	632 ( $\text{H}^+$ )	795

\* The porphyrins were usually observed as the monoprotonated molecular ions. One mass unit has been subtracted to give the value reported.

\*\* The most intense ion (that due to the major isotope of zinc,  $^{64}\text{Zn}$ ) is reported.

\*\*\*The isotope pattern due to the presence of two chlorines was observed. The reported value is that of the most intense ( $^{35}\text{Cl}$ ) ion.

units. Thus the molecular ion observed for a given pigment corresponds to the sum of the molecular weights of protoporphyrin IX dimethyl ester plus the substrate plus 16 mass units (Table 3).

The single deviation from this pattern is the norethisterone pigment, which gave an apparent molecular ion at  $m/e$  909. A hypothesis consistent with the formation of this ion is that it is the sodium-complexed, dehydrated adduct. Sodium complexation (cationization) has been observed in FDMS studies (Derrick, 1977) and is a likely possibility in view of the fact that the emitters used in this study were etched in sodium chloride solution. In fact, a steady stream of sodium ions could be observed desorbing from the emitter surface in the mass spectrometer. The loss of 18 mass units (dehydration) may have occurred as a result of the particularly high emitter temperatures required to obtain this spectrum. These harsh conditions were not required for the other metal free pigments. The strongest evidence to support this rationalization remains the fact that the norethisterone adduct is the only pigment which deviates from the previously discussed adduct stoichiometry.

The purified pigments have been shown to exhibit essentially identical electronic absorption spectra and to produce FDMS molecular ions equal to the sum of the molecular weights of protoporphyrin IX dimethyl ester plus the substrate plus 16 mass units. Since aerobic oxidation of the

acetylenes is required for destruction to occur (White and Muller-Eberhard, 1977), and substrate oxidation by cytochrome P-450 terminates in the transfer of atomic oxygen to the substrate, the source of the extra 16 mass units is likely to be atomic oxygen. That the additional 16 mass units are due to oxygen is shown in the next section.

### 2.35 PROTON NUCLEAR MAGNETIC RESONANCE STUDIES

Catalytic processing of terminal acetylenes by cytochrome P-450 isozymes present in phenobarbital induced rat liver is abruptly terminated by alkylation of the heme prosthetic group of the enzyme by a reactive intermediate generated in situ. The alkylated hemes have been isolated by a procedure which removes the iron (DeMatteis, 1978) and methylates the two porphyrin carboxyl groups. Nine of the porphyrins have been purified by high pressure liquid chromatography and analyzed by electronic absorption spectroscopy and field desorption mass spectrometry. The visible absorption spectra of the porphyrins have been shown to be highly similar. FDMS studies have allowed the formulation of an alkylation stoichiometry which clearly establishes incorporation of the destructive agent into each of the green pigments.

The most definite evidence relevant to elucidation of the porphyrin adduct structure has been provided by proton

magnetic resonance studies. Even at high magnetic field strengths (360 MHz) a ten-fold higher amount of the pigments was required for NMR studies than for FDMS studies. Accordingly, the biological reactions were scaled up to deliver 200 to 300 micrograms of pigment.

The first acetylene adduct obtained in sufficient quantity and purity to allow a structural assignment to be made was that obtained with propyne. The 360 MHz NMR of the chloro-zinc complex of this adduct is presented in Figure 10 and discussed more fully in section 3.5. This spectrum provides proof that the various peripheral substituents of heme survive the alkylation reaction and the purification procedure unscathed. All four meso protons (10-10.5 ppm, 4H), the two internal vinyl protons (7.8-8.3 ppm, 2H, 4 lines each proton due to cis and trans coupling with external vinyl protons), the 4 external vinyl protons (6-6.4 ppm, 4 H, 2 lines each), the four methylene protons on the two carbons beta to the carboxyl groups (4.2-4.4 ppm, 4H, vicinal coupled), the six methyl groups (3.5-3.8 ppm, 18H, one methyl per pyrrole ring plus the two ester methyls), and the 4 methylene protons of the carbons alpha to the carboxyl groups (3.2-3.4 ppm, 4H, vicinally coupled) are all accounted for in this spectrum. The apparent molecular weight of the propyne adduct is 646 (Table 3). The proton signals from the 56 mass units remaining after subtraction of 590 due to protoporphyrin IX dimethyl ester are not found

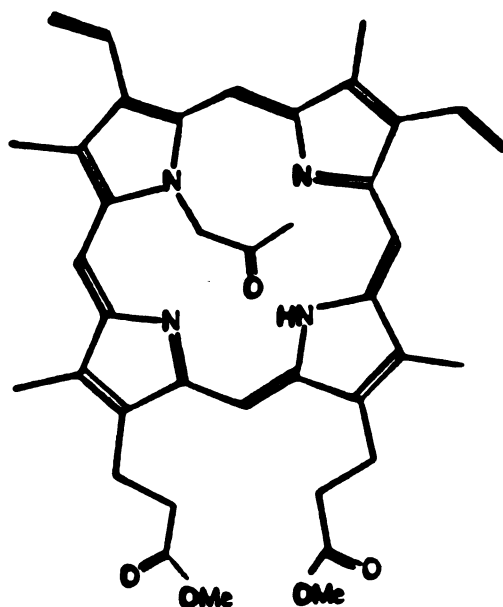
FIGURE 10

NMR SPECTRUM OF THE CHLORO-ZINC COMPLEX  
OF THE PROPYNE PIGMENT

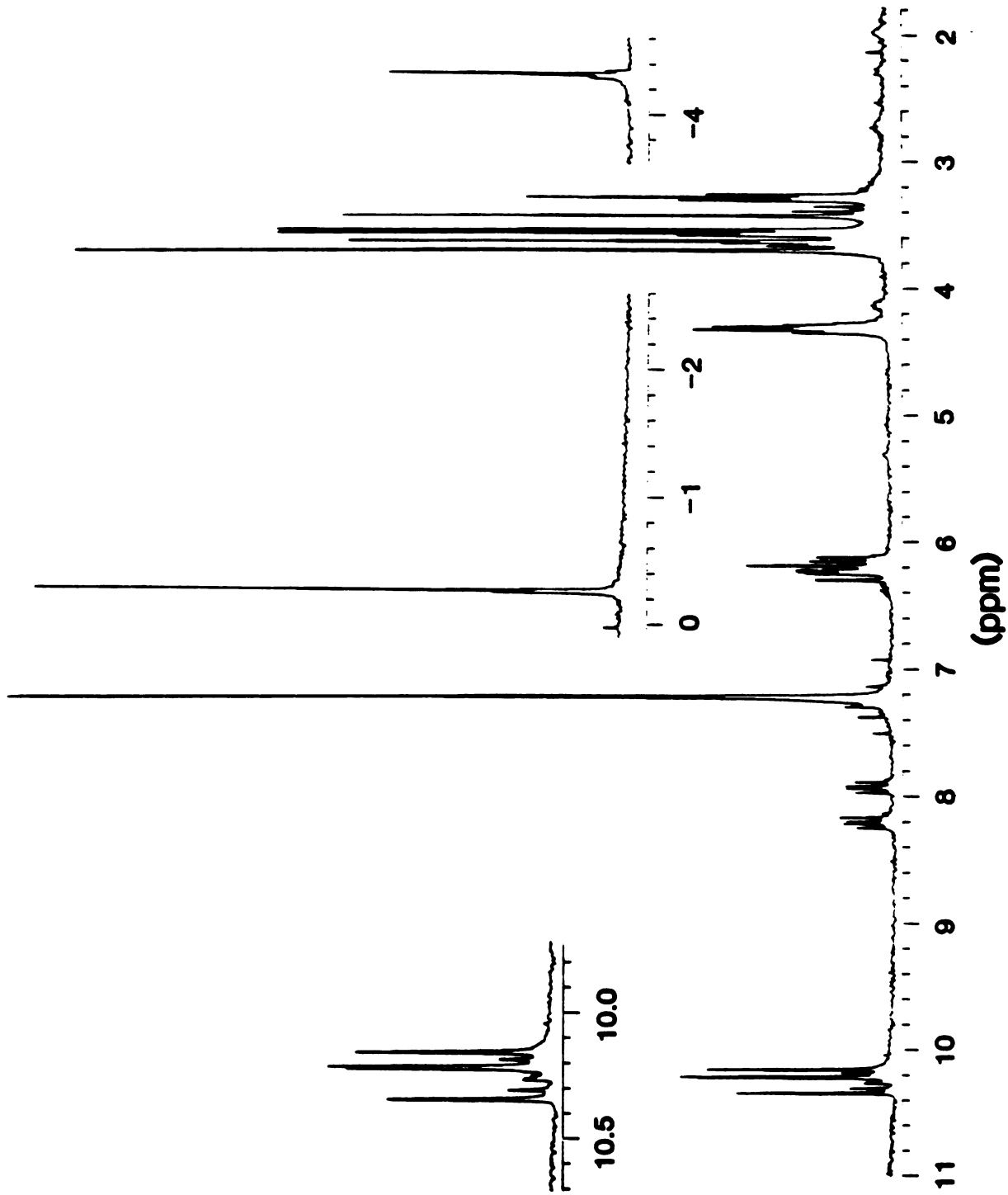
360 MHz NMR spectrum (next page) of the zinc complex of the of the propyne adduct in deuteriochloroform. The region of the spectrum between 0 and 2 ppm is not shown. The only signals in the deleted region are due to impurities and water. The baseline of the upfield region of the spectrum is displaced upwards and to the left. The meso region of the spectrum has been expanded in the inset.

FIGURE 11

STRUCTURE OF THE METAL-FREE PROPYNE ADDUCT







in the region from 2 to 11 ppm. Instead, a three proton singlet at -0.15 ppm and a two proton singlet at -4.35 ppm are observed. The abnormally high field position of the signals associated with these protons is only consistent with their placement in the shielding cone of the porphyrin ring current. The appearance of a two proton singlet at -4.35 ppm locates these protons on a carbon directly attached to a pyrrole ring nitrogen since this is the only position where the ring current effects are of sufficient strength to cause such an upfield shift. The remaining protons must be those of an acetyl group since only this formulation allows for the three proton singlet observed at -0.15 ppm. The propyne adduct is therefore one of the four isomers of N-(2-oxopropyl)-protoporphyrin IX dimethyl ester. The one remaining ambiguity, that is, which pyrrole nitrogen bears the N-alkyl group, has been resolved by a combination of NMR techniques (section 3.5). The structure of the major propyne adduct determined in those experiments is given in Figure 11.

Examination of the meso region of the NMR spectrum (Figure 10, inset) reveals that minor amounts of at least one of the other four isomers of N-(2-oxopropyl)-protoporphyrin IX are also formed in the bioalkylation reaction. The presence of isomers is also detectable in the methyl region (3.4-3.8 ppm) and the 2-oxopropyl-methyl region (-0.15 ppm) of the spectrum. Thus, the alkylative

sequence overwhelmingly favors the A ring pyrrole nitrogen but is not specific for it.

Insertion of metals into porphyrins involves replacement of the two pyrrole hydrogens with the metal, generating a neutral compound. For instance, insertion of divalent zinc (as zinc acetate) into protoporphyrin IX produces the neutral zinc complex plus two equivalents of acetic acid. On the other hand, insertion of zinc into an N-alkylated porphyrin produces a salt since the metal free porphyrin has only one proton to lose. The remaining positive charge on the metal is balanced by a counterion. The counterion can be exchanged by washing with salt solutions. The fact that the zinc-complexed pigments, now known to be salts, are much more polar by HPLC analysis than the metal free adducts is therefore readily understood.

The field desorption mass spectra of the zinc-complexed pigments give molecular ion patterns consistent with the insertion of zinc. These molecular ions (after adjustments are made for the natural isotopic distribution of zinc) are 63 mass units heavier than the molecular weights of the metal-free porphyrins. This requires that the metal complexes desorb from the emitter as the intact metalloporphyrins minus the counterion.

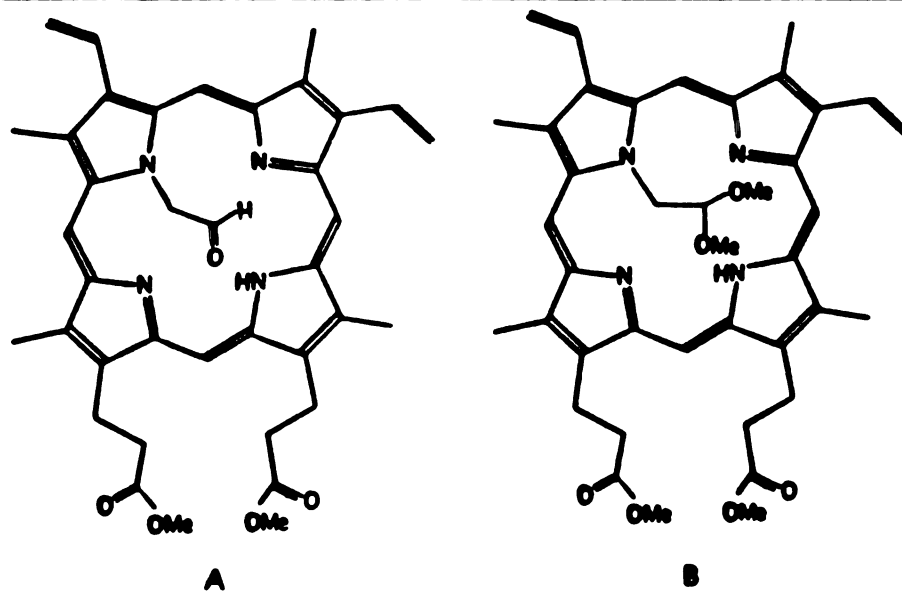
The similarity in absorption spectra and the consistency to the alkylation stoichiometry revealed by the **FDMS** studies leave little doubt that the destruction of

cytochrome P-450 caused by catalytic processing of terminal acetylenes is due to N-alkylation of the heme prosthetic group of the enzyme by the activated acetylene. Support for this conclusion is provided by the NMR spectrum (obtained in collaboration with Hal Beilan of this laboratory) of pigments isolated from rats treated with acetylene gas. The acetylene pigments proved to be particularly difficult to obtain in pure form. Especially frustrating was the fact that the metal-free pigments were irreversibly bound by the HPLC columns. On one occasion it was possible to collect two chromatographically distinct forms of the pigment. The 360 MHz NMR spectrum of one of these fractions, as the chloro-zinc complexed porphyrin, is presented in Figure 12. Peak by peak analysis of the spectrum clearly revealed that it is composed of a number of isomers. However, signals associated with protons attached to a carbon bound to a pyrrole nitrogen could be observed at -4.5 to -5ppm. These signals correspond to two protons when compared with the meso proton signals by integration. In light of the FDMS data, and in analogy with the propyne pigment structure, these signals must be due to methylene groups bound directly to isomeric pyrrole nitrogens. This leaves one proton unaccounted for. Since the FDMS data (Table 3) require the presence of a carbon and an oxygen, these adducts must be the isomers of N-(2-oxoethyl)-protoporphyrin IX dimethyl ester. Additional evidence for this conclusion has been obtained by exchange experiments (Figure 12, inset).

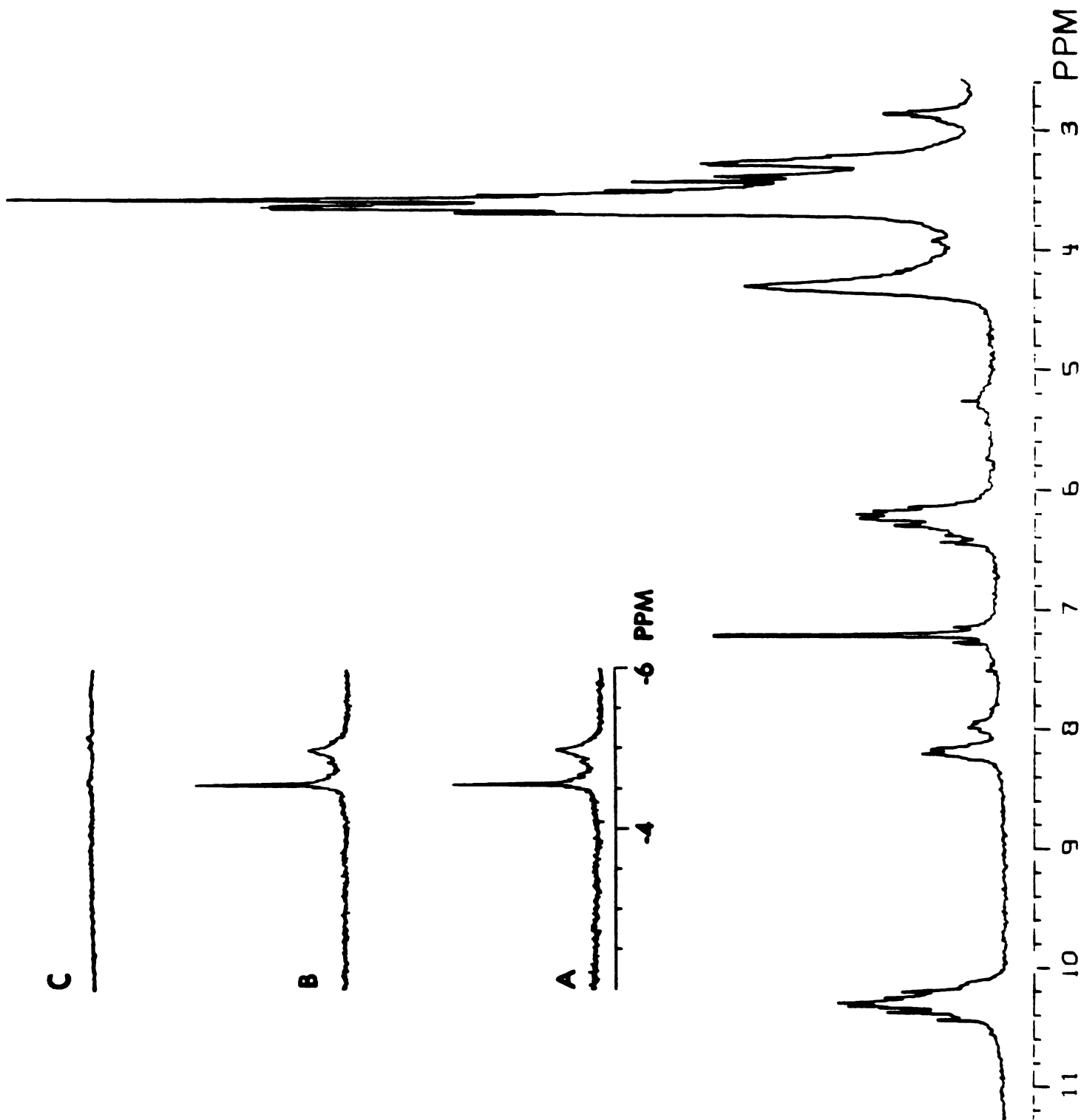
FIGURE 12

NMR SPECTRUM OF CHLORO-ZINC COMPLEXED  
PIGMENTS ISOLATED FROM ACETYLENE-TREATED RATS

360 MHz NMR spectrum of the zinc-complexed pigments isolated from the livers of rats treated with acetylene gas. The pigments in this sample represent one of two approximately equal HPLC fractions of the crude pigment. The upfield (-2 to -6 ppm) region has been displaced upwards and to the left (A). The upfield region after addition of  $D_2O$  to the NMR sample (B). The same region after addition of  $D_2O$  and a trace of deuterated trifluoroacetic acid (C). The region from 2.5 to -2 ppm is not shown. The spectrum is shown on the next page.



Structure of (A) one of the four possible isomers of dimethyl esterified N-(2-oxoethyl)-protoporphyrin IX and (B) the corresponding dimethyl acetal derivatives. The other three isomers are those with the alkyl group on each of the other three nitrogens of protoporphyrin IX

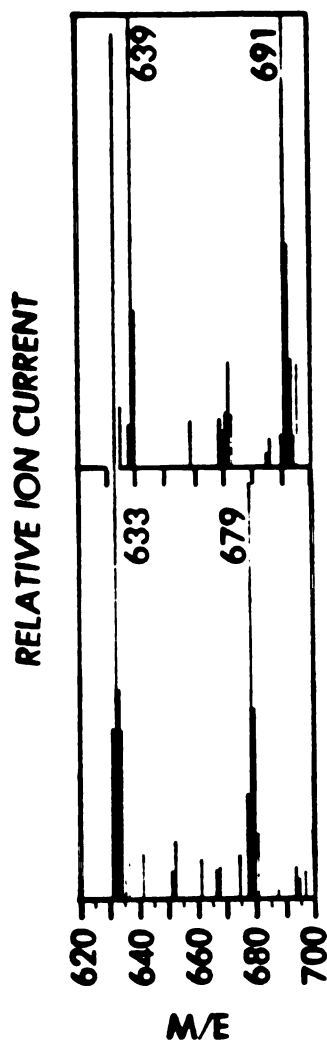


Addition of deuterium oxide and a trace of trifluoroacetic acid to the NMR sample caused the upfield signals to rapidly disappear. Addition of deuterium oxide alone had no effect on the intensities of these signals. The methylene protons therefore undergo acid catalyzed exchange with water. This is consistent with the proposed structure of these pigments since they would be expected to undergo rapid, acid catalyzed enolization, reactions. Similar results have also been obtained for other N-(2-oxoalkyl)-porphyrins (Ortiz de Montellano and Beilan, manuscript in preparation).

N-2-oxoethyl isomers of protoporphyrin IX are also formed during catalytic processing of 2,2,2-trifluoroethyl vinyl ether (fluroxene) by cytochrome P-450 (Kunze et al, 1981). Common to the FDMS spectra of the metal free pigments isolated from fluroxene and acetylene treated animals are ions at  $m/e$  633 and  $m/e$  679. The relative intensities of these ions varied with the sample and the emitter, although the former peak was always much more intense. The presence of the ion at  $m/e$  679 in the spectra of the fluroxene pigment has been explicitly shown to arise from the formation of the dimethyl acetal of the aldehyde in the N-alkyl group. The bottom trace of Figure 13 is the FD spectrum of the fluroxene pigment. The upper trace shows the same pigment after treatment with acidic trideuteromethanol. The ion at  $m/e$  633 (lower trace) has been replaced by an ion at  $m/e$  639 due to transesterification of the methyl ester

FIGURE 13

## FIELD DESORPTION MASS SPECTRUM OF THE METAL-FREE FLUOXENE ADDUCT



Field desorption mass spectrum of the metal-free green porphyrin isolated from fluoxetine-treated rats. The upper spectrum is that obtained when the sample was treated overnight with 5%  $H_2SO_4$  in trideuteromethanol and was reisolated. Essentially the same mass spectrum is obtained with the acetylene adduct (see text).



groups with the deuterated methanol. The ion at  $m/e$  679 (lower trace) has been replaced by ion at  $m/e$  691 (upper trace) due to the same treatment. This twelve mass unit shift is due to incorporation of four trideuteromethyl groups into the porphyrin, two into the ester methyl positions and two into the dimethyl acetal. The NMR spectrum presented in Figure 12 therefore also contains signals from the dimethyl acetals as well as the different regioisomers of N-(2-oxoethyl)-protoporphyrin IX dimethyl ester. The NMR spectrum of the other fraction collected from the HPLC column similarly represents a number of isomeric porphyrins as well as their dimethyl acetals (not shown). While it is not possible to precisely define the isomeric distribution of the acetylene adducts, the convergent lines of evidence presented here leave little doubt that the initially formed adduct contains the N-2-oxoethyl group as the N-alkyl substituent.

Identification of the propyne adduct as N-(2-oxopropyl)-protoporphyrin IX allows a tentative prediction to be made for the structures of other terminal acetylene adducts. The destructive interaction involves a mechanism which leads to addition of the terminal carbon of activated propyne to pyrrole nitrogen of heme. Similarly, the other terminal acetylenes probably also add to heme to give the ketone rather than the aldehyde product. The single exception to this rule is, of course, acetylene itself, since it

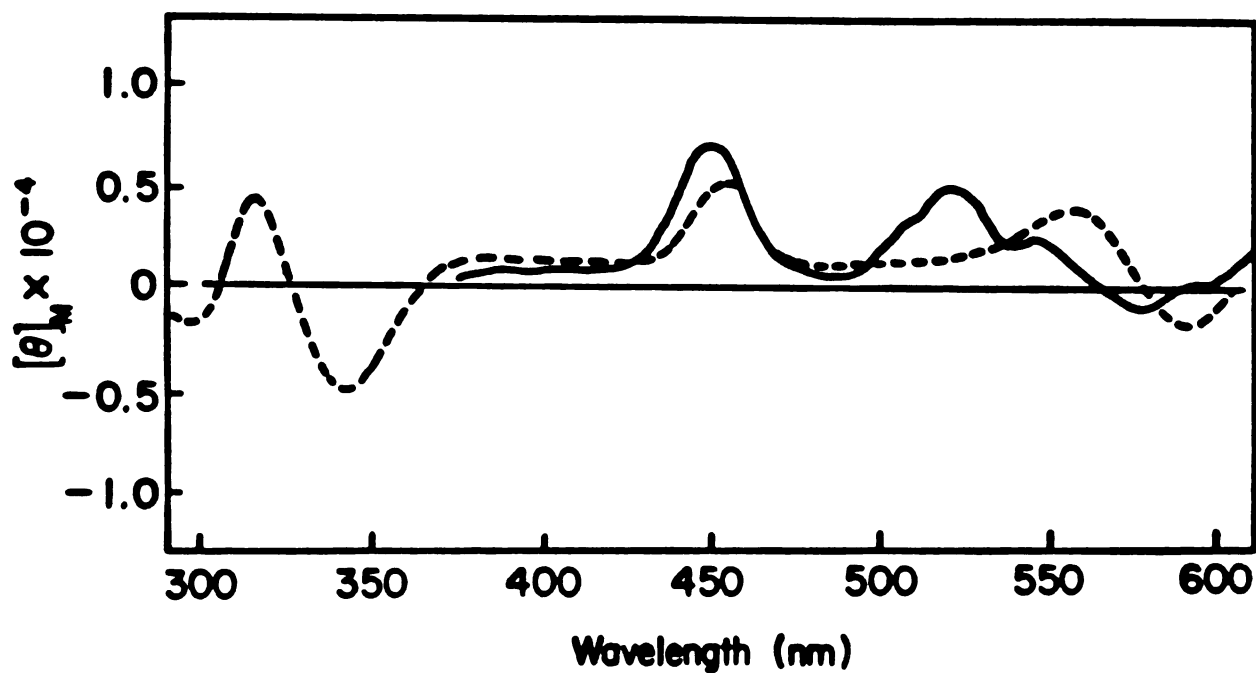
can only give the aldehyde derivative.

### 2.35 CIRCULAR DICHROISM SPECTRA OF THE PROPYNE ADDUCT: THE TWO FACES OF HEME

The two sides of protoporphyrin IX defined by the plane of the porphyrin ring are prochiral. N-alkylation of one of the pyrrole nitrogens removes this symmetry element and generates two enantiomeric porphyrins. An equal mixture of the two enantiomers will exhibit no optical activity, whereas each enantiomer will give an equal and opposite rotation of circularly polarized light. The purified propyne adduct has been found to be composed of essentially one isomer of N-(2-oxopropyl)-protoporphyrin IX dimethyl ester. The three carbon centers of the N-alkyl group are not chiral. The possibility that the propyne adduct is optically active was investigated by measuring the circular dichroism spectra of the pigment. The CD spectra of the metal-free adduct (solid line) and of the zinc acetate salt of the pigment (dotted line) are presented in Figure 14. Both the free base and the zinc-complexed pigment were found to be optically active. Moreover, the obvious differences in the optical activity of the two forms of the pigment definitively attributes the observed optical activity to the porphyrin itself rather than to an optically active impurity in the sample.

FIGURE 14

CIRCULAR DICHROISM SPECTRA OF THE  
METAL-FREE AND ZINC-COMPLEXED PROPYNE ADDUCT



Circular dichroism spectrum of the propyne adduct (solid line) and of its zinc complex (dotted line) in methylene chloride. The high absorbance of the sample precluded determination of the shorter wavelength region of the spectrum of the metal-free form of the porphyrin. Ellipticity has been calculated on the assumption that the extinction coefficient of the zinc-complexed porphyrin at 423 nm is 125,000.

These results suggest that N-alkylation of the cytochrome P-450 prosthetic heme by oxidatively activated propyne is stereoselective for one face of prosthetic heme. A single ambiguity prevents use of the word stereospecific rather than stereoselective. The optical purity of the porphyrin cannot be determined from this data. Therefore, it cannot be stated with certitude that one enantiomer is present to the complete exclusion of the other.

A number of scenarios can be envisioned, in the absence of optical purity data, which would be consistent with the CD results. The first of these is that the propyne adduct is only one of the two possible enantiomers, in which case N-alkylation of prosthetic heme only occurs at one face of the porphyrin. The most logical explanation in this case would be that the heme is bound in the active site in such a manner that only one face of the heme is presented to the alkylating substrate. Hemoglobin, for instance, always presents the same side of heme to oxygen. If the pigment is not optically pure, however, one is left with less clear-cut alternatives, including stereospecific alkylation of different isozymes containing oppositely oriented heme groups or stereoselective, but not stereospecific, insertion of heme into the apoprotein. Additional studies are in progress to determine the optical purity of these and similar adducts.

### 2.36 POTENTIAL MECHANISMS FOR TERMINAL ACETYLENE MEDIATED DESTRUCTION OF CYTOCHROME P-450

Catalytic processing of terminal acetylenes by cytochrome P-450 terminates in the production of a reactive intermediate which destroys the enzyme by alkylation of the heme prosthetic group. The nature of the reactive intermediate formed, and the chemical events leading to its formation and subsequent attachment to a pyrrole nitrogen of prosthetic heme, have yet to be defined. Structural elucidation of the pigments isolated from propyne- and acetylene-treated animals, however, provides a firm base from which mechanistic arguments may be proposed. The isolated pigments contain the three elements of the ternary complex present in the active site immediately prior to the destructive sequence. These are heme, atomic oxygen and the acetylene molecule. While it has not been explicitly demonstrated that the activated oxygen is the oxygen atom eventually incorporated into the pigments, the fact that oxygen is required for destruction to occur (White and Muller-Eberhard, 1977) clearly favors this possibility. Destruction of cytochrome P-450 by acetylenes is not attenuated by glutathione in vitro, indicating that a short-lived species, one that remains in the confines of the active site, is responsible for destruction. In the analogous case of olefin-mediated destruction of cytochrome P-450, the destructive process has been explicitly demonstrated to be

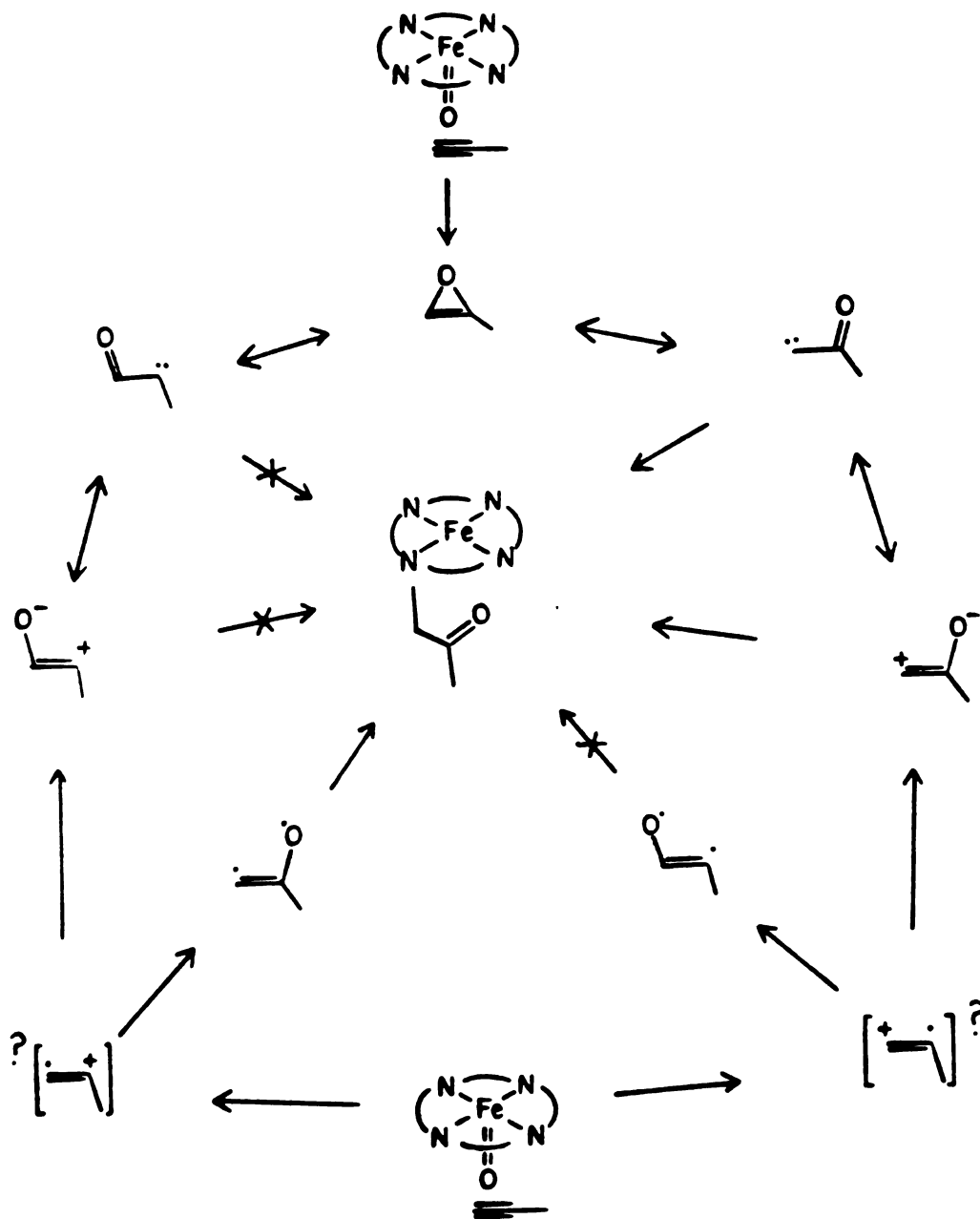
suicidal by kinetic analysis, a result which specifically excludes the intervention of a diffusible intermediate (Ortiz de Montellano and Mico, 1981 ).

The mechanistic alternatives considered in this discussion are predicated on the supposition that the alkylating intermediate is generated during an abortive attempt to oxidize the acetylene triple bond. Cytochrome P-450-dependent oxidation of this functionality has been demonstrated (Wade et al, 1980, Ortiz de Montellano and Kunze, 1980f; 1981b) and is discussed in section 2.4. Concerted transfer of activated oxygen to the triple bond would give an oxirene (Figure 14). The highly unstable, antiaromatic, oxirene ring has never been observed (see Ciabattoni et al, 1970; Tanaka and Yoshimine, 1980). Its short-lived presence has, however, been inferred (Zeller, 1977; Russel and Rowland, 1970). The lifetime calculated for the oxirene ring is too short to allow chemical trapping or stabilization by low temperature matrix isolation techniques (Strauz et al, 1976). The most refined calculations to date indicate that the potential energy barrier between oxirene and ketocarbene is low or non-existent, and that the ketocarbene is energetically favored (Tomioka, 1980). Moreover, chemical oxidation of acetylenes leads to the products expected from decomposition of the ketocarbene, not the oxirene. Therefore, if the oxygen transfer is concerted, the resulting ketocarbene is the most likely alkylating agent. Exit from

FIGURE 15

## DESTRUCTION OF CYTOCHROME P-450 BY PROPYNE:

## POTENTIAL ALKYLATING SPECIES



the oxirene-ketocarbene manifold is possible via ketocarbene to ketene rearrangement. A ketene is not the alkylating agent since it would not give the observed propyne adduct. A calculated minimum corresponding to the zwitterionic oxovinyl cation, a resonance form of the ketocarbene, has not been observed (Tomioaka, 1980), although its presence in the active site may be favored by the proximity of the iron of heme.

Entry into a second array of reactive intermediates can be envisioned if transfer of the oxygen to the triple bond is non-concerted (Figure 14). Destruction of cytochrome P-450 by terminal, monosubstituted olefins apparently proceeds via an acyclic precursor to the epoxide (Ortiz de Montellano and Mico, 1980a,b). The initial step might then be either be asymmetric transfer of the oxygen to give the iron-ligated oxovinyl cation, a resonance structure of the ketocarbene, or single electron removal from a pi orbital, in analogy to aliphatic hydroxylation reactions (Groves et al, 1977), followed by recombination of the oxygen at either carbon to give the radical or oxovinyl cation.

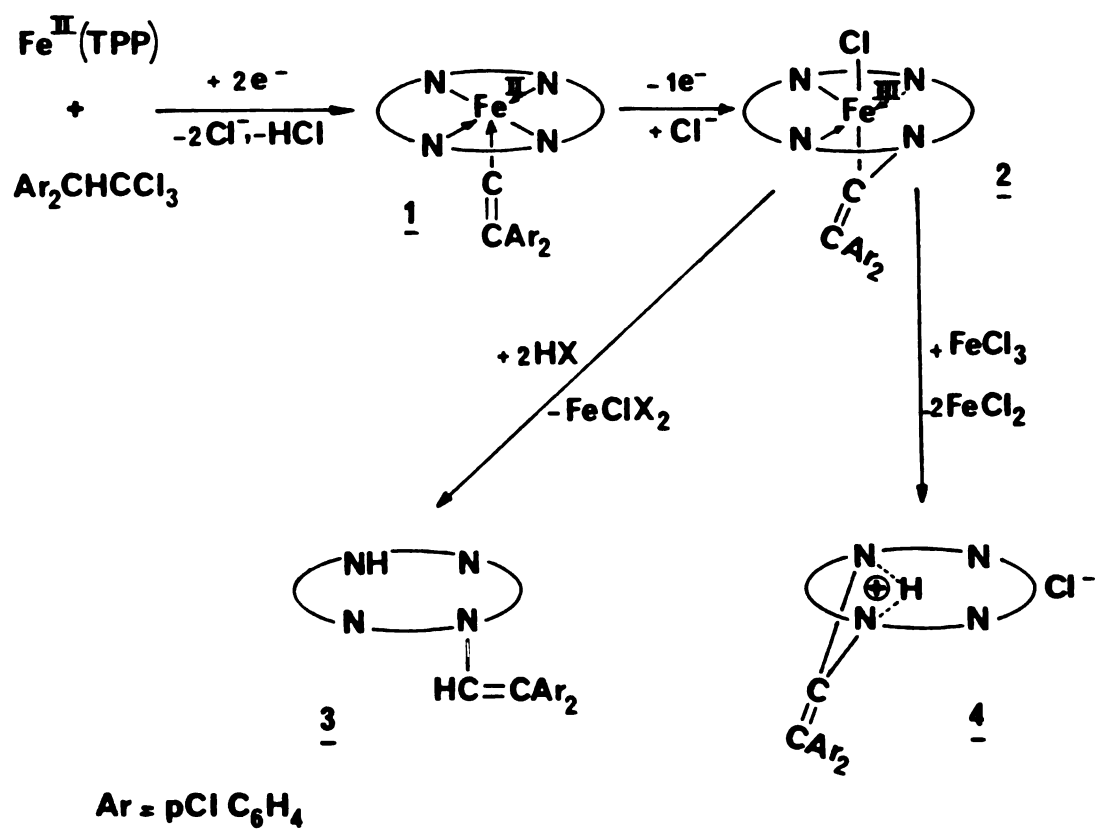
The battery of potential alkylating species is presented in Figure 14. Three of the six proposed intermediates may be ruled out since they would react with heme to give the aldehyde rather than the observed ketone adduct. The remaining three species merely represent different distributions of electrons among the two carbons and oxygen.



Calculations indicate that the ketocarbene will predominate. The potential for an equilibrium between the alternatives, perhaps aided by the iron, however, makes a firm prediction difficult.

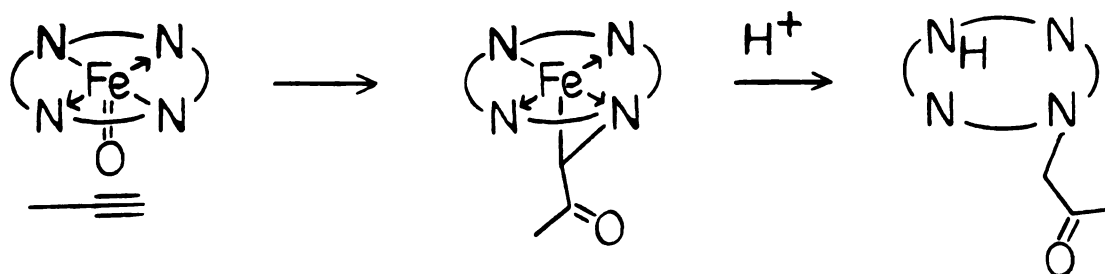
Recently, workers in a number of laboratories have demonstrated the ability of carbenes to react with metalloporphyrins to give, after further reactions, N-alkylated porphyrins. Particularly relevant to our work is the demonstration that an iron II carbene complex of tetraphenyl porphyrin undergoes a one electron oxidation to a carbon bridged species which, upon acid treatment, rearranges with loss of iron to an N-substituted tetraphenyl porphyrin (Lange and Mansuy, 1981; Latos-Grayzyski et al, 1981). These reactions are summarized in Figure 16. Related reactions have been demonstrated for zinc, nickel and cobalt porphyrins (Callot et al, 1978; Callot and Schaffer, 1980; Johnson and Ward, 1976; Johnson et al, 1975). In particular, the reaction of ethyl diazoacetate with cobalt III porphyrins has been shown to give the carbon-cobalt-pyrrole nitrogen bridged species directly. Therefore, if the ketocarbene enters the manifold of reactive intermediates generated during oxidation of acetylenes in the enzyme, it may directly insert into the ferric iron-pyrrole nitrogen bond of heme. Rearrangment with loss of iron might then be expected to occur during the acid workup of the pigments, in analogy with the results of Lange and Mansuy (1981) and

REACTION OF CARBENES WITH IRON TETRAPHENYLPORPHYRIN\*



\*Taken from Lange and Mansuy (1981)

Latos-Grayzynski et al (1981).



The alkylation sequence with propyne could conceivably generate as many as eight different N-alkylated porphyrins. Thus each of the four pyrrole nitrogens could bear either a 2-oxopropyl group or a 1-methyl-2-oxoethyl group. (Actually 24 isomers are possible when the potential for enantiomers and diastereomers is also taken into consideration.) Our results show that one major isomer, that with a 2-oxopropyl group attached to pyrrole ring A, as well as a trace of as many as two other N-2-oxopropyl isomers, are formed. The acetylene alkylation reaction seems to be less specific. High alkylation selectivity has also been observed in the case of the ethylene and propene adducts (see section 3.4). Selectivity could, in principle, be mediated by specific binding of the substrate, orientation of the reactive intermediate species in the active site, or a combination of the two. Pyrrole ring specificity may also be due to differential reactivities of the pyrrole nitrogens. If the reactive intermediate is sufficiently short lived, initial orienta-

tion may be dominant. An intermediate with sufficient longevity to assume a number of orientations might be expected to give less specific alkylation.

Why is it that only the terminal carbon of activated propyne adds to heme? Again, a number of possibilities come to mind. If the ketocarbene is the proximate alkylating species, it may be that the terminal carbene is formed exclusively or preferentially. It is also possible that if the disubstituted carbene is formed, it immediately rearranges to the ketene by a 1,2 hydrogen shift (see section 2.4) rather than alkylating the heme. It remains to be shown that dialkyl carbenes can add to heme, so it is also possible that the reaction is sterically disfavored. Internal acetylenes, which could only give dialkyl carbenes, do destroy cytochrome P-450 but do not give green pigments.

#### 2.4 OXIDATION OF THE TRIPLE BOND BY CYTOCHROME P-450: THE UC SHIFT

The first evidence that acetylenes are oxidized by mammalian systems was provided by El Masri et al (1958), who found that 50% of an oral dose of phenyl acetylene was excreted in the urine of rabbits as phenylacetic acid. More recently, biphenylacetylene (Wade et al, 1979; 1980) and 4'-ethynyl-2-fluorobiphenyl (Sullivan et al, 1979) have been shown to be transformed in vivo to the corresponding aryl-

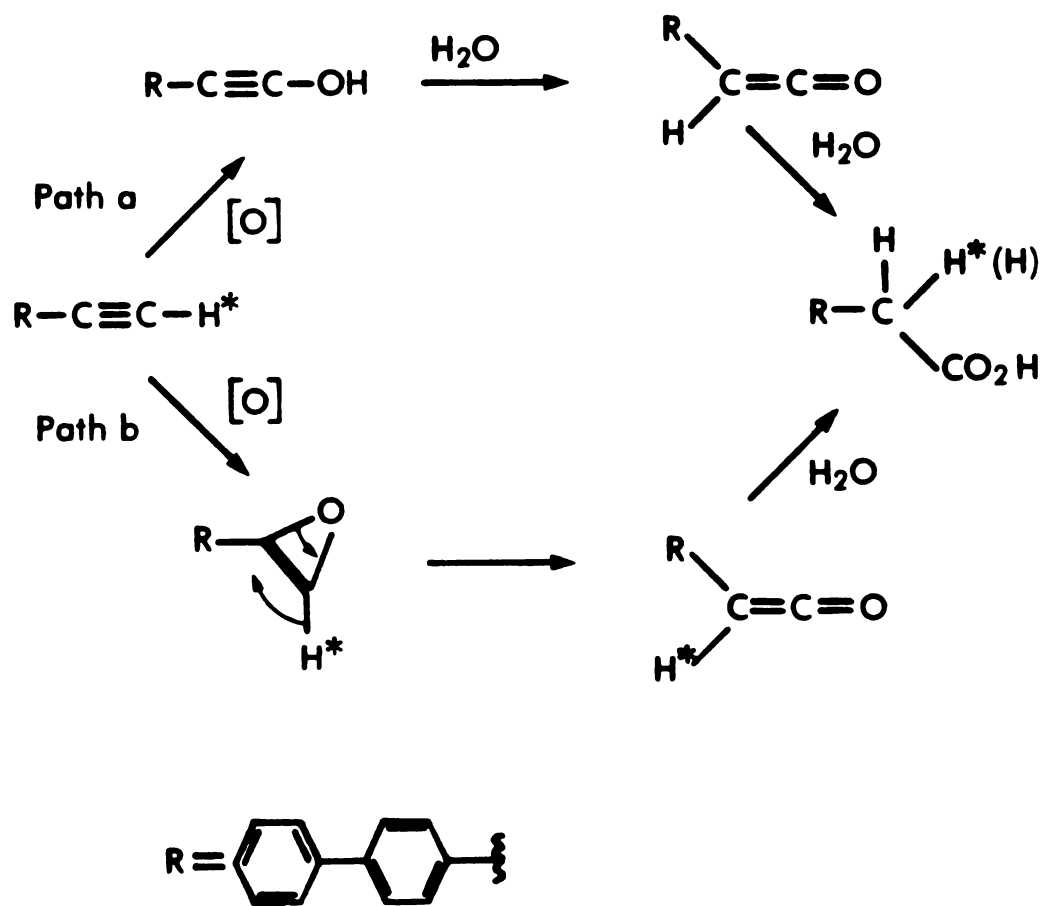
substituted acetic acids. The conversion of biphenyl acetylene to biphenyl acetic acid by hepatic microsomes requires NADPH and is inhibited by carbon monoxide. Furthermore, the rate of oxidation varies with the induction state of the animals. Induction with phenobarbital or 3-methylcholanthrene accelerates the in vitro microsomal oxidation reaction compared with that in untreated liver microsomes. These results demonstrate that the oxidation reaction is catalyzed by isozymes of cytochrome P-450.

Two mechanisms have been proposed for this oxidation reaction. One group (Sullivan et al, 1979) has postulated that the oxidative step is a cytochrome P-450 catalyzed insertion of oxygen into the acetylene carbon-hydrogen bond. The initially formed hydroxy-acetylene then is suggested to rapidly tautomerize to the ketene and to be hydrolyzed to the acid (Figure 18, path a). Alternatively, oxidation could proceed by oxygen insertion into the triple bond to give an oxirene which, via ketene formation and hydrolysis, also gives the corresponding acid (Figure 18, path b; Wade et al, 1980).

These mechanistic alternatives can be differentiated by labeling the acetylene proton with deuterium and looking for the presence of this isotope in the acid product. Oxidation via path a would give the oxirene which rearranges to the ketene via a 1,2 shift. The acetylene proton would therefore be conserved in the acid product. Product formation

FIGURE 17

ALTERNATIVE PATHWAYS FOR CYTOCHROME P-450 CATALYZED  
OXIDATION OF THE TRIPLE BOND OF BIPHENYLACETYLENE



via path b would involve loss of the acetylene proton to the environment since retention of the alcohol proton would require a sigmatropically non-allowed 1,3 hydride shift or two allowed, but energetically unfavorable, 1,2 shifts. Calculations suggest that the rearrangement of hydroxyacetylene to ketene with retention of the acetylene proton would involve the latter of the two mechanisms but that the required energy of activation would be in excess of 90 kilocalories/mole (Tanaka and Yoshimine, 1980). Thus, any rearrangement involving acid formation would require removal of the labeled alcohol proton. Appearance of this proton in the acid is viable but unattractive since it requires highly specific off-return mechanisms. Oxirene rearrangement to ketene, on the other hand, is thermodynamically favored, and follows a reaction coordinate which presents little or no activation barrier, and does not involve loss of the acetylene proton.

Monodeuterated biphenylacetylene was chosen as a probe of these two mechanistic alternatives since the role of cytochrome P-450 in its oxidation has been established (Wade et al, 1980). Treatment of biphenylacetylene with n-butyl lithium, followed by addition of D<sub>2</sub>O, gave the monodeuterated biphenylacetylene with no detectable residual protons on the acetylene carbon. The 1-<sup>2</sup>H-biphenylacetylene was incubated with hepatic microsomes isolated from phenobarbital induced rats. The biphenylacetic acid formed

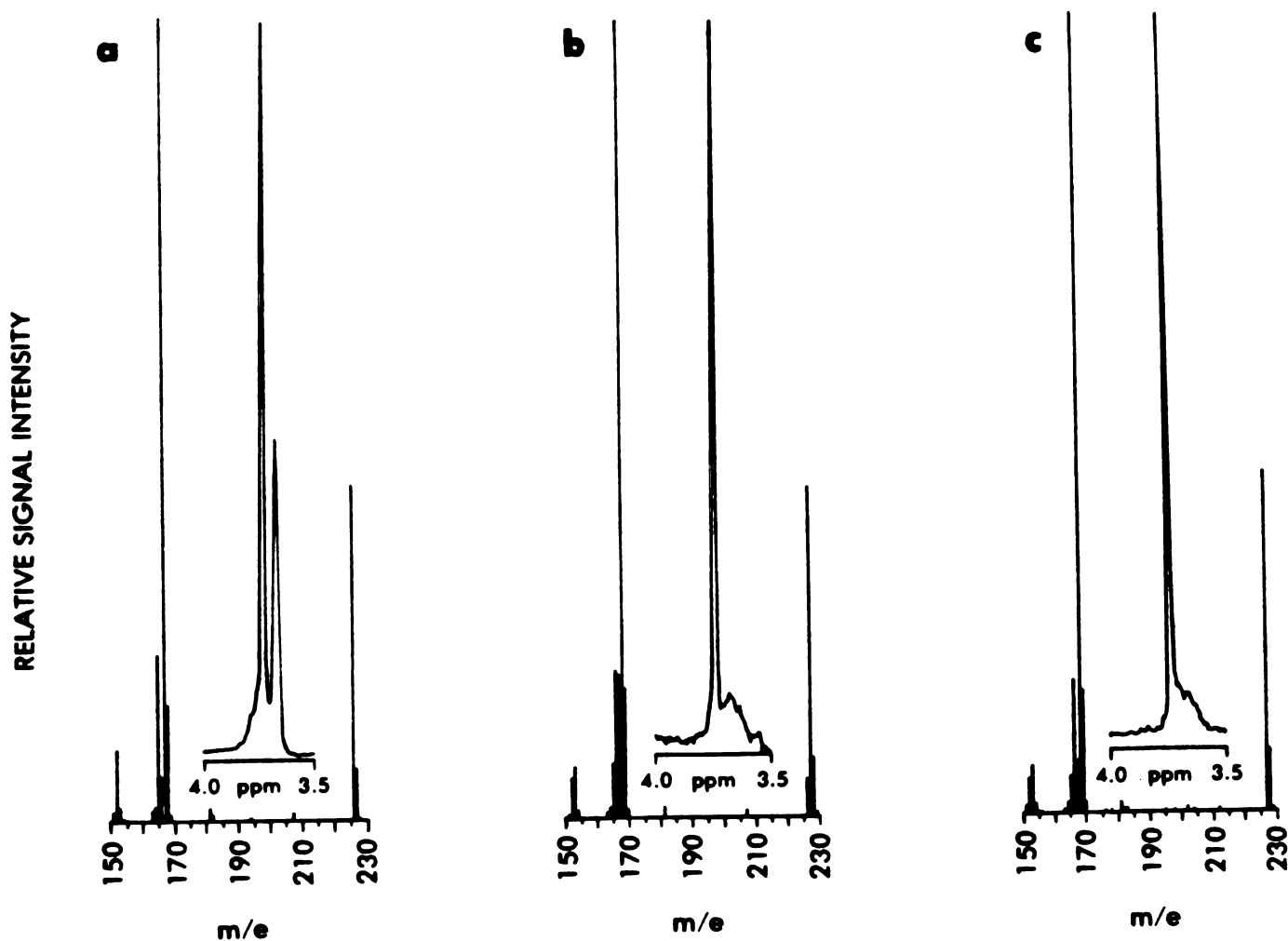
in this reaction was extracted into dichloromethane after careful acidification of the incubation mixture to pH 5. Extreme care was taken to avoid exposure of the arylacetic acid to highly acidic or basic conditions because rapid exchange of the methylene protons would be expected to occur under these conditions. The combined organic extracts were dried (anhydrous magnesium sulfate) and the solvent removed. The residue was treated with ethereal diazomethane to methylate the metabolite. The solvent was removed under a stream of nitrogen and the residue analyzed by coupled GC-EIMS. The methyl-biphenyl acetate was further purified by low pressure liquid chromatography on silica gel and analyzed by NMR.

The high mass region of the electron impact spectrum of unlabeled methyl biphenyl acetate is shown in Figure 19, panel A. The base peak in the spectrum is the 4-phenylbenzyl cation at  $m/e$  157. A strong (40% of the base peak) molecular ion at  $m/e$  226 is also observed. The region of the NMR spectrum containing the methyl (3.77 ppm, 3H) and methylene (3.34 ppm, 2H) proton signals is inset in this figure. The corresponding spectral regions of the microsomally-generated biphenylacetic acid (as the methyl ester) are shown in Figure 19, panel B. The molecular ion ( $m/e$  227) and the base peak benzyl cation ( $m/e$  158) were one mass unit higher than the unlabeled ions in panel A. This shift of one mass unit was attributed to the presence of a



FIGURE 18

NMR AND EIMS SPECTRA OF METHYL BIPHENYLACETATE OBTAINED FROM  
 CHEMICAL AND MICROSOMAL OXIDATION OF 1-<sup>2</sup>H-2-BIPHENYLACETYLENE



Electron impact (70ev) mass spectra and 80 MHz NMR spectra (inset) of (a) authentic unlabeled methyl 2-biphenylacetate, (b) methyl 2-biphenylacetate obtained by esterification of the acid formed on incubation of monodeuterated biphenylacetylene with hepatic microsomes, (c) methyl 2-biphenylacetate obtained by m-chloroperbenzoic acid oxidation of monodeuterated biphenylacetylene.

deuterium on the methylene carbon by NMR (Figure 18, panel B). The two proton methylene singlet of the unlabeled compound was replaced by a broad (H-D geminal coupling) one proton signal at 3.34 ppm. A trace of unlabeled methylbiphenyl acetate was observed in the mass spectrum and may be due to minor exchange of the methylene proton during workup.

Peracid oxidation of monosubstituted arylacetylenes is known to give arylacetic acids as products (McDonald and Schwab, 1964), yet definitive proof that the reaction proceeds through ketene has not been offered. Dialkyl acetylene oxidation, on the other hand, has been shown to involve 1,2 alkyl migration to give the ketene intermediate (Stille and Whitehurst, 1964; Concannon and Ciabattonia, 1973; Ciabattonia et al, 1970). Accordingly, deuterated biphenylacetylene was treated with meta-chloroperbenzoic acid in dichloromethane solution containing 1% methanol (as a ketene trap). The purified ester product was analyzed by GCMS and NMR (Figure 19, panel C). Essentially quantitative retention of deuterium in the ester product was observed by MS, and the position of the deuterium at the methylene positions was confirmed by NMR.

The retention of deuterium during enzymatic and peracid oxidation of biphenylacetylene to biphenyl acetic acid rules out the intermediacy of the hydroxy acetylene in both reaction sequences. Therefore, these reactions must proceed via attack of an activated oxygen species on the acetylene pi

bond. Two mechanistically-distinguishable routes can be invoked to rationalize these results. Both routes proceed through the ketene, one via a 1,2 hydride shift (Figure 20, path a) and the other via a 1,2 shift of the biphenyl group (Figure 20, path b). To distinguish between these two alternatives, methyl biphenyl-acetate was generated in both the chemical and biological systems from 1-<sup>13</sup>C-biphenylacetylene and was examined for label content and position by GCMS.

The synthesis of 1-<sup>13</sup>C-biphenyl acetylene was patterned after a similar synthesis of radiolabeled biphenylacetylene (Wade et al, 1979). The two step synthesis involved Friedel-Crafts alkylation of biphenyl with 1-<sup>13</sup>C-acetyl chloride (90% isotopically labeled) followed by treatment of the resulting 4-phenyl acetophenone with PCl<sub>5</sub> in pyridine to give the acetylene.

The specifically labeled biphenylacetylene was incubated with hepatic microsomes obtained from phenobarbital induced rats and was also oxidized with meta-chloroperbenzoic acid. The labeled methyl-biphenylacetate obtained from these two procedures was analyzed by GCMS. The molecular ion obtained by the enzymatic (Figure 21, panel c) and peracid (Figure 21, panel b) oxidation reactions was, as expected, m/e 227. Both spectra also displayed small (ca 10%) molecular ions at m/e 226 due to the 10% <sup>12</sup>C present in the acetyl chloride reagent. The

FIGURE 19

THE 1,2 SHIFT DURING TRIPLE BOND OXIDATION:

ARYL VERSUS HYDRIDE

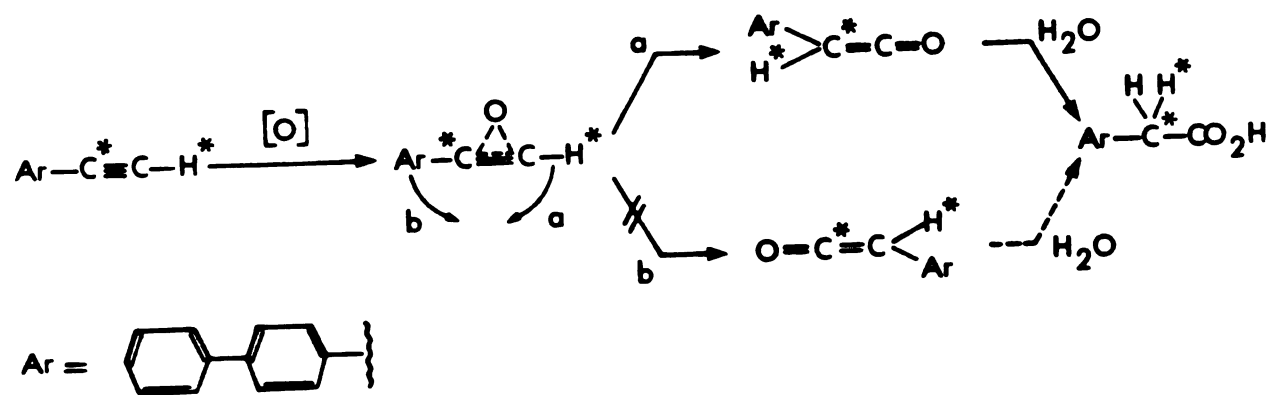
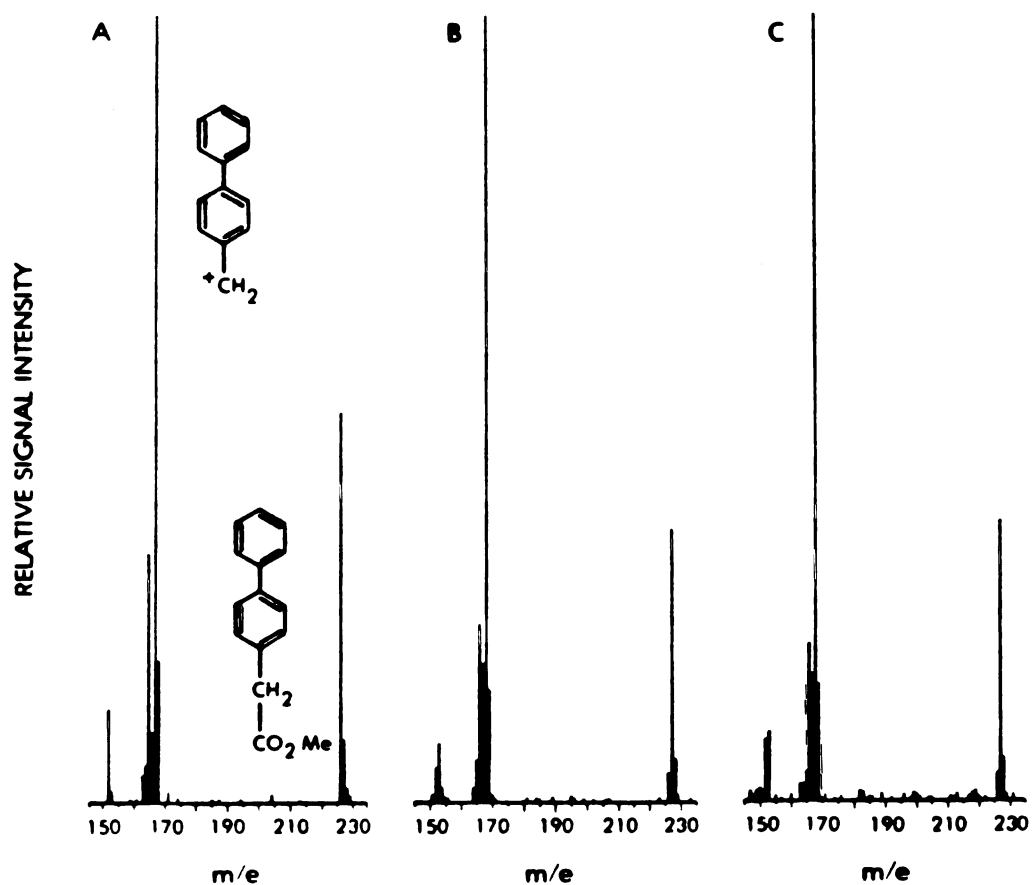


FIGURE 20

ELECTRON IMPACT MASS SPECTRA OF METHYL BIPHENYLACETATE OBTAINED BY CHEMICAL AND MICROSOMAL OXIDATION OF 1-<sup>13</sup>C-1-BIPHENYLACETYLENE



Electron impact (70 ev) mass spectra of (a) authentic unlabeled methyl 2-biphenylacetate, (b) methyl 2-biphenylacetate obtained by metachloroperbenzoic acid oxidation of 1-<sup>13</sup>C-1-biphenylacetylene in the presence of methanol, and (c) methyl 2-biphenylacetate obtained by esterification with diazomethane of the acid formed on incubation of 1-<sup>13</sup>C-1-biphenylacetylene with hepatic microsomes from phenobarbital pretreated rats.

base peak due to the 4-phenyl-benzyl cation fragment is diagnostic for the position of the labeled carbon in the acid product. Biphenyl migration would place the label at the carbonyl carbon, whereas hydrogen migration places the label at the benzylic carbon (Figure 20). The methyl-biphenyl acetate obtained from both oxidation systems fragmented in the mass spectrometer to give the benzyl cation at  $m/e$  168, demonstrating that the benzylic carbon was labeled. Thus, both oxidation reactions involve oxygen attack at the acetylene pi bond and a 1,2 hydride shift to the ketene. This 1,2 shift is similar to the 1,2 hydride shift (NIH shift) observed subsequent to cytochrome P-450 catalyzed oxidation of aromatic pi bonds to the highly reactive arene oxides. Both reaction sequences involve initial attack of activated oxygen on a pi bond to give a highly reactive intermediate which rapidly rearranges, via a 1,2 hydrogen shift, to a more stable product.

These results show that cytochrome P-450 catalyzed oxidation of biphenylacetylene, and very likely other acetylenes as well, proceeds by attack of enzymatically activated oxygen at the acetylene pi bond. This attack, if concerted, should give an extremely short-lived oxirene which would immediately isomerize to the ketocarbene. A rapid exit from the oxirene-ketocarbene manifold is expected due to the extreme reactivity of these species. One mode of deactivation has been shown to be a 1,2 shift of the ace-

tylenic hydrogen to give the ketene. A second pathway involves addition to the heme prosthetic group of the enzyme (section 2.3). Additional pathways may also be operative. An example of such a secondary reaction is the peracid oxidation of cycloalkynes to give transannular insertion reactions expected of carbene intermediates (Concannon and Ciabtoni, 1973).

## CHAPTER III

SYNTHESIS AND IDENTIFICATION OF  
N-ALKYLATED DERIVATIVES OF PROTOPORPHYRIN IX3.0 INTRODUCTION

Catalytic processing of terminal olefin and acetylene pi bonds by hepatic cytochrome P-450 isozymes leads to the formation of reactive intermediates that inactivate the enzyme via alkylation of the heme prosthetic group. The covalent attachment of these activated substrates to heme has been elucidated by spectroscopic studies of the iron-free dimethyl-esterified porphyrin adducts. FDMS and NMR studies have demonstrated the pigments to be stoichiometrically composed of protoporphyrin IX dimethyl ester plus the substrate plus atomic oxygen. The ethylene (Ortiz de Montellano et al, 1981a; section 3.4), propene (section 3.4), and propyne (section 2.4; Ortiz de Montellano and Kunze, 1981g) adducts have been characterized by proton NMR studies and found to be N-alkylated derivatives of protoporphyrin IX dimethyl ester. The major propyne adduct is one of the four regioisomers of N-(2-oxopropyl)-protoporphyrin IX dimethyl ester. The ethylene adduct is a single isomer of N-(2-hydroxyethyl)-protoporphyrin IX dimethyl ester. The propene adduct is a single isomer of N-(2-hydroxypropyl)-



protoporphyrin IX dimethyl ester. The alkylation sequences partially unveiled by these studies display a surprisingly high selectivity for individual pyrrole nitrogens of heme. The acetylene adduct, on the other hand, is composed of an as yet undetermined distribution of the four isomers of N-(2-oxoethyl)-protoporphyrin IX dimethyl ester (section 2.4) indicating that more than one pyrrole nitrogen is susceptible to alkylation. Moreover, both activated propene and propyne are bound to heme through the terminal unsaturated carbon. Mechanistic alternatives consistent with these results have been suggested for destruction mediated by terminal olefins (Ortiz de Montellano et al, 1980c; 1981a; 1981h) and terminal acetylenes (Ortiz de Montellano and Kunze, 1981g; section 2.4).

The high regiospecificity exhibited by these alkylation reactions suggests that the destructive sequence is rigidly controlled by steric and electronic factors. Unfortunately it is not a simple task to determine, from the NMR spectra, which of the four pyrrole nitrogens bears the N-alkyl group. Such a determination for a number of different destructive agents would provide a means by which the active site topology of the enzyme can be explored. In order to facilitate such studies, we have developed techniques to differentiate the four isomers of N-methyl and of N-ethyl protoporphyrin IX dimethyl ester. These studies are presented in the next sections. This methodology, which includes spin decoupling,

nuclear Overhauser effect, and spin lattice relaxation studies, has subsequently been applied to the elucidation of the structures of the ethylene, propene, and propyne adducts (sections 3.3-3.4).

### 3.1 THE FOUR ISOMERS OF N-METHYL PROTOPORPHYRIN IX DIMETHYL ESTER

Synthetic access to the N-alkylated porphyrins has been reviewed (Jackson, 1978; Jackson and Dearden, 1973). The first N-alkylated porphyrin known, N-methyl etioporphyrin I, was synthesized by the high temperature, sealed tube, reaction of methyl iodide with etioporphyrin I (McEwen, 1952). This reaction exemplifies the most general procedure used to synthesize N-alkylated porphyrins, that is electrophilic attack by an electrophile on a porphyrin pyrrole nitrogen. The most common electrophiles employed for this purpose are methyl iodide, ethyl iodide, and methyl fluorosulphonate. The types of porphyrins examined have been limited to the simple, symmetrical porphyrins such as etioporphyrin, octaethyl porphyrin, coproporphyrin and meso-tetraphenylporphyrin.

The synthesis of N-methyl protoporphyrin IX is complicated by the fact that this porphyrin contains two highly reactive vinyl sidechains which must survive the alkylation conditions unscathed. Attempts to form the desired deriva-

tives of this porphyrin by high temperature alkylation with alkyl halides yielded only insoluble tars. Since similar reactions with porphyrins not containing vinyl sidechains give excellent yields of the N-alkylated products it appears that the vinyl sidechains participate in polymerization reactions. Methyl fluorosulphonate, however, was found to give good yields of the desired N-methylated derivatives of protoporphyrin IX.

### 3.11 SYNTHESIS AND SEPARATION OF THE FOUR N-METHYL ISOMERS

The reaction of excess methyl fluorosulphonate with protoporphyrin IX dimethyl ester in dichloromethane was marked by a gradual change in the color of the reaction mixture from red to brown. (The use of methyl fluorosulphonate requires extreme caution due to its toxic effects, see experimental section for details). After three days the reaction was terminated and worked up. The residue obtained after work up was fractionated by column chromatography on silica gel. Three major fractions were eluted from the column. The first of these was unreacted protoporphyrin IX dimethyl ester. The second and major fraction was found to contain the four regioisomers of N-methyl protoporphyrin IX dimethyl ester. The final fraction was found to consist of the many isomers of N,N'-dimethyl protoporphyrin IX dimethyl

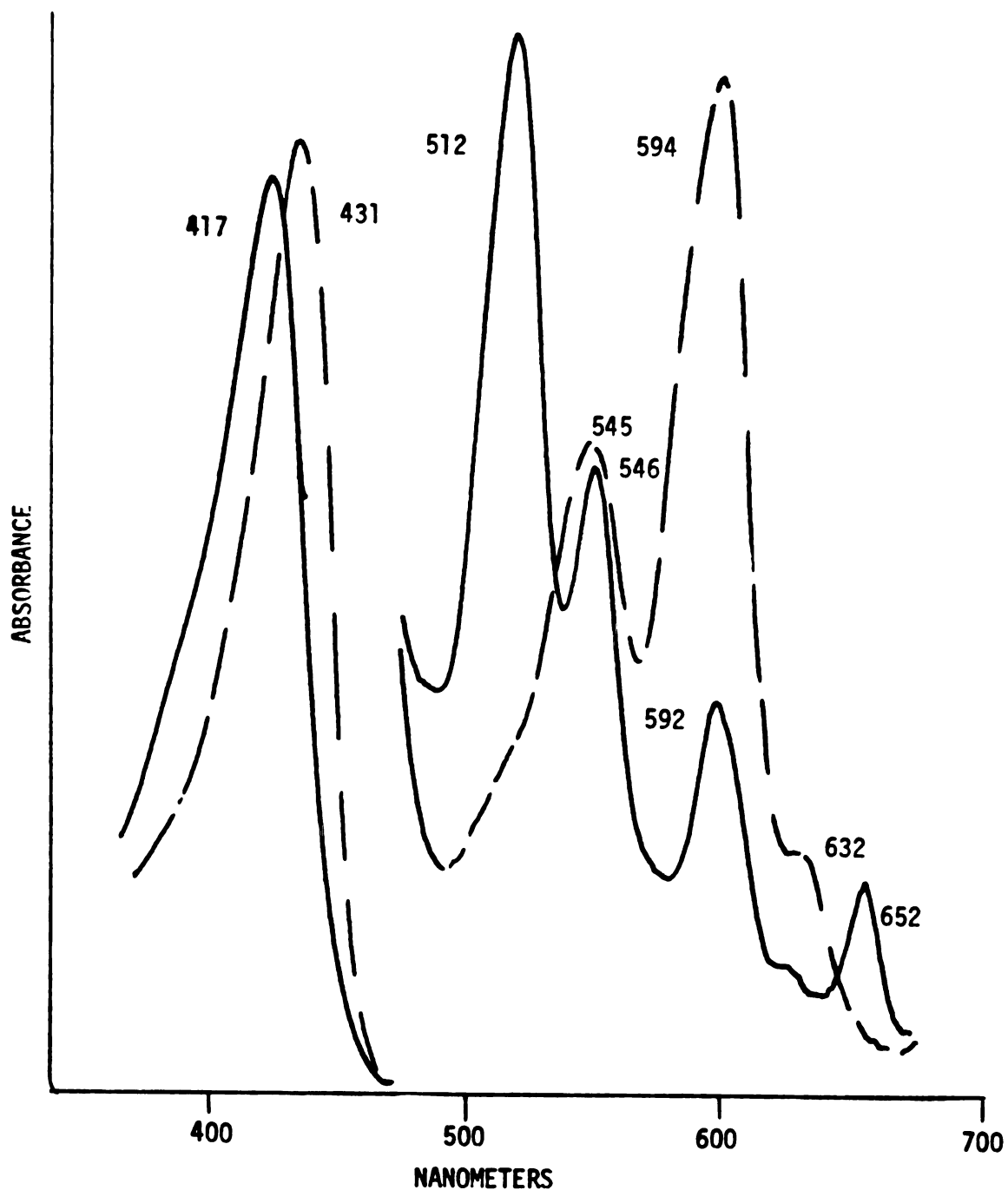
ester. The four isomers of N-methyl protoporphyrin IX dimethyl ester were dissolved in hot chloroform and precipitated from solution by the addition of cold hexane.

The electronic absorption spectra of the metal-free and zinc-complexed N-methyl isomer mixture are given in Figure 21. These spectra are essentially identical to those of the biologically obtained green pigments. The molar absorptivity values for the Soret bands are also comparable (free bases, 417 nm (116,000); zinc complexes, 431 nm (124,000); norethisterone free base pigment, 417 nm (116-118,000); norethisterone zinc-complexed pigment, 432 nm (123-125,000). Moreover the zinc-complexed N-methyl protoporphyrin IX spectrum exhibits the three long wavelength absorptions characteristic of all the pigments. Thus, by all appearances, the visible spectra of the pigments and of N-methyl protoporphyrin IX are indistinguishable.

Analysis of the N-methyl protoporphyrin mixture by FDMS resulted in spectacular ion currents at  $m/e$  604 and  $m/e$  605 (Figure 22). The molecular weight of N-methyl protoporphyrin IX dimethyl ester is 604. These ions correspond, therefore, to the protonated and non-protonated molecular ions. Generally, a greater proportion of the monoprotinated molecular ion was present at higher emitter currents.

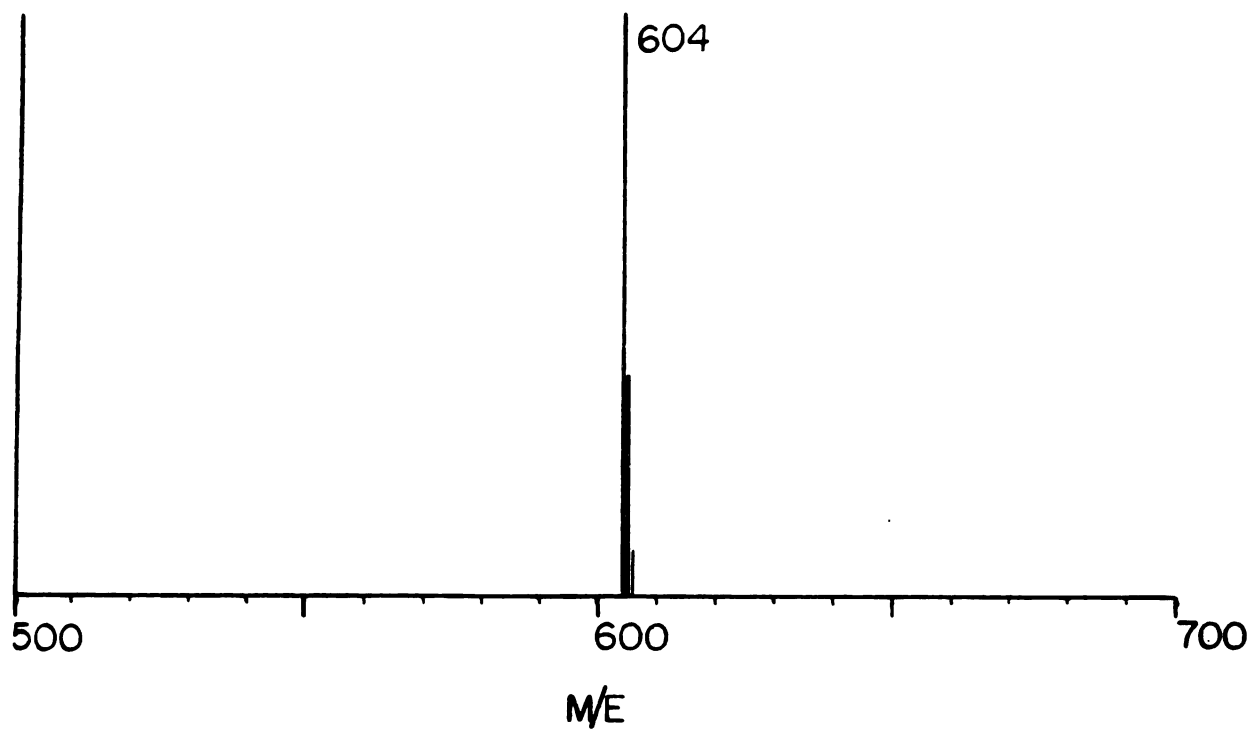
The mixture of N-methylated protoporphyrin IX dimethyl ester isomers was resolved into four fractions by high pressure liquid chromatography (Figure 23). These fractions are

ELECTRONIC ABSORPTION SPECTRA OF  
METAL-FREE AND ZINC-COMPLEXED  
N-METHYL PROTOPORPHYRIN IX DIMETHYLESTER



Electronic absorption spectra of metal-free (solid line) and zinc-complexed (dashed line) N-methyl protoporphyrin IX dimethylester. in chloroform. The Soret bands are attenuated ten-fold.

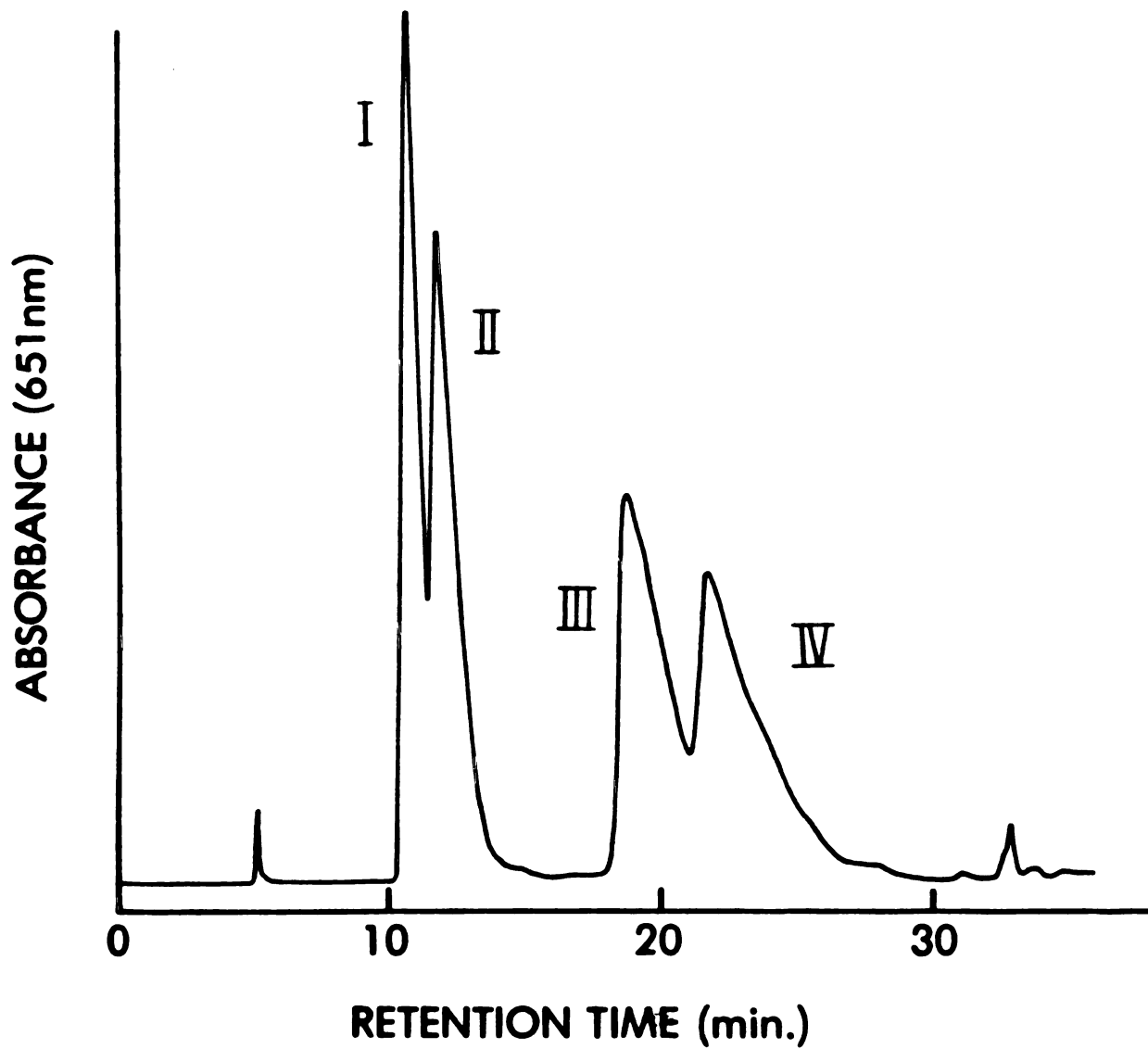
FIELD DESORPTION MASS SPECTRUM OF A MIXTURE  
OF THE N-METHYL PROTOPORPHYRIN IX DIMETHYL ESTER ISOMERS



labeled according to their relative elution pattern in Figure 23. The visible absorption spectrum of each isomer was essentially identical in both the metal free and zinc-complexed forms to the corresponding spectrum of the mixture of isomers (Figure 21). A slight longwavelength shoulder was observed in the spectra of the zinc complexes of isomers I and II. Similar shoulders have been observed with some of the pigments. Each of the metal-free isomers I-IV gave a molecular ion pattern similar to that of the unresolved mixture shown in Figure 22. NMR spectra of each porphyrin in the metal-free, monoprotonated, diprotonated and zinc-complexed forms were recorded. The zinc-complexed porphyrins were chosen for further study since their NMR spectra were insensitive to the presence of trace amounts of acids.

The 360 MHz NMR spectra of the four chloro-zinc complexes of the N-methyl protoporphyrin IX dimethyl ester isomers shown in Figure 24, are labeled I-IV as in the HPLC chromatogram (Figure 23). The NMR spectra of metallo-N-alkylated porphyrins have been shown to differ significantly when the counterion used to neutralize the remaining positive charge on the metal is varied (Jackson and Dearden, 1973). The samples of zinc-complexed I-IV were, therefore, washed with aqueous solutions of sodium chloride to insure that chloride was the uniform counterion. Each spectrum contains all of the resonances associated with the porphyrin protons: (a) meso (10.1-10.4 ppm, 4H), (b) internal vinyl

HPLC SEPARATION OF THE FOUR ISOMERS OF  
N-METHYL PROTOPORPHYRIN IX DIMETHYL ESTER



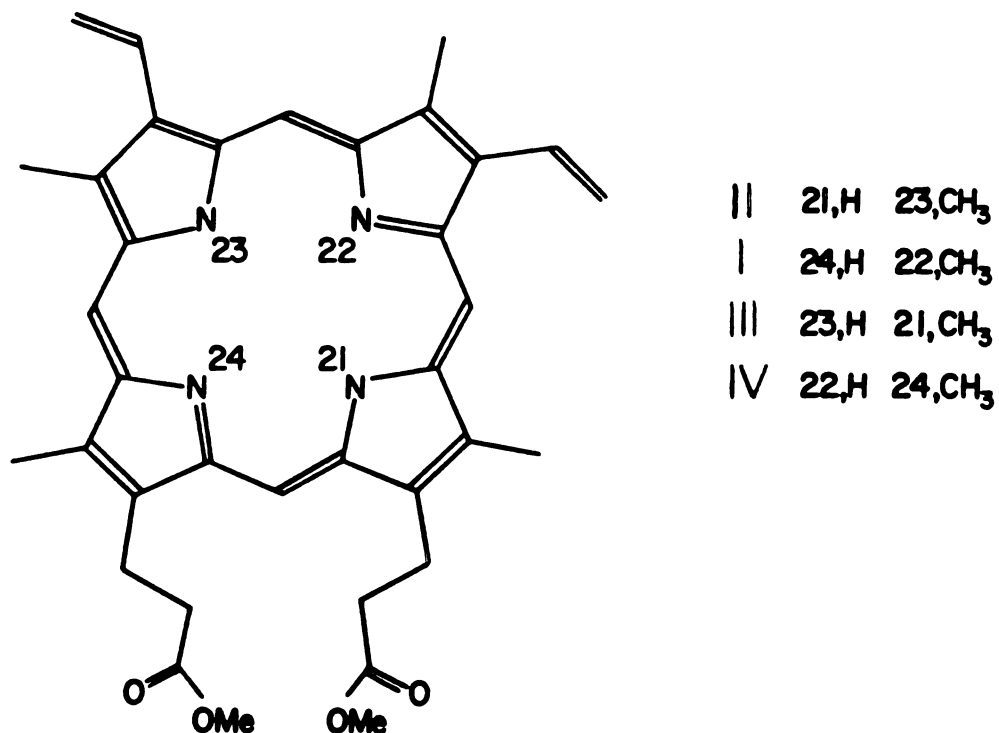
Separation of the four isomers of N-methyl protoporphyrin IX dimethyl ester by HPLC (9.4 X 250 mm Whatman Partisil 10-PAC column, hexane/THF/methanol 97:97:6). The isomers are labeled I-IV in order of elution from the column.

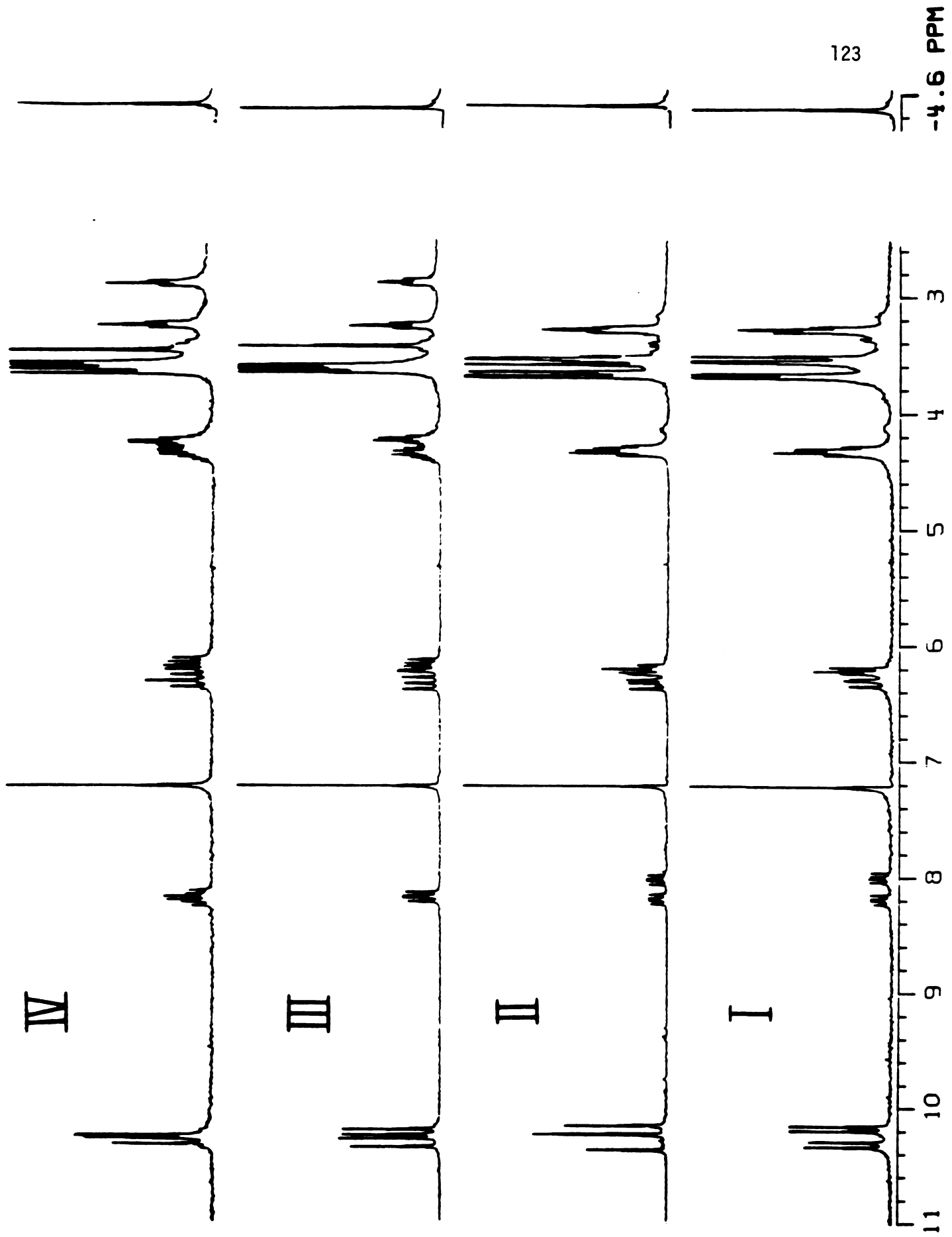


FIGURE 24

360 MHZ NMR SPECTRA OF THE CHLOROZINC-COMPLEXED ISOMERS  
OF N-METHYL PROTOPORPHYRIN IX DIMETHYL ESTER

NMR spectra of the zinc chloride complexed isomers of N-methyl protoporphyrin IX dimethyl ester (next page) in deuteriochloroform. Each spectrum is labeled with the number of the porphyrin isomer (Figure 23) from which the zinc complex was prepared. The methyl group signals are truncated (see Figure 26 for expansion of this region). The structures of the four isomers are given below.





(7.9-8.3 ppm, 2H), (c) terminal vinyl (6.0-6.4 ppm, 4H), (d) benzylic methylene (methylene protons adjacent to the ring) (4.0-4.4 ppm, 4H), (e) ester and ring methyl (3.4-3.8 ppm, 18H), (f) carboxyl methylene (sidechain methylene protons adjacent to the carbonyls) (2.7-3.3 ppm, 4H), and (g) N-methyl (-4.5 ppm, 3H). The unusual three proton singlet at approximately -4.5 ppm is due to the three N-methyl protons nestled in the shielding region of the porphyrin ring current.

The identity of the N-alkylated pyrrole ring in each of the four isomers I-IV cannot be determined directly from the NMR spectra. The position of the N-methyl group may, however, be localized on one of the two types of pyrrole rings present in the protoporphyrin IX macrocycle. Pyrrole rings A and B bear a methyl and a vinyl substituent whereas rings C and D bear a methyl and a methyl propionate substituent. NMR studies of other N-alkylated porphyrins have shown that the proton signals associated with peripheral substituents attached to an N-alkylated pyrrole ring occur approximately 0.1 to 0.2 ppm to higher field than the corresponding signals of the same substituent on the non-alkylated pyrrole rings (Jackson and Dearden, 1973). This upfield shift is due to changes in the structure of the porphyrin macrocycle caused by the presence of the N-alkyl substituent. Structural determinations of N-alkylated porphyrins by X-ray crystallography have shown that the alkylated pyrrole ring

is sharply tilted out of the plane of the porphyrin ring defined by the four meso carbons (Lavallee et al, 1978; Anderson and Lavallee, 1977; Lavallee and Anderson, 1977; Grigg et al, 1970; McLaughlin, 1974). The position of the substituent protons on the alkylated pyrrole ring relative to the porphyrin ring current is sufficiently altered by this perturbation to cause the signals associated with these protons to appear at higher field in the NMR spectrum. Application of this chemical shift correlation permits a partial assignment of the four isomers of N-methyl protoporphyrin IX. A 0.1 ppm upfield shift is observed for one of the two internal vinyl multiplets in the spectra of I and II but not of III and IV (each internal vinyl proton signal is observed as a four line multiplet due to cis and trans scalar coupling to the external vinyl protons ( $J(\text{cis})=12\text{Hz}$ ,  $J(\text{trans})=15\text{Hz}$ ). The benzylic methylene proton signals, on the other hand, are observed as a single set of multiplets in the NMR spectra of I and II whereas one set of multiplets is displaced 0.2 ppm to higher field in the spectra of III and IV. A similar result obtains for the carboxyl methylene proton signals as well. Spin decoupling experiments (not shown) have established that the higher field benzylic and carboxyl methylene protons are on the same side chain. Thus, upfield shifts are observed for one of the two internal vinyl proton multiplets of I and II but not of III or IV, while the protons on one of the two methylene sidechains are displaced to higher field in III and IV but not in I and II.

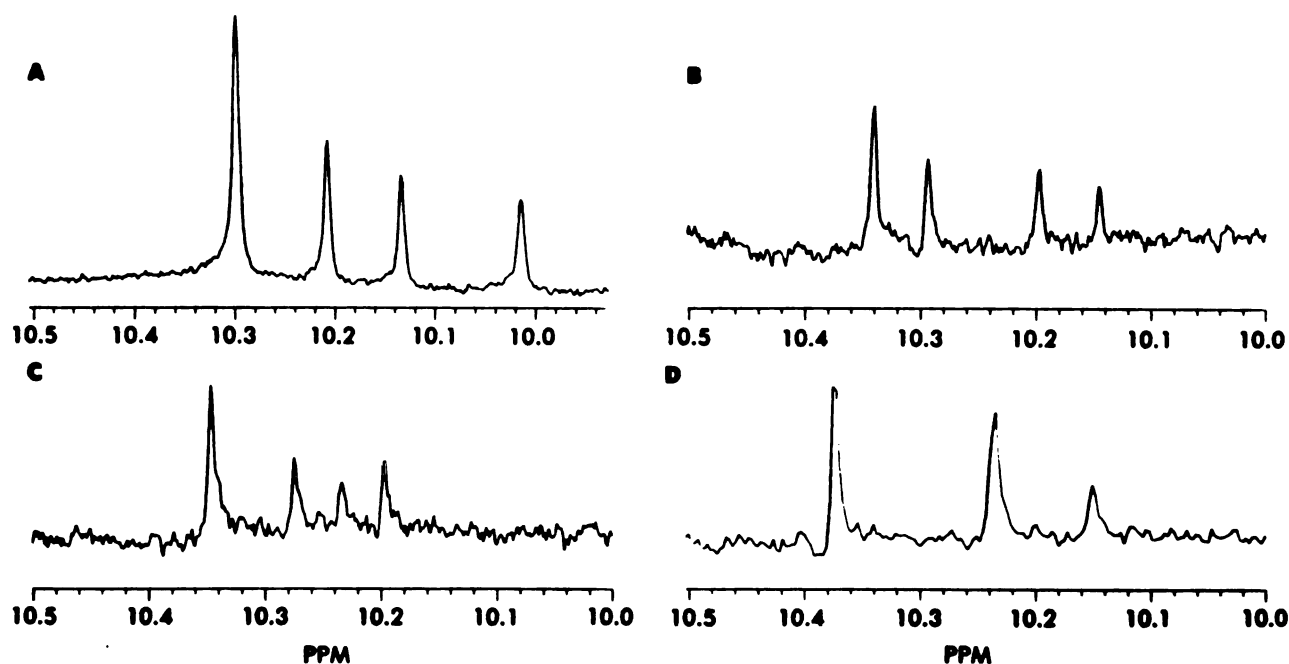
These self-consistent observations lead directly to the assignment of I and II as the isomers of N-methyl protoporphyrin IX dimethyl ester bearing an N-methyl group on a vinyl-substituted pyrrole ring (rings A and B), and III and IV as the two isomers alkylated on propionate-substituted pyrrole rings (rings C and D). Final structural assignments are not possible in the absence of more specific identification of the porphyrin peripheral proton signals. The requisite signal assignments have been made by a combination of techniques including synthesis of the four N-methyl isomers with different but known amounts of deuterium incorporated into the meso positions, determination of spin lattice relaxation times for the peripheral methyl and meso protons, and the use of nuclear Overhauser enhancements (NOE) to establish the spatial relationships of the peripheral protons.

Synthesis of Meso-Deuterated Isomers of N-Methyl Protoporphyrin IX Dimethyl Ester: Assignment of the Alpha and Gamma Meso Protons

The identity of the meso proton signals in the spectra of I-IV can be determined by synthesis of the isomers from protoporphyrin IX containing known, but different, amounts of deuterium at the meso positions. The reaction of mono-deuterated *p*-toluenesulfonic acid with protoporphyrin IX

FIGURE 25

MESO REGIONS OF THE NMR SPECTRA OF PARTIALLY-DEUTERATED  
N-METHYL ISOMERS I-III AND PROTOPORPHYRIN IX DIMETHYLESTER



Meso proton region in the NMR spectra of dimethyl-esterified, partially-deuterated (a) zinc protoporphyrin IX (spectrum taken in the presence of 5 mM perdeuteropyridine), (b) zinc-complexed isomer I of N-methyl protoporphyrin IX, (c) zinc-complexed II, (d) zinc-complexed III. The meso signal identities in (a) are, from right to left: delta, gamma, beta, and alpha.

dimethyl ester has been shown to effect such a differential incorporation of deuterium into the four porphyrin meso positions (Smith et al, 1979). The relative vulnerabilities of the meso positions to acid-catalyzed deuteration has been demonstrated to be, in decreasing order:

gamma,delta,beta,alpha. This exchange reaction gave, in our hands, a 45% yield of deuterated protoporphyrin IX dimethyl ester which was further treated with methyl fluorosulphonate to give partially deuterated I-IV. The reaction mixture, following normal work-up, was fractionated by column chromatography. Unreacted protoporphyrin IX dimethyl ester was complexed with zinc and assayed for deuterium content by NMR to insure that no back-exchange reactions had occurred during methylation and work-up. The ratio of deuterium incorporated into the meso positions of protoporphyrin IX (Figure 25, panel a) was similar to that reported by Smith et al (1979), although, the integrated intensities of the beta and delta meso signals were not significantly different from each other. Significant intensity differences were observed for the alpha and gamma proton signals. The meso regions of the NMR spectra of chlorozinc-complexed I, II, and III are shown and labeled in Figure 25. The assignment of the alpha and gamma meso signals follows directly from the relative amounts of deuterium known to be incorporated into each of the meso positions. The identity of the gamma meso proton signal has been independently confirmed by the relaxation time measurements discussed in the next section. The meso

signal assignments for IV are given in Figure 26.

Spin-Lattice Relaxation Time Measurements: Assignment of the Ester Methyl Proton Signals

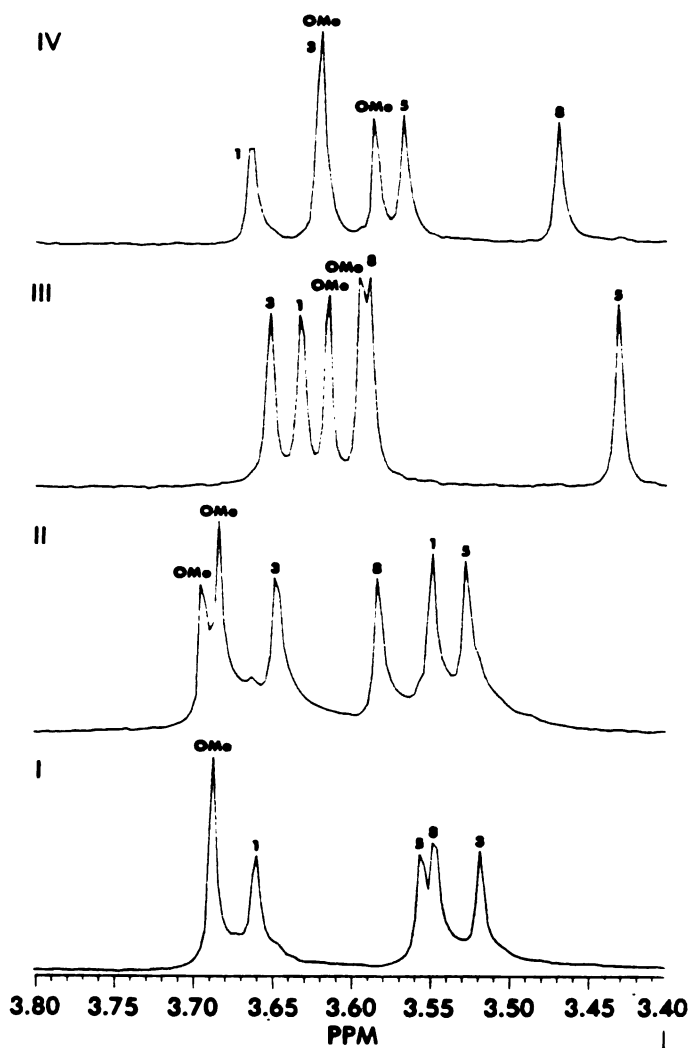
A single isomer of N-methyl protoporphyrin IX dimethyl ester contains six peripheral methyl groups. Four of these methyl groups are pyrrole ring substituents while the remaining two methyl groups are due to the methyl esters on the propionate sidechains of rings C and D. The six methyl groups all give rise to signals within a relatively congested region of the NMR spectrum (Figure 26). Partial dissection of this region can be accomplished by examination of the spin lattice relaxation time ( $T_1$ ) of the protons of each methyl group. This procedure, first implemented by Sanders et al (1978) in studies on protoporphyrin IX and dihydroporphyrins, directly assigns the two methyl ester signals. Sanders and coworkers noted that the aromatic methyl protons of protoporphyrin IX dimethyl ester relax 1.5 to 2 times more rapidly than the ester methyl protons. This difference is due to the fact that the aromatic methyl protons are rigidly held in proximity to the vinyl, methylene, and meso protons, whereas the ester methyl protons are relatively unconstrained. The primary mode of spin lattice relaxation for protons attached to small molecules of this type in deuterated solvents involves radiationless transfer



of magnetization to other nuclei, primarily protons, via through-space dipolar coupling. This relaxation process is accelerated in the case of the porphyrin aromatic methyl protons due to their proximity to the other ring substituent protons. The ester methyl protons, in contrast, spend a large percentage of their time in contact with the solvent (deuterated solvents are poor promoters of relaxation), and relax more slowly. Accordingly, the spin lattice relaxation times were determined for the methyl protons of I-IV. Each of isomers I-IV was found to contain two sets of methyl protons which relaxed much more slowly (ca 1.3 seconds) than the protons of the remaining four methyl groups (ca 0.7 seconds). One ester methyl signal was found to overlap with an aromatic methyl signal in the spectrum of IV. The  $T_1$  value calculated in this case (0.9 seconds) has no real significance since it represents a simultaneous fit to two different, exponentially-decaying functions. The  $T_1$  values measured in these experiments are given in Table 4.

The spin lattice relaxation times for the meso protons were also determined. Sanders et al (1979) reported that the gamma meso proton of metal-free and zinc-complexed protoporphyrin IX dimethyl ester relaxes more rapidly than the remaining three meso protons. A conclusive rationale for this observation was not offered by Sanders, nor is one readily apparent, but the effect was reproducible. The selective deuteration experiments described previously unam-

FIGURE 26

NMR SPECTRA OF THE METHYL PROTON REGION  
OF N-METHYL ISOMERS I-IV

Methyl proton region of the NMR spectra of the four zinc-complexed N-methylprotoporphyrin IX dimethylester isomers. The isomer number is given with each spectrum. The identity of each of the methyl signals is given.

TABLE 4

CHEMICAL SHIFT AND RELAXATION TIMES ( $T_1$ ) VALUES FOR  
MESO AND METHYL PROTONS IN THE FOUR N-METHYLPROTOPORPHYRIN IX  
 DIMETHYL ESTER ISOMERS

<u>GROUP</u>	<u>ISOMER</u> <sup>a</sup>			
	<u>I</u>	<u>II</u>	<u>III</u>	<u>IV</u>
1-methyl	3.659 (0.71)	3.548 (0.66)	3.630 (0.72)	3.663 (0.67)
3-methyl	3.517 (0.65)	3.646 (0.71)	3.650 (0.66)	3.620 (0.98) <sup>c</sup>
5-methyl	3.554 (0.67)	3.526 (0.65)	3.429 (0.65)	3.566 (0.64)
8-methyl	3.546 (0.67)	3.582 (0.64)	3.587 (0.80)	3.469 (0.64)
6-methoxy	3.686 (1.32)	3.682 (1.32) <sup>b</sup>	3.592 (1.14)	3.619 (0.98) <sup>c</sup>
7-methoxy	3.686 (1.36)	3.693 (1.33) <sup>b</sup>	3.613 (1.30)	3.548 (1.24)
N-methyl	-4.492	-4.530	-4.497	-4.535
<u>alpha meso</u>	10.338 (1.16)	10.373 (1.12)	10.344 (1.19)	10.315 (1.07)
<u>beta meso</u>	10.291 (1.10)	10.233 (1.05) <sup>c</sup>	10.272 (1.12)	10.265 (1.10)
<u>gamma meso</u>	10.142 (0.65)	10.150 (0.66)	10.232 (0.70)	10.247 (0.90) <sup>c</sup>
<u>delta meso</u>	10.193 (1.04)	10.236 (1.05) <sup>c</sup>	10.193 (1.08)	10.245 (0.90) <sup>c</sup>

(a). Chemical shifts in ppm ( $T_1$  values in parenthesis in seconds).

(b). These two methoxy groups could not be specifically assigned.

(c). Relaxation time is an average for two superimposed signals

biguously established the identity of the gamma meso signal in each of the four spectra. Examination of the  $T_1$  data for the meso protons of I-III revealed the presence of one rapidly relaxing ( $T_1$ , 0.65-0.70 seconds) and three slowly-relaxing ( $T_1$ , 1.0-1.2 seconds) protons. In each instance the previously assigned gamma meso proton signal coincided with the rapidly relaxing meso proton. The gamma meso signal overlapped with another meso signal in the spectrum of IV. The coincidence of this assignment, based on relaxation data, extends the applicability of Sander's results and provides an independent method for determining the identity of the gamma meso signal in porphyrins such as the green pigments.

#### Proton-Proton Nuclear Overhauser Effects: The Missing Link

Accelerated relaxation of the porphyrin ring methyl protons relative to the ester methyl protons demonstrated in the previous section is due to strong dipole-dipole interactions with adjacent ring substituents held rigidly in place by the porphyrin ring. Through-space dipole dipole interactions provide a conduit through which energy is transferred from proton to proton by radiationless processes. Irradiation of a proton in a magnetic field with energy of a frequency equal to its Larmor precessional frequency induces rapid transitions between its two nuclear spin energy lev-

els. If the irradiated proton is strongly dipole coupled with another proton, a portion of the absorbed energy will be transferred to the second proton and the absorption signal of this second proton in the NMR experiment will be altered. For small molecules this alteration in intensity is observed as an enhancement of the signal arising from the second proton. This phenomenon, known as the Nuclear Overhauser Effect (NOE), is not confined to proton-proton interactions (see Noggle and Schirmer, 1971 for a complete discussion). The enhancement observed is dependent upon the strength of the dipole-dipole coupling which falls off as the sixth power of the internuclear distance. Thus the observation of a signal enhancement in an appropriately designed NMR experiment establishes the proximity of two protons.

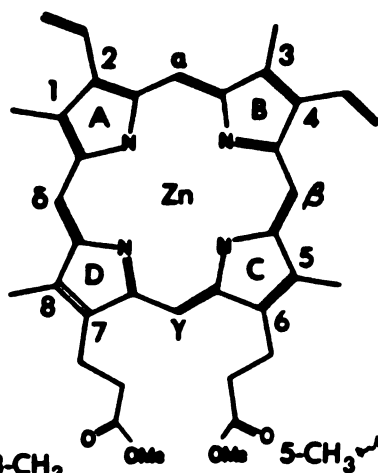
The applicability of nuclear Overhauser effects to porphyrin systems was first demonstrated by Sanders et al (1979). These investigators found that nuclear Overhauser enhancement of the meso signals of zinc protoporphyrin IX dimethyl ester could be observed when the protons immediately adjacent the meso protons were irradiated. For instance, irradiation of the benzylic methylene protons caused an enhancement of the gamma meso proton signal. Due to the rigid positioning of the substituent protons around the periphery of the porphyrin ring, large (15-30%) enhancements were observed (50% enhancement is the theoretical

limit; Noggle and Schirmer, 1971). The application of this technique to the four isomers of N-methyl protoporphyrin IX leads to specific assignments of the methyl groups, once the identity of the meso protons is known. The alpha and gamma meso proton signals for I-IV have been assigned. Assignment of one of the two remaining meso proton signals identifies the last by difference.

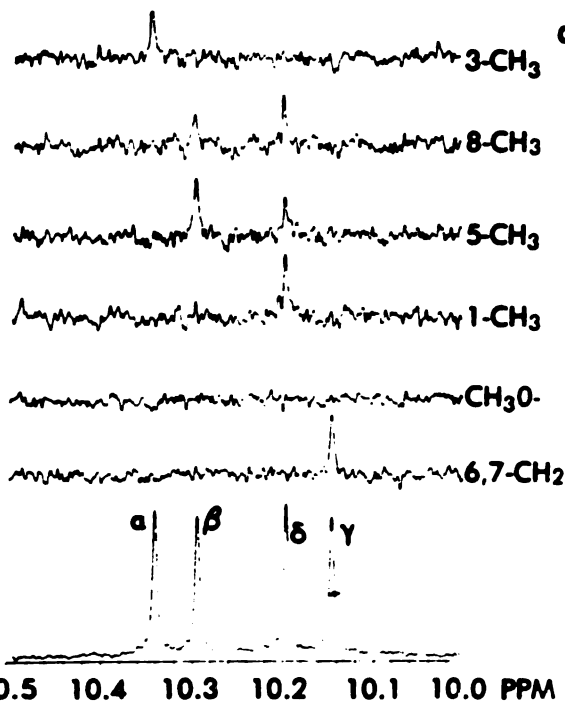
The NMR signals arising from the methyl protons of I-IV are shown in Figure 25. The use of high magnetic fields was absolutely required since selective irradiation of the methyl protons at lower field strengths is not possible. Selective NOE experiments were performed by sequentially irradiating the methyl and methylene protons with sufficient power to saturate their absorption signals in the NMR spectrum. Immediately after the selective pulse was terminated, a broad band  $90^{\circ}$  pulse was applied, and the free induction decay recorded. This sequence was repeated until the required signal-to-noise ratio was achieved. A control spectrum was also recorded using an identical presaturation pulse which did not excite any of the porphyrin protons. The Fourier-transformed spectrum from each experiment was subtracted from the control transformed spectra. Peaks present in the resulting difference spectrum indicate the presence of a signal enhancement. The results of these experiments are shown in Figure 27. The bottom plot in each panel is the meso region spectrum of the isomer in question.

NUCLEAR OVERHAUSER EFFECT ENHANCEMENT  
OF THE MESO PROTON SIGNALS OF I-IV

Nuclear Overhauser effect (NOE) enhancement of the meso proton signals in each isomer of zinc-complexed N-methyl protoporphyrin IX dimethyl ester due to sequential irradiation first of the low-field side-chain methylene protons (Figure 24) and then of each of the methyl groups shown in the corresponding spectrum in Figure 26. The results of these NOE experiments, going from low to high field are shown from the bottom to the top in the panel which corresponds to each isomer. Each NOE result is given as the difference between the meso proton region in the specifically irradiated sample and the meso proton region of a control spectrum. The presence of a peak thus indicates a signal enhancement: (a) isomer I, (b) isomer II, (c) isomer III, and (d) isomer IV. The structure of zinc protoporphyrin IX dimethylester is given at the top. The ring methylated as well as the identity of the meso protons and the group irradiated in each NOE each NOE experiment are given for each isomer. Spectra are shown on the following page.

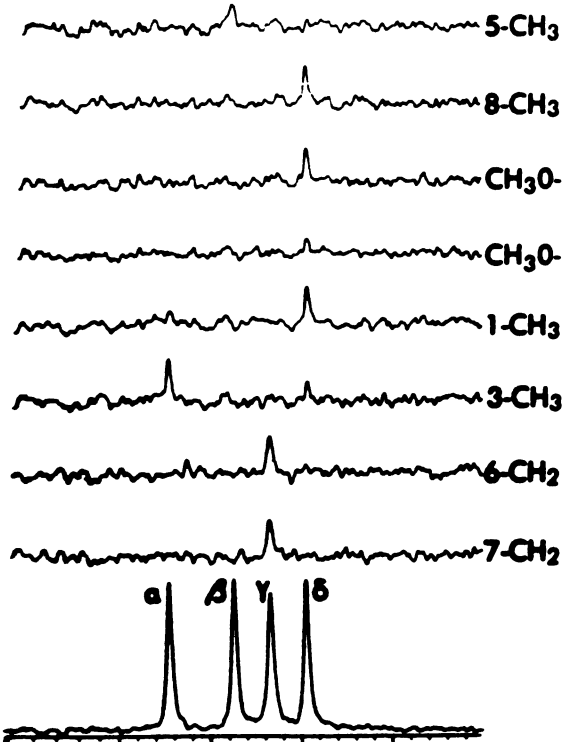


Isomer I Ring B



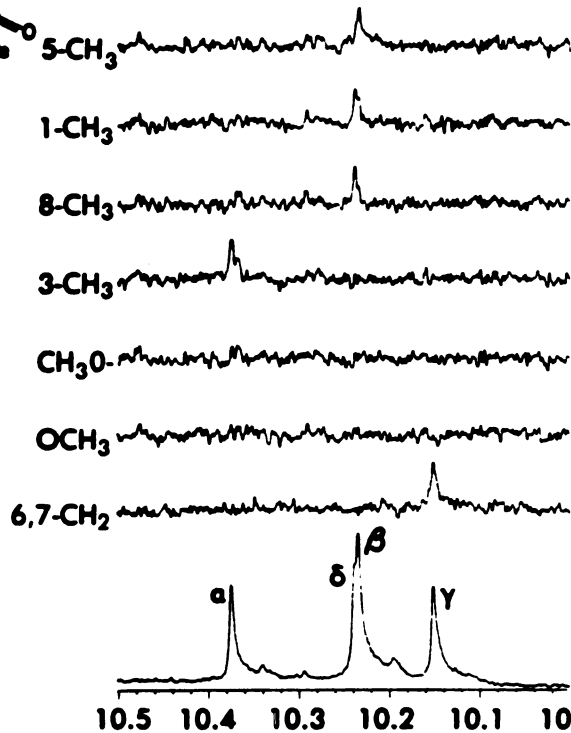
10.5 10.4 10.3 10.2 10.1 10.0 PPM

Isomer III Ring C



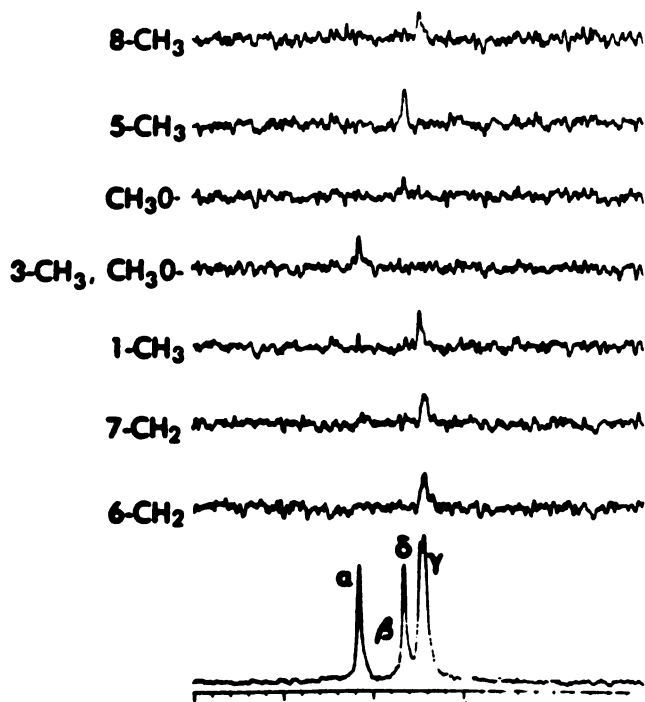
10.5 10.4 10.3 10.2 10.1 10.0 PPM

Isomer II Ring A



10.5 10.4 10.3 10.2 10.1 10.0 PPM

Isomer IV Ring D



10.5 10.4 10.3 10.2 10.1 10.0 PPM



The difference spectra directly above the reference spectrum represent experiments involving sequential irradiation, from low to high field, of each set of methylene or methyl protons. The identity of the set of protons irradiated is given beside the appropriate difference spectrum.

Irradiation of the benzylic methylene protons (I and II, bottom difference spectra; III and IV, bottom two difference spectra) gives rise to an enhancement of the meso proton signal previously assigned as the gamma meso signal. Selective irradiation of each of the methyl protons was not always possible since, in some instances, their resonant frequencies were almost identical. Fortunately, even in these cases, the relative meso proton signal enhancements were sufficiently different to allow assignments to be made (see isomer I where the 5 and 8-methyl proton frequencies differ by only 2.5 Hz). Irradiation of the previously assigned (from the relaxation experiments) ester methyl protons gave rise to no detectable meso signal enhancements except when ring methyl protons were also excited due to spin tickling effects (see III and IV, Figure 27 and 28).

Enhancement of the alpha meso proton signal, previously assigned by the selective deuteration experiments, is only observed when the neighboring 3-methyl protons are irradiated. The NOE experiment, therefore, assigns the 3-methyl proton signal. Enhancement of the delta meso signal will be observed by irradiation of either the 1 or 8-methyl protons.

The identity of the delta meso proton signal is, therefore, uniquely defined since it is the only meso proton flanked by two methyl groups. Assignment of the delta meso proton signal immediately isolates the beta meso proton signal as the only unassigned meso signal. The 5-methyl proton signal is then assignable since it is dipolar-coupled to the beta meso proton (see Figure 27 for enhancements). The only ambiguities remaining are differentiation of the 1 and 8-methyl proton signals and the final structural assignments.

### Isomer Assignments

The NMR spectrum of an N-alkylated porphyrin differs from that of its non-alkylated counterpart in a number of ways. Crucial to this study is the fact that the proton signals associated with the peripheral substituents on the alkylated pyrrole ring are shifted 0.1 to 0.2 ppm to higher field than the signals associated with similarly substituted protons on the vicinal rings. This phenomenon, due to twisting of the alkylated pyrrole ring out of the plane of the porphyrin ring, has been demonstrated for simple N-alkylated porphyrins such as zinc N-methyl octamethyl porphyrin (Jackson and Dearden, 1973). This result has been applied to the four isomers of N-methyl protoporphyrin IX by examination of the internal vinyl and benzylic methylene proton signal chemical shifts. Isomers I and II bear N-

methyl substituents on pyrrole ring A or B, while III and IV bear N-methyl groups on ring C or D.

The 3- and 5-methyl proton signals has been identified by a combination of nuclear Overhauser enhancement, spin lattice relaxation, and chemical exchange studies. The 3-methyl proton signal for isomer I is shifted approximately 0.1 ppm upfield from its position in the other three isomers (Table 4). Isomer I is therefore N-alkylated on the nitrogen of pyrrole ring B.

The 5-methyl proton signals for I-IV exhibit the same pattern except that the 5-methyl signal occupies a highfield position in the spectrum of isomer III (Table 4). The previous conclusion that this isomer is alkylated on ring C or D, supports the assignment of III as the isomer of N-methyl protoporphyrin IX dimethyl ester in which pyrrole ring C is alkylated.

The preceding assignments lead directly, even without specific assignment of the 1- and 8-methyl proton signals, to the identification of isomer II as A ring alkylated and isomer IV as D ring alkylated. (The structural assignments are given in Figure 24) The 1- and 8-methyl signals can be assigned on the basis of chemical shift correlations. The 1- and 3-methyl proton signals of zinc protoporphyrin IX dimethyl ester occur approximately 0.1 ppm downfield from the 5 and 8-methyl proton resonances due to the inductive effects of the adjacent vinyl groups. The chemical shifts

of the 3- and 5-methyl proton signals in the four isomers accurately mirror this difference. It is to be expected, therefore, that the 1-methyl proton signal will be consistently downfield from the 8-methyl signal except perhaps for the isomer where pyrrole ring A is alkylated. This chemical shift correlation has been applied to make the final signal assignments given in Table 4. The identity of the 1-methyl proton signal in isomer II has been confirmed through spin decoupling experiments in which the 1-methyl signal was observed to sharpen when the internal vinyl protons were irradiated. This correlation has also been validated by NMR experiments on the four isomers of N-ethyl protoporphyrin IX dimethyl ester presented in section 3.2.

Both the alkylated pyrrole ring and the pyrrole ring trans to it, the latter to a much lesser degree, have been shown to be tilted out of the plane of the porphyrin ring defined by the two vicinal rings by X-ray crystallographic studies of simple metallo N-alkylated porphyrins (McLaughlin, 1974; Grigg et al, 1970; Lavalley et al, 1978; Anderson and Lavalley, 1977; Lavalley and Anderson, 1977). We have also observed this effect in solution by correlation of the chemical shifts of the methyl group resonances. The average of the two chemical shifts for each methyl group when present on a ring vicinal to an alkylated ring have been computed and are given in Table 5. This value is then compared with the chemical shifts of each methyl group signal

TABLE 5

UPFIELD SHIFT OF THE RING METHYL GROUPS WHEN PRESENT ON THE  
N-ALKYLATED RING OR ON THE RING OPPOSITE TO IT

METHYL GROUP	REFERENCE CHEMICAL SHIFT VALUE <sup>a</sup> (IN PPM)	UPFIELD SHIFT WHEN ON ALKYLATED RING <sup>b</sup> (IN PPM)	UPFIELD SHIFT WHEN ON OPPOSITE RING <sup>c</sup> (IN PPM)
1	3.661 (0.004)	0.113	0.031
3	3.648 (0.004)	0.130	0.028
5	3.560 (0.012)	0.131	0.024
8	3.585 (0.005)	0.116	0.039

- (a). The chemical shift values for the given methyl when on neither the alkylated ring nor on the ring opposite to it (Table 4) have been averaged. The difference between the two averaged values is given in parenthesis.
- (b). The difference between the chemical shift value for the given methyl when on the alkylated ring and the average (reference) value calculated in the first column.
- (c). The difference between the chemical shift value for the given methyl when on the ring opposite to that which is alkylated and the reference value in the first column

when present on the alkylated ring or on the ring trans to the alkylated ring. An upfield shift of 0.113 to 0.131 ppm is observed when the chemical shifts of the alkylated ring methyl signals are compared with the averaged reference value. An upfield shift of 0.028 to 0.039 ppm is observed when the averaged value is compared with the chemical shift of each methyl when present on the ring trans to the alkylated ring. These results indicate that the ring trans to the alkylated ring is also tilted out of the porphyrin plane, but less so than the alkylated ring, in agreement with the X-ray results.

3.12 N-METHYL PROTOPORPHYRIN IX DIMETHYL ESTERS: THE PORPHYRINS ISOLATED FROM RATS TREATED WITH 3,5 DIETHOXYCARBONYL-1,4-DIHYDROCOLLIDINE

Administration of 3,5-diethoxycarbonyl-1,4-dihydrocollidine (DDC) to mice reduces hepatic heme and cytochrome P-450. Concurrently, the levels of heme precursors such as protoporphyrin IX become elevated due to inhibition of mitochondrial ferrochelatase, the enzyme which inserts iron into protoporphyrin IX to make heme. The inhibition of ferrochelatase is indirect since in vitro preparations of the enzyme are unaffected by DDC. Recently, the inhibitory effect of DDC on ferrochelatase in vivo has been ascribed to ill-defined green pigments isolated from the

livers of treated animals (Tephly et al, 1979; DeMatteis et al, 1980). The hepatic pigments formed due to administration of DDC have been found to inhibit in vitro preparations of ferrochelatase.

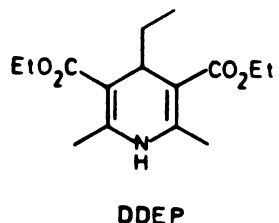
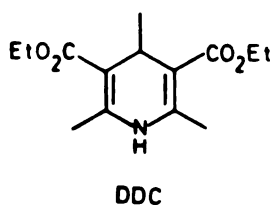
The identity of the pigments isolated from DDC treated animals has recently been established by Hal Beilan of this laboratory. The pigments, isolated as the dimethyl esterified porphyrins, have been examined by HPLC, electronic absorption spectroscopy, NMR, and FDMS and found to be composed of the four isomers of N-methyl protoporphyrin IX dimethyl ester (Ortiz de Montellano et al, 1981d). The isomer of N-methyl protoporphyrin IX alkylated on pyrrole ring A is formed to the greatest extent in the biological system. Minor amounts of isomers I and III (B and C ring methylated) are also formed, as well as a trace of isomer IV.

The pigments isolated from DDC treated animals, as the metal-free, non-esterified porphyrins, have been shown to be potent inhibitors of mitochondrial ferrochelatase (Tephly et al, 1979; DeMatteis, 1980). The relative proportions of the four N-methyl isomers was, of course, unknown (as was the overall structure of the pigments), leaving open the question of differential inhibitory potencies of the four isomers. Accordingly, the four isomers of N-methyl protoporphyrin IX have been tested in a collaborative effort with Gerald Marks and Susan Cole of Queen's University for inhibition of chick embryo liver ferrochelatase activity and

found to be equally-potent inhibitors of the enzyme (Ortiz de Montellano et al, 1980g).

3.2 SYNTHESIS AND CHARACTERIZATION OF THE FOUR ISOMERS OF N-ETHYL PROTOPORPHYRIN IX DIMETHYL ESTER: THE PORPHYRINS ISOLATED FROM RATS TREATED WITH 3,5-DICARBETHOXY-2,6-DIMETHYL- 4-ETHYL-1,4-DIHYDROPYRIDINE

The administration of 3,5-dicarbethoxy-1,4-dihydrocollidine (DDC) to rats results in the formation of abnormal hepatic pigments which have been identified as an unequal mixture of the four isomers of N-methyl protoporphyrin IX (Ortiz de Montellano et al, 1981d). More recently the mysterious origin of the N-methyl group has been investigated by Hal Beilan of this laboratory. Administration of 3,5-dicarbethoxy-2,6-dimethyl-4-ethyl-1,4-dihydropyridine (DDEP), an analog of DDC bearing an ethyl instead of a methyl group at the 4 position, to rats results in the accumulation of hepatic pigments.



The pigments were fractionated by HPLC and found to consist



of four porphyrins. NMR and FDMS studies revealed that the purified pigments were the four isomers of N-ethyl-protoporphyrin IX dimethyl ester. These and other experiments (Ortiz de Montellano et al, 1981e) demonstrate that metabolic transformation of DDC and DDEP by cytochrome P-450 generates a reactive species capable of donating the dihydropyridine 4-alkyl group to a pyrrole nitrogen of prosthetic heme. Heme alkylation by activated DDC occurs primarily at the nitrogen of pyrrole ring A. The alkylation reaction in the case of DDEP is pyrrole ring selective as well. In order to better characterize the destructive interaction, the four isomers of N-ethyl protoporphyrin IX have been synthesized, separated, and the isomers assigned.

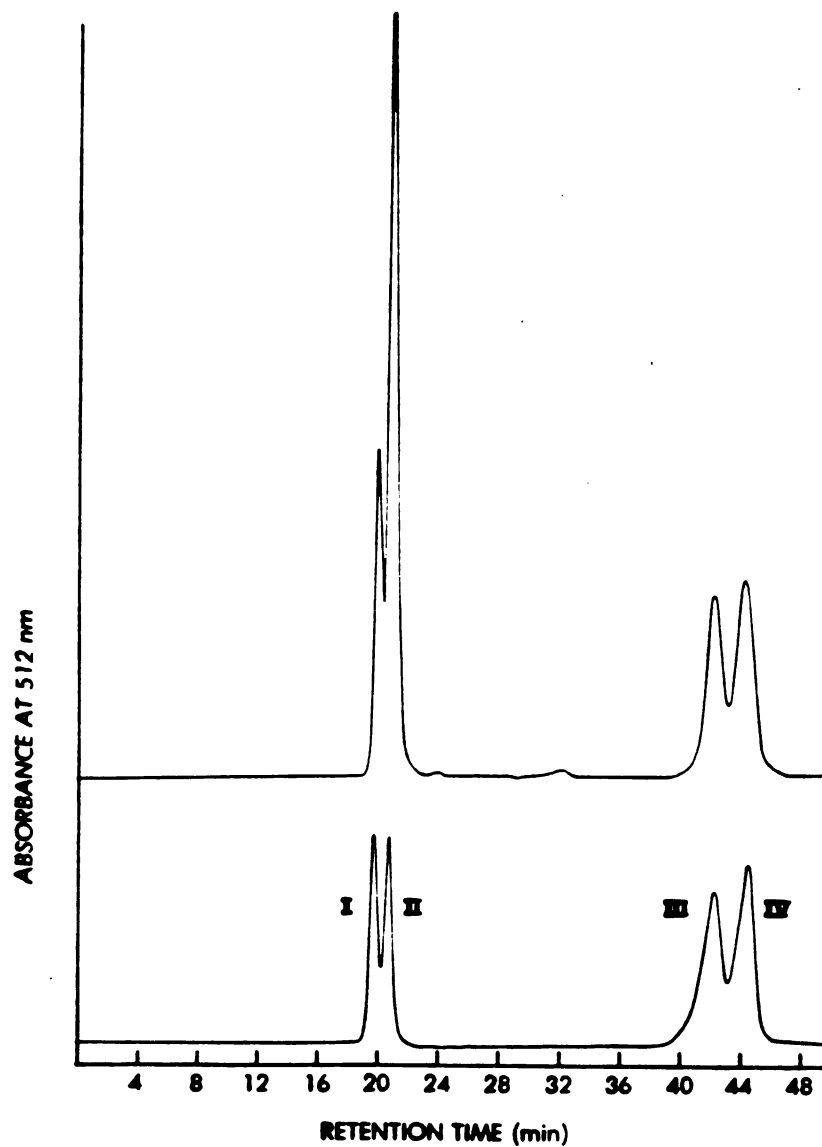
### 3.21 SYNTHESIS AND SEPARATION OF THE FOUR ISOMERS

A dichloromethane solution of ethyl fluorosulphonate (6 mmol) and protoporphyrin IX dimethyl ester (0.84 mmol) was stirred in the dark for 3 days. The residue obtained after work-up was dissolved in acidic methanol and left overnight to insure that the porphyrin carboxyl groups were methyl esterified (some of the ethyl esters were detected by preliminary NMR studies). The porphyrins were then chromatographed on silica gel to give 130 mg of the desired N-ethyl isomers. The four isomers were separated by HPLC. The bottom trace (Figure 28) shows the chromatographic profile of

the four synthetic isomers. The upper trace (Figure 28) shows the elution pattern of the four isomers isolated from the livers of DDEP-treated animals.

The visible absorption spectra of the four metal-free porphyrins were indistinguishable from one another and highly similar to that of the mixture of N-methyl isomers (Figure 21). The spectra of the zinc-complexed porphyrins were essentially identical to the N-methyl spectra (Figure 21) including the presence of a slight shoulder on the longwavelength side of the Soret bands of I and II. Each of the four metal-free pigments gave a molecular ion at  $m/e$  618 when analyzed by FDMS. The same ion was observed in the spectra of the mixture of four isomers (Figure 29).

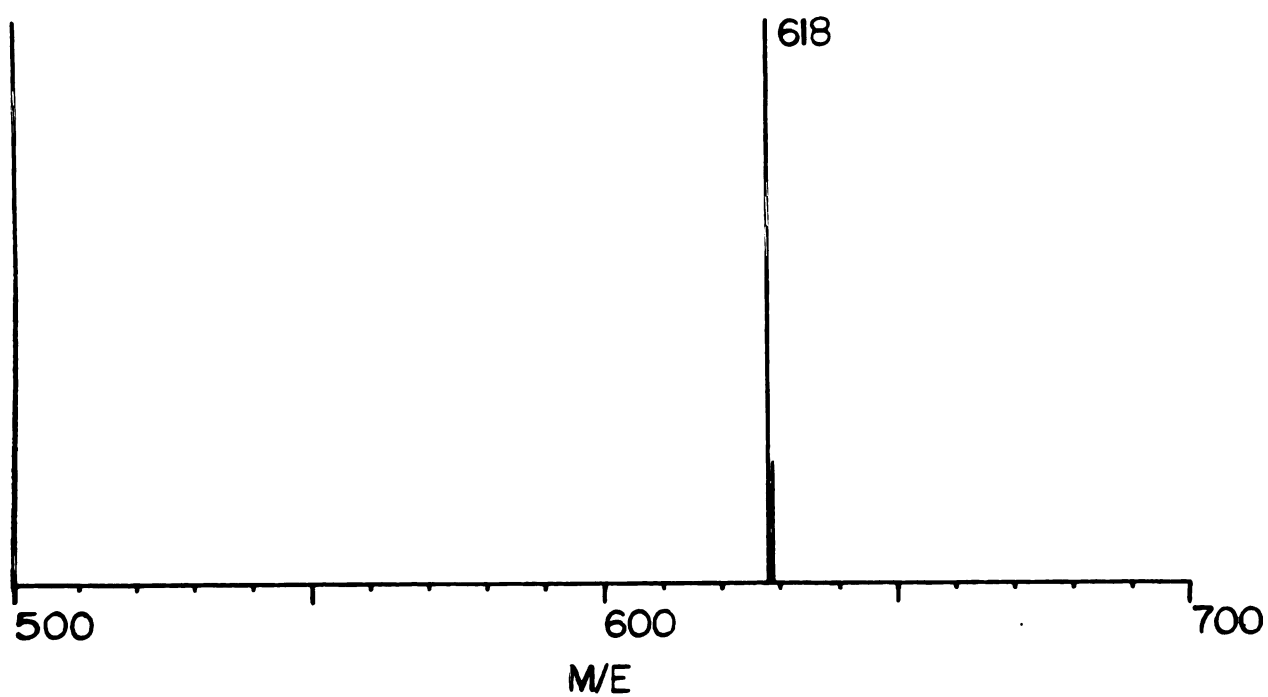
The NMR spectra of the chloro-zinc complexes of the four isomers of N-ethyl protoporphyrin dimethyl ester are shown in Figure 30 and labeled according to increasing HPLC retention times. The signals associated with the various porphyrin protons were present in each spectrum: (a) meso (10.0-10.5 ppm, 4H); (b) internal vinyl (8.0-8.5 ppm, 2H); (c) external vinyl (6.0-6.5 ppm, 4H); (d) benzylic methylene (4.0-4.5 ppm, 4H); (e) benzylic and ester methyl (3.5-3.75 ppm, 18H); (f) carboxyl methylene (2.9-3.3 ppm, 4H); (g) methyl of N-ethyl (-2.0 ppm, 3H); and (h) methylene of N-ethyl (-5 ppm, 2H). The signal at 7.21 ppm is due to chloroform.

SEPARATION BY HPLC OF THE FOUR ISOMERS OF  
N-ETHYL PROTOPORPHYRIN IX DIMETHYL ESTER

HPLC analysis of the abnormal porphyrin isolated from DDEP-treated rats (top) and the mixture of the four synthetic isomers of N-ethyl protoporphyrin IX dimethyl ester. The isomers are numbered I-IV in order of elution from the column. A 9.4 X 500 mm Partisil 10-PAC column eluted with hexane/THF/methanol 12:12:1 was used for the purification.

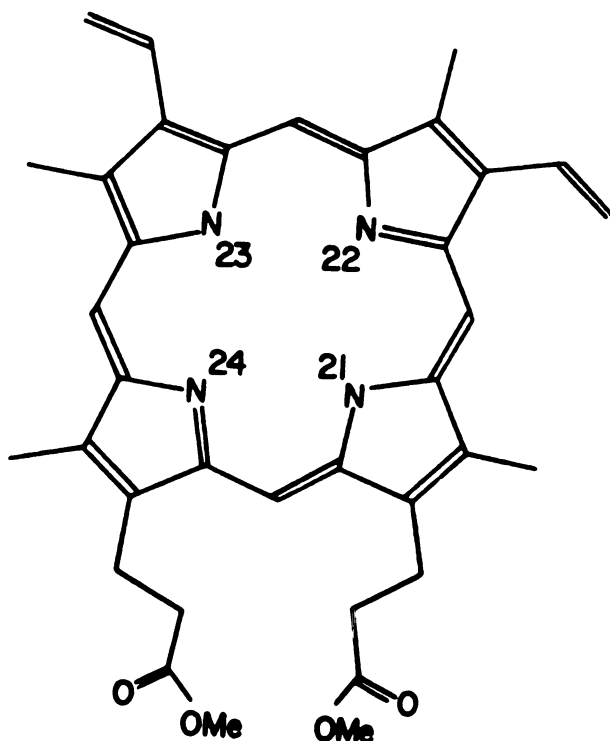
FIGURE 29

FIELD DESORPTION MASS SPECTRUM OF  
A MIXTURE OF THE N-ETHYL PROTOPORPHYRIN IX DIMETHYL ESTER  
ISOMERS

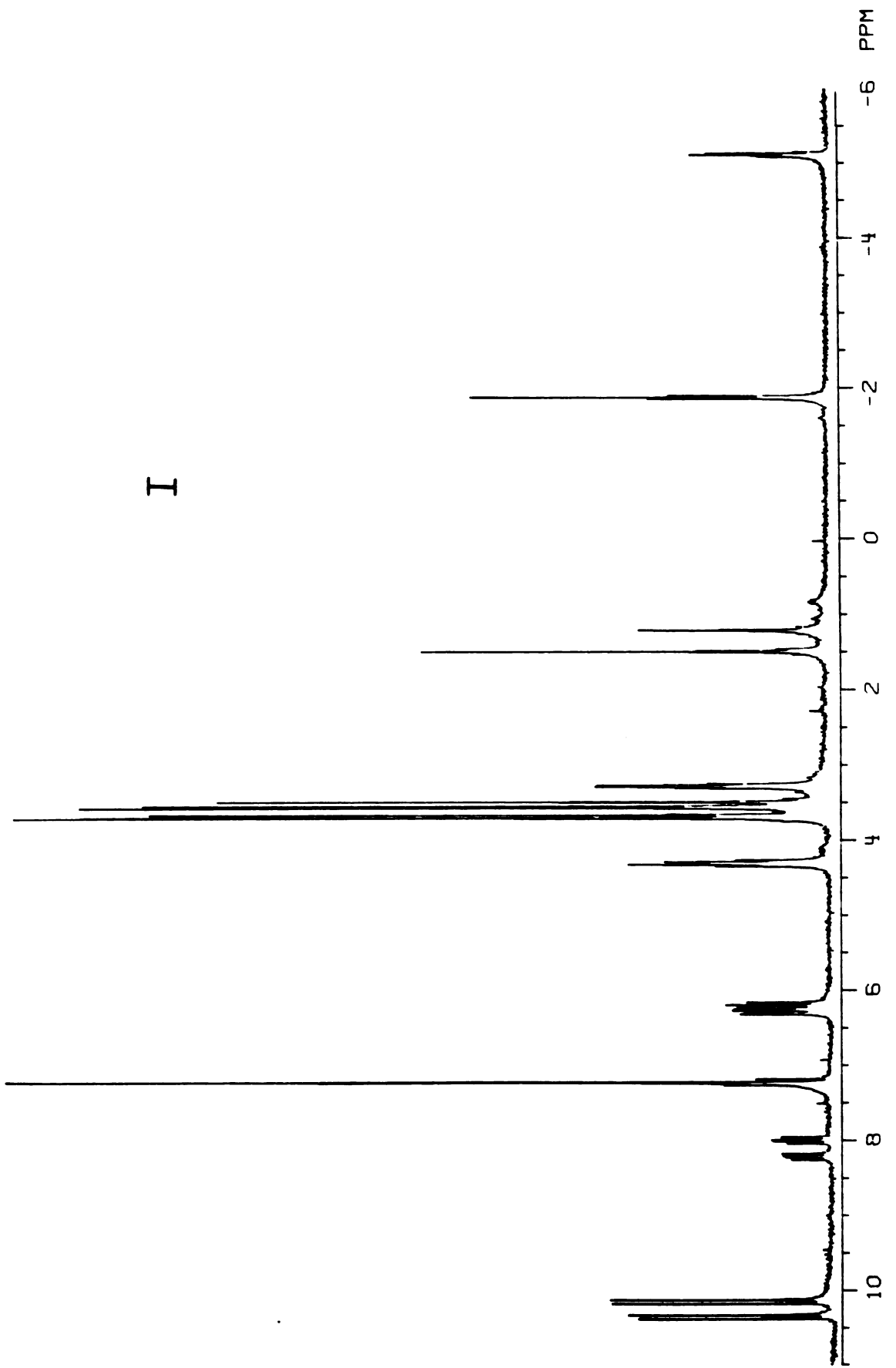


360 MHZ NMR SPECTRA OF THE CHLOROZINC-COMPLEXED ISOMERS  
OF N-ETHYL PROTOPORPHYRIN IX DIMETHYL ESTER

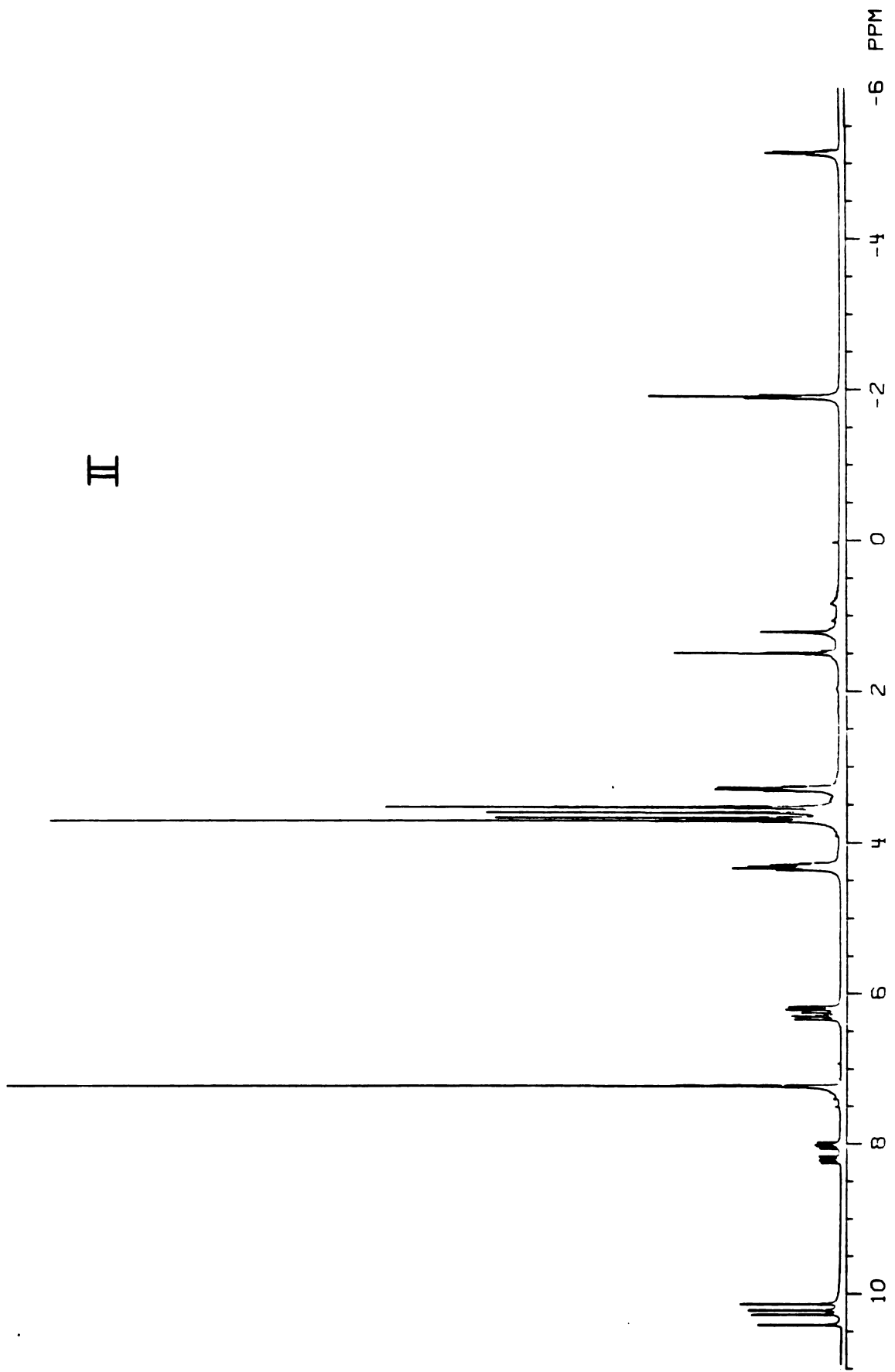
NMR spectra in deuterated chloroform of the zinc chloride complexed isomers of N-ethyl protoporphyrin IX dimethyl ester (next four pages). Each spectrum is labeled with the number of the porphyrin isomer (figure 28) from which the zinc complex was prepared. The structures of the four isomers are given below.



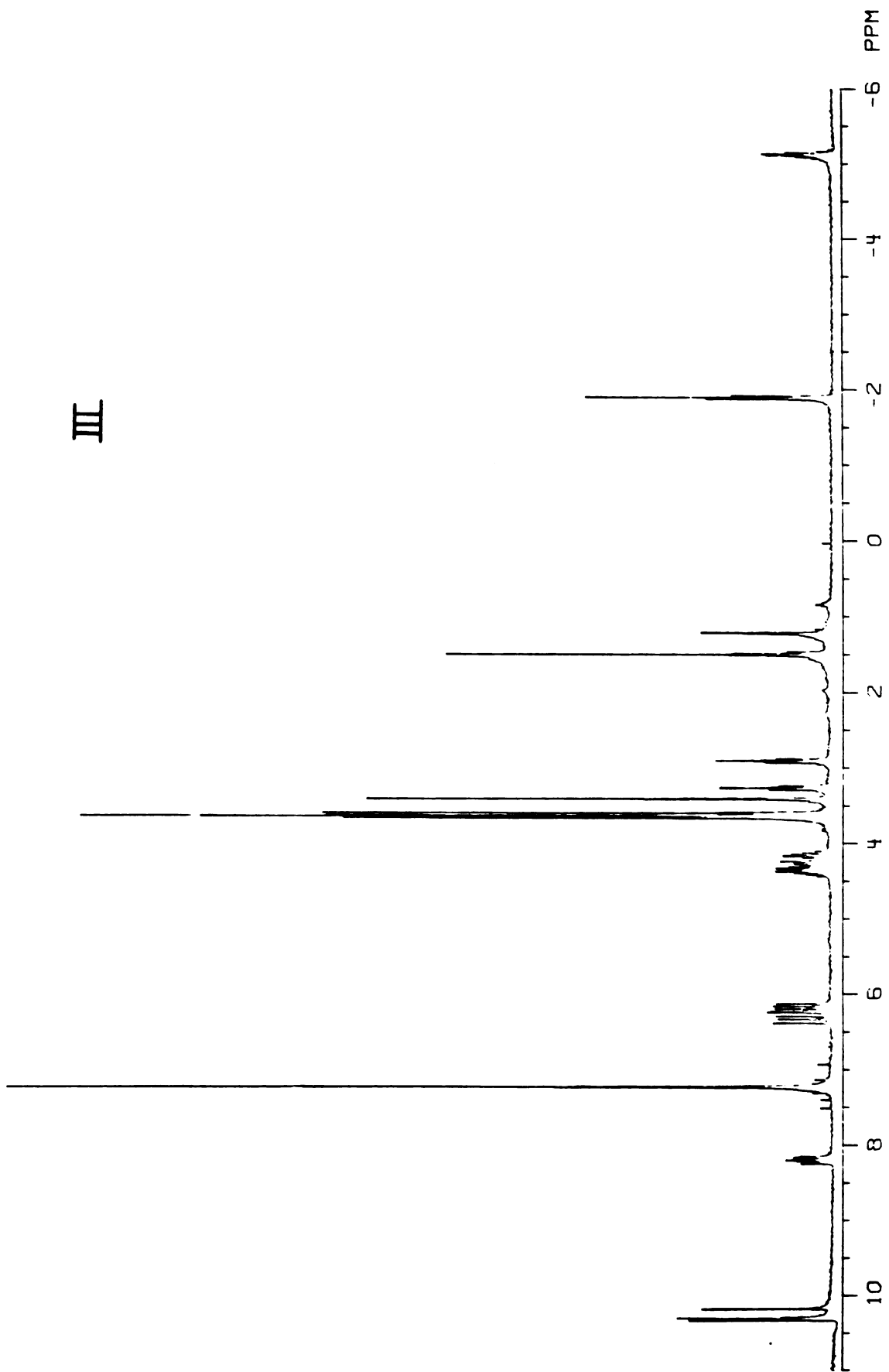
II	21, H	23, -CH <sub>2</sub> CH <sub>3</sub>
I	24, H	22, -CH <sub>2</sub> CH <sub>3</sub>
III	23, H	21, -CH <sub>2</sub> CH <sub>3</sub>
IV	22, H	24, -CH <sub>2</sub> CH <sub>3</sub>



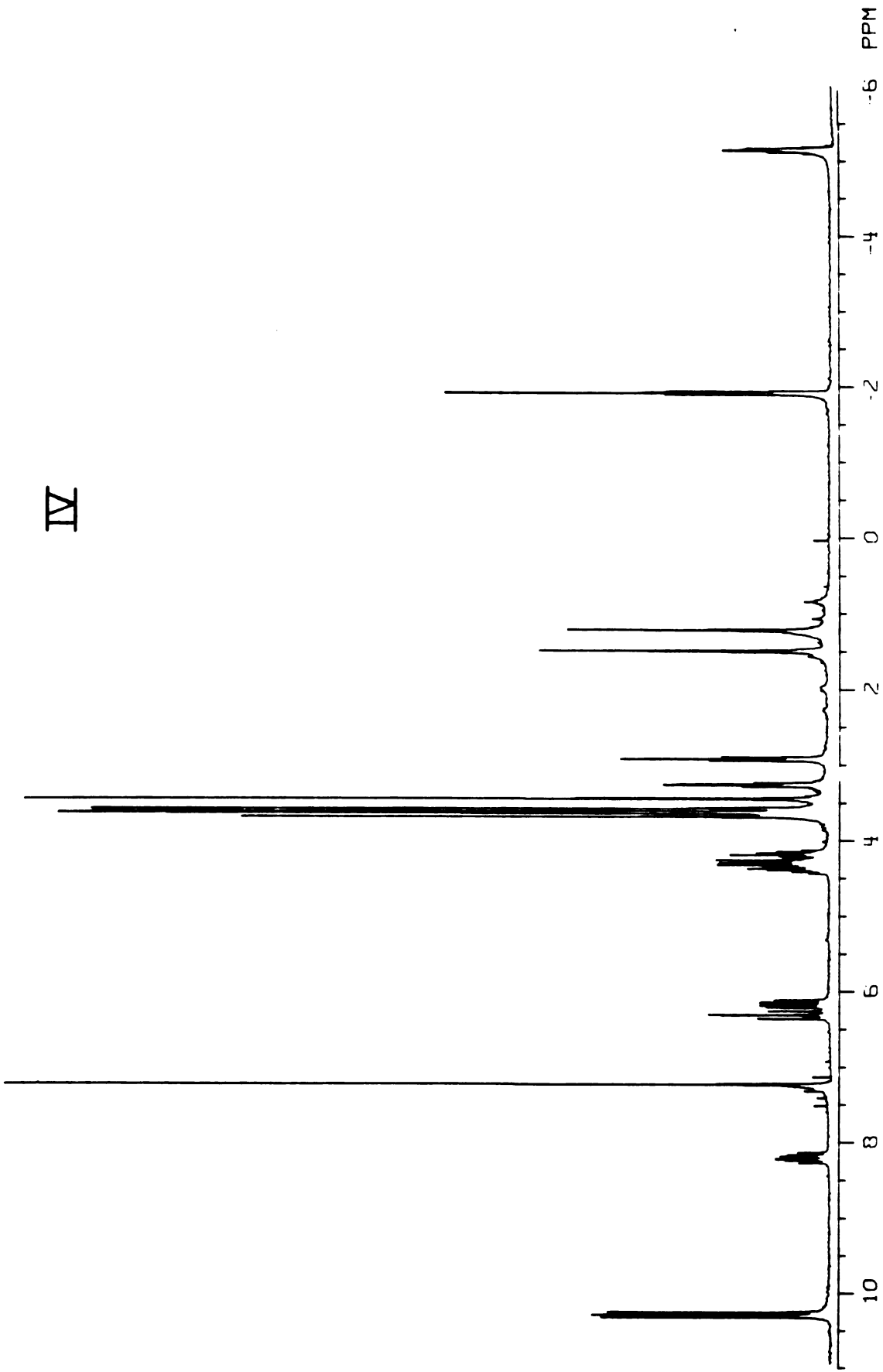
II



III







### Strategy of Peripheral Proton Assignments

The strategy employed to assign the peripheral resonances has been refined to the point that the selective meso proton deuteration experiments utilized in the N-methyl isomer assignment studies are no longer required. The two additional experiments which make this possible are the detection of scalar coupling between the internal vinyl protons and the methyl protons on pyrrole ring A and B and detection of dipolar, through space coupling between the alpha and beta meso protons and their neighboring 2 and 4 internal vinyl protons. Similar connectivities have been observed for protoporphyrin IX dimethyl ester (Sanders et al, 1979). Isomers I and III will be used as examples of these techniques.

### Gamma Meso Proton Signal

The gamma meso proton signal may be identified by two independent methods. The first of these requires measurement of the meso proton spin lattice relaxation times. These values are reported in Table 6. The gamma meso proton is more rapidly relaxed by its surroundings than the remaining three meso protons. The rapidly relaxing meso proton, thus identified as the gamma meso proton signal, is at 10.117 ppm for isomer I and 10.292 ppm for isomer III (see Table 6). These assignments are confirmed by the presence of through-space dipolar coupling, detected by nuclear Overhauser

enhancement studies, between the benzylic methylene protons and these same meso protons (Figure 31a,c).

#### Ester Methyl Proton Signals

The signals arising from the methyl ester protons are determined from the  $T_1$  data (Table 6). The ester methyl protons relax significantly more slowly (1.5 to 2.0 times) than the ring methyl protons. The ester methyl  $T_1$ 's varied from 1.1 to 1.2 seconds while the ring methyl proton  $T_1$ 's fell within the range of 0.55 to 0.70 seconds. The  $T^1$  data does not uniquely assign the ester methyl protons. The assignments are confirmed by the fact that irradiation of the ring methyl protons gives rise to an enhancement of a meso proton signal whereas irradiation the ester methyl protons does not.

#### Delta Meso Proton Signal

The delta meso proton is uniquely flanked by two methyl groups (1 and 8) and may be assigned by the NOE experiment. The delta meso signal is at 10.167 ppm for isomer I (Figure 35a) and at 10.196 ppm for isomer III (Figure 35c).

#### 1,3,8 Methyl Proton Signals

The 1-methyl proton (ring A) shares its pyrrole ring with a vinyl group (2 vinyl) whereas, the 8-methyl group shares the D ring with a beta-carboxy-ethyl group. The 1

and 3 methyl protons are slightly coupled (0.8 Hz) with the 2 and 4 internal vinyl protons respectively. This coupling can be eliminated by irradiation of the 1 and 3-methyl group protons. Once the coupling is removed, the internal vinyl proton resonances are observed to sharpen. Figure 31b,d shows the effects of irradiating (in a spin decoupling experiment) each of the methyl protons (identities given on the right) on the internal vinyl signals. The bottom trace corresponds to the signal without irradiation. Sharpening can be observed in the second (from the bottom) and fifth spectra of isomer I (Figure 31b) and in the second and third spectra of isomer III (Figure 31d). The 1-methyl protons are therefore identified as those which are dipolar-coupled to the delta meso proton and scalar-coupled to an internal vinyl proton (I, 3.658 ppm; III, 3.623 ppm). The 8-methyl protons are assigned, by difference, as being dipolar-coupled to the delta meso proton but not scalar-coupled to an internal vinyl proton (I, 3.539 ppm; III, 3.589 ppm). The 3-methyl protons are also assigned by difference since they are scalar-coupled to an internal vinyl proton but are not dipolar-coupled to the delta meso proton (I, 3.483 ppm; III, 3.648 ppm).

#### Alpha and Beta Meso, and 5 Methyl, Proton Signals

Irradiation of the 3-methyl protons (just assigned) produces a nuclear Overhauser enhancement of the alpha meso

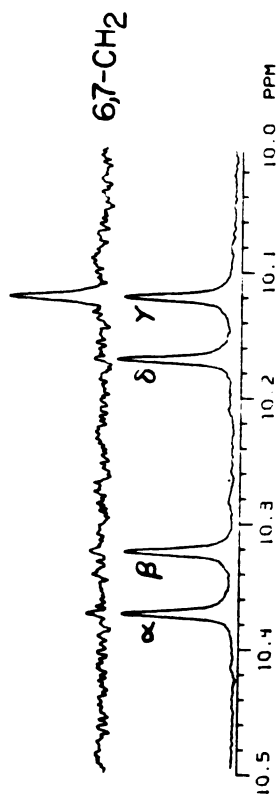
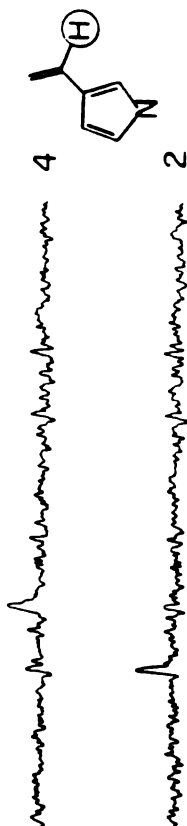
N-ETHYL PROTOPORPHYRIN IX DIMETHYL ESTER ISOMERS I AND III:  
NOE ENHANCEMENT OF THE MESO SIGNALS  
AND METHYL TO VINYL PROTON COUPLING

Nuclear Overhauser effect (NOE) enhancement of the meso proton signals in isomers I (a) and III(c) of zinc-complexed N-ethyl protoporphyrin IX dimethyl ester due to irradiation of the methylene, internal vinyl, and methyl protons (Figure 30). The identity of the irradiated protons is given on the right side of each difference spectrum. Each NOE result is given as the difference between the meso proton region in the specifically irradiated sample and the meso proton region of a control spectrum.

Sharpening of the internal vinyl proton signals of isomers I(b) and III (d) of zinc-complexed N-ethyl protoporphyrin IX dimethyl ester due to specific irradiation of each set of methyl group protons (identity given on right side of each spectrum). The identity of the internal vinyl proton signals is given at the top of the figure. The sharpening observed is due to removal of scalar coupling (0.8 Hz) between an internal vinyl proton and the methyl group protons which share a common pyrrole ring.

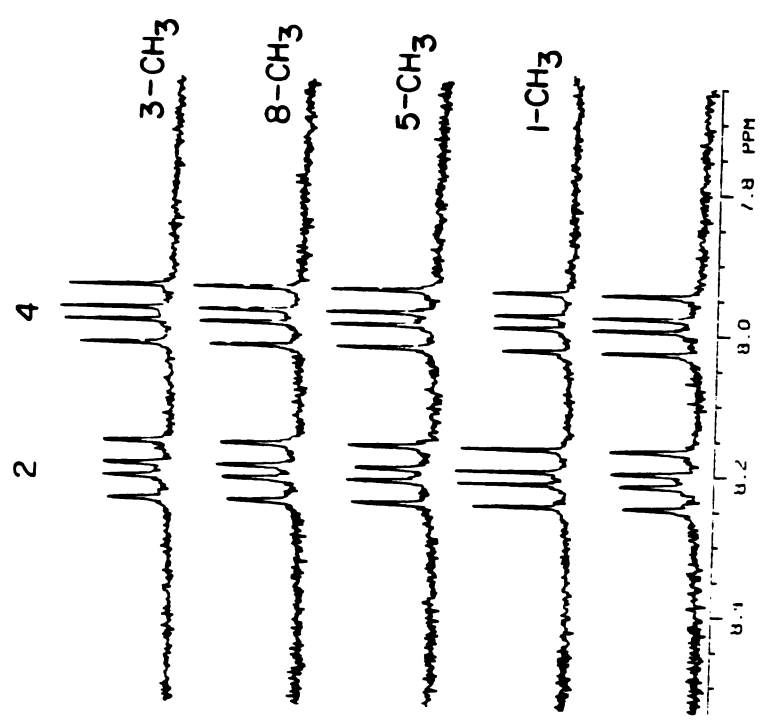
Spectra for I are shown on the next page. Spectra for III are shown on the following page.

a

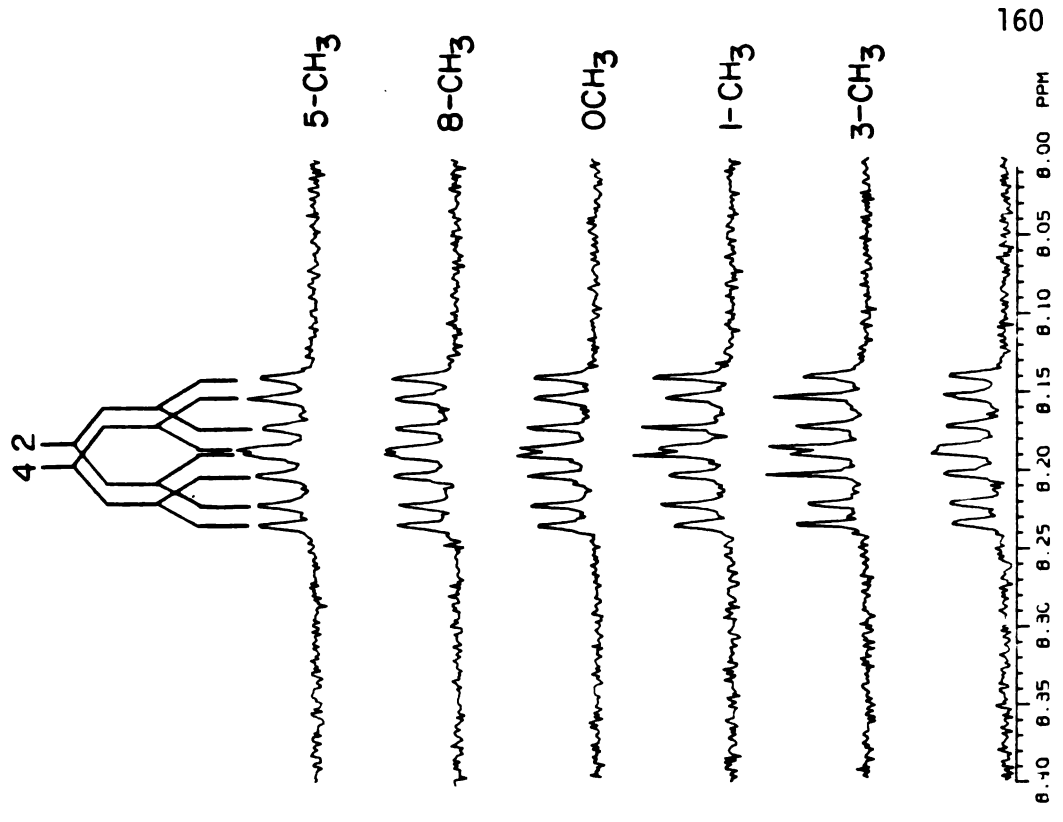


10.5 10.4 10.3 10.2 10.1 10.0 PPM

b



d



c

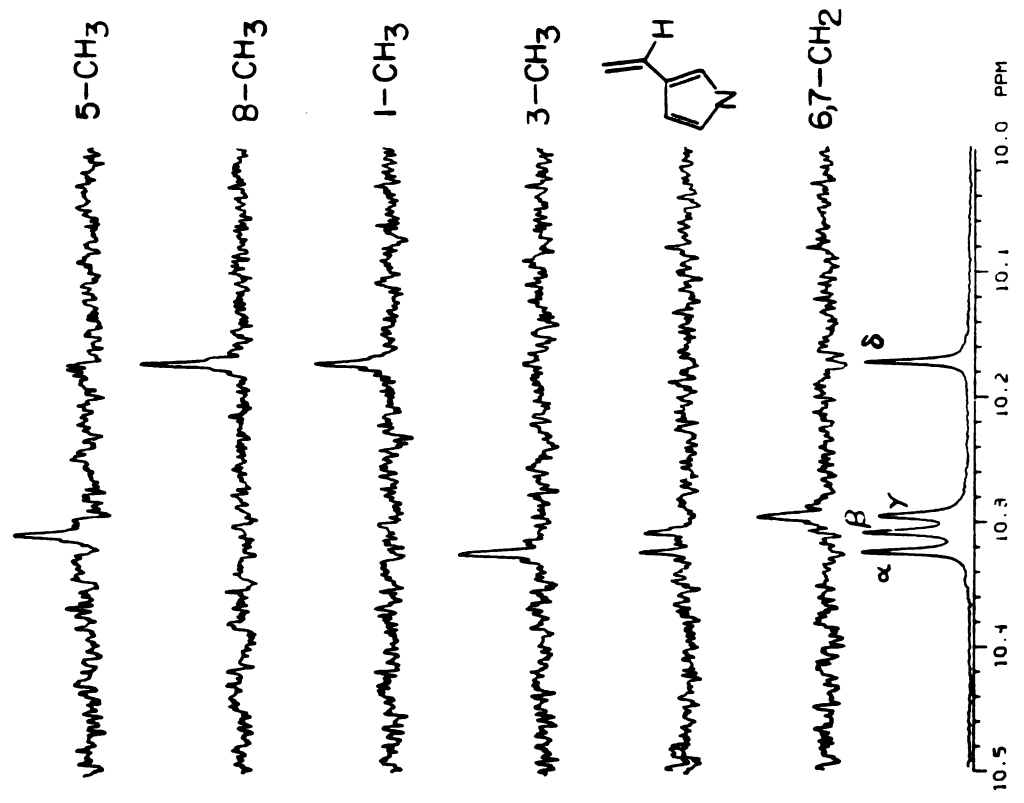


TABLE 6

CHEMICAL SHIFT AND RELAXATION TIME ( $T_1$ ) VALUES FOR THE  
MESO AND METHYL PROTONS IN THE FOUR N-ETHYLPROTOPORPHYRIN IX  
 DIMETHYL ESTER ISOMERS

<u>GROUP</u>	<u>ISOMER</u> <sup>a</sup>			
	<u>I</u>	<u>II</u>	<u>III</u>	<u>IV</u>
1-methyl	3.658 (0.62)	3.519 (0.58) <sup>b</sup>	3.623 (0.77) <sup>b</sup>	3.672 (0.64)
3-methyl	3.483 (0.60)	3.655 (0.60)	3.648 (0.61)	3.615 (0.68)
5-methyl	3.563 (0.58)	3.513 (0.58) <sup>b</sup>	3.397 (0.61)	3.565 (0.62)
8-methyl	3.539 (0.59)	3.589 (0.55)	3.583 (0.58)	3.436 (0.62)
methoxy	3.690 (1.20)	3.695 (1.16)	3.619 (0.77) <sup>b</sup>	3.626 (1.16)
methoxy	3.701 (1.20)	3.695 (1.16)	3.611 (1.13)	3.606 (1.15)
<u>alpha meso</u>	10.369 (1.06)	10.402 (0.98)	10.320 (1.01)	10.294 (1.05)
<u>beta meso</u>	10.319 (1.01)	10.206 (1.04)	10.305 (0.96)	10.243 (0.93)
<u>gamma meso</u>	10.117 (0.64)	10.122 (0.63)	10.292 (0.63)	10.303 (0.64)
<u>delta meso</u>	10.167 (0.95)	10.264 (1.05)	10.196 (1.03)	10.278 (1.04)
N-CH <sub>2</sub> -CH <sub>3</sub>	-5.107	-5.138	-5.131	-5.143
N-CH <sub>2</sub> -CH <sub>3</sub>	-1.884	-1.908	-1.902	-1.923

(a). Chemical shifts in ppm ( $T_1$  values in parenthesis in seconds).

(b). Relaxation time is an average for two superimposed signals.



proton signal (I, 10.369 ppm; III, 10.320 ppm). The beta meso and 5-methyl proton signals can then be assigned since they are the only two remaining signals. The observation of NOE enhancements of the beta meso signals (I, 10.319 ppm; III, 10.305 ppm) upon irradiation of the 5-methyl protons (I, 3.563 ppm; III, 3.397 ppm) confirms the assignments.

#### Isomer Assignment and Chemical Shift Correlations

The identity of the alkylated pyrrole ring may be deduced from the chemical shifts of the peripheral proton resonances. The methyl, internal vinyl and benzylic resonances are found 0.1 to 0.2 ppm to higher field, compared to their corresponding values when occupying rings vicinal to an alkylated ring, when the protons giving rise to these signals are found on the alkylated pyrrole ring. We have also observed that the signals associated with the peripheral substituents on a ring trans to an alkylated ring are shifted upfield approximately 0.040 ppm. Examination of the chemical shifts for the ring methyl proton signals (Table 6) leads directly to the final isomer assignments. Four values (one for each isomer) are presented for the chemical shifts of each methyl group. A dramatic upfield shift is observed for the 1-methyl group protons of isomer II as well as a smaller 0.042 ppm shift in isomer III when compared with the averaged value for the two remaining isomers. Thus isomer II is the porphyrin alkylated on pyrrole ring A. A similar

TABLE 7

UPFIELD SHIFT OF THE RING METHYL GROUPS WHEN PRESENT ON THE  
N-ALKYLATED RING OR ON THE RING OPPOSITE TO IT

METHYL GROUP	REFERENCE CHEMICAL SHIFT VALUE <sup>a</sup> (IN PPM)	UPFIELD SHIFT WHEN ON ALKYLATED RING <sup>b</sup> (IN PPM)	UPFIELD SHIFT WHEN ON OPPOSITE RING <sup>c</sup> (IN PPM)
1	3.665 (0.014)	0.149	0.042
3	3.651 (0.017)	0.168	0.036
5	3.564 (0.002)	0.167	0.048
8	3.586 (0.006)	0.150	0.047

- (a). The chemical shift values for the given methyl when on neither the alkylated ring nor on the ring opposite to it (Table 6) have been averaged. The difference between the two averaged values is given in parenthesis.
- (b). The difference between the chemical shift value for the given methyl when on the alkylated ring and the average (reference) value calculated in the first column.
- (c). The difference between the chemical shift value for the given methyl when on the ring opposite to that which is alkylated and the reference value in the first column.

analysis of the remaining isomers and methyl group resonances irrevocably leads to the assignment of I as B ring alkylated, III as C ring alkylated, and IV as D ring alkylated (see Figure 30 for structures). A mean upfield shift of 0.158 ppm ( $\pm 0.010$ ) in chemical shift is observed when a methyl group is on an alkylated ring compared to the average of its chemical shift when it is attached to a pyrrole ring vicinal to an alkylated ring (Table 7). A more modest, but significant, 0.043 ppm ( $\pm 0.005$ ) shift is observed when the methyl proton is on the ring trans to the alkylated ring. These difference values are slightly higher than those obtained for the N-methyl isomers (Table 5). This may be due to the effect of the increased size of the N-alkyl substituent.

### 3.22 CONCLUSIONS AND APPLICATIONS

The NMR studies outlined in the preceding section provide a practical methodology for determination of the structure of N-alkylated derivatives of protoporphyrin IX. Consistent and significant upfield shifts of proton signals on substituents attached to an alkylated pyrrole ring have been cataloged. A firm base has therefore been established from which the ultimate structures of the green pigments may be ascertained (see 3.3 and 3.4).

The major isomer of N-ethyl protoporphyrin IX formed during alkylation of the prosthetic heme group of cytochrome P-450 by an enzymatically-activated form of DDEP is that bearing the N-ethyl group on pyrrole ring A. Exactly the same ring is preferentially alkylated during destruction by DDC. The fact that a significantly greater proportion of the other ring alkylated isomers is formed in the case of DDEP than DDC raises some intriguing questions about substrate binding and the heme alkylation reaction.

Each of the four isomers of N-methyl protoporphyrin IX was found to be equally potent as an inhibitor of chick embryo liver ferrochelatase (Ortiz de Montellano et al, 1980g). The four N-ethyl isomers of non-esterified protoporphyrin IX have also been examined for inhibition of this enzyme. Isomers I and II were found to be equally-potent inhibitors of ferrochelatase, whereas isomers III and IV were 30-100 times less potent. Isomers I and II gave inhibition profiles very similar to those of the N-methyl isomers (Ortiz de Montellano, P.R., Kunze, K. L., Cole, S.B., and Marks, G.; submitted for publication).

### 3.3 STRUCTURES OF THE GREEN PIGMENTS ISOLATED FROM RATS TREATED WITH ETHYLENE AND PROPENE

#### The Ethylene Adduct

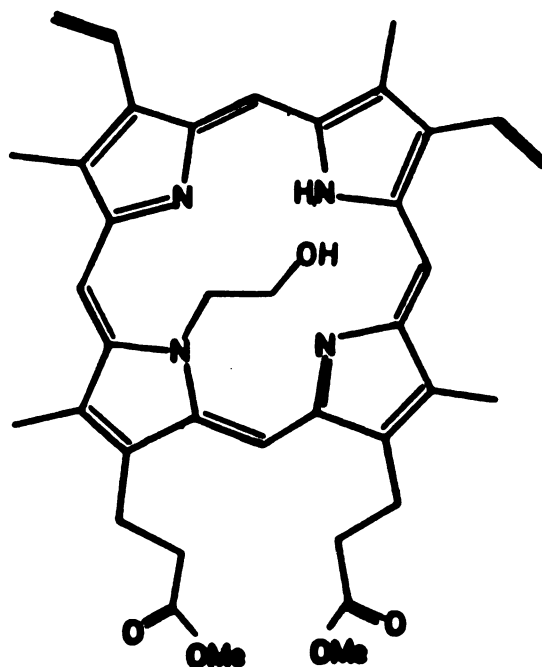
Purification of the ethylene adduct has been reported (Ortiz de Montellano et al, 1981a). The procedure used included two steps involving chromatography on thin layer silica plates, passage down an alumina column, and two separate fractionations by HPLC. In all these steps the porphyrin was observed to chromatograph as a single band. The electronic absorption spectra have been reported (Ortiz de Montellano and Mico, 1980b). The metal-free pigment is characterized by a FDMS monoprotinated molecular ion at  $m/e$  635. This value corresponds to the one expected from addition of the molecular weights of protoporphyrin IX dimethyl ester (590) plus ethylene (28) plus atomic oxygen (16). The 360 MHz NMR spectrum of the chloro-zinc complex of the ethylene adduct is shown in Figure 32. The signals associated with the peripheral protons are: (a) meso (10.2-10.4 ppm, 4H); (b) internal vinyl (8.0-8.5 ppm, 2H); (c) external vinyl (6.0-6.5 ppm, 4H); (d) benzylic methylene (3.9-4.5 ppm, 4H); (e) ring and ester methyl (3.3-3.8 ppm, 18H); and (f) carboxyl methylene (3.0-3.3 ppm; 4H). Irradiation of the internal vinyl protons removes scalar coupling to the external vinyl protons and collapses the 8 line signal to a

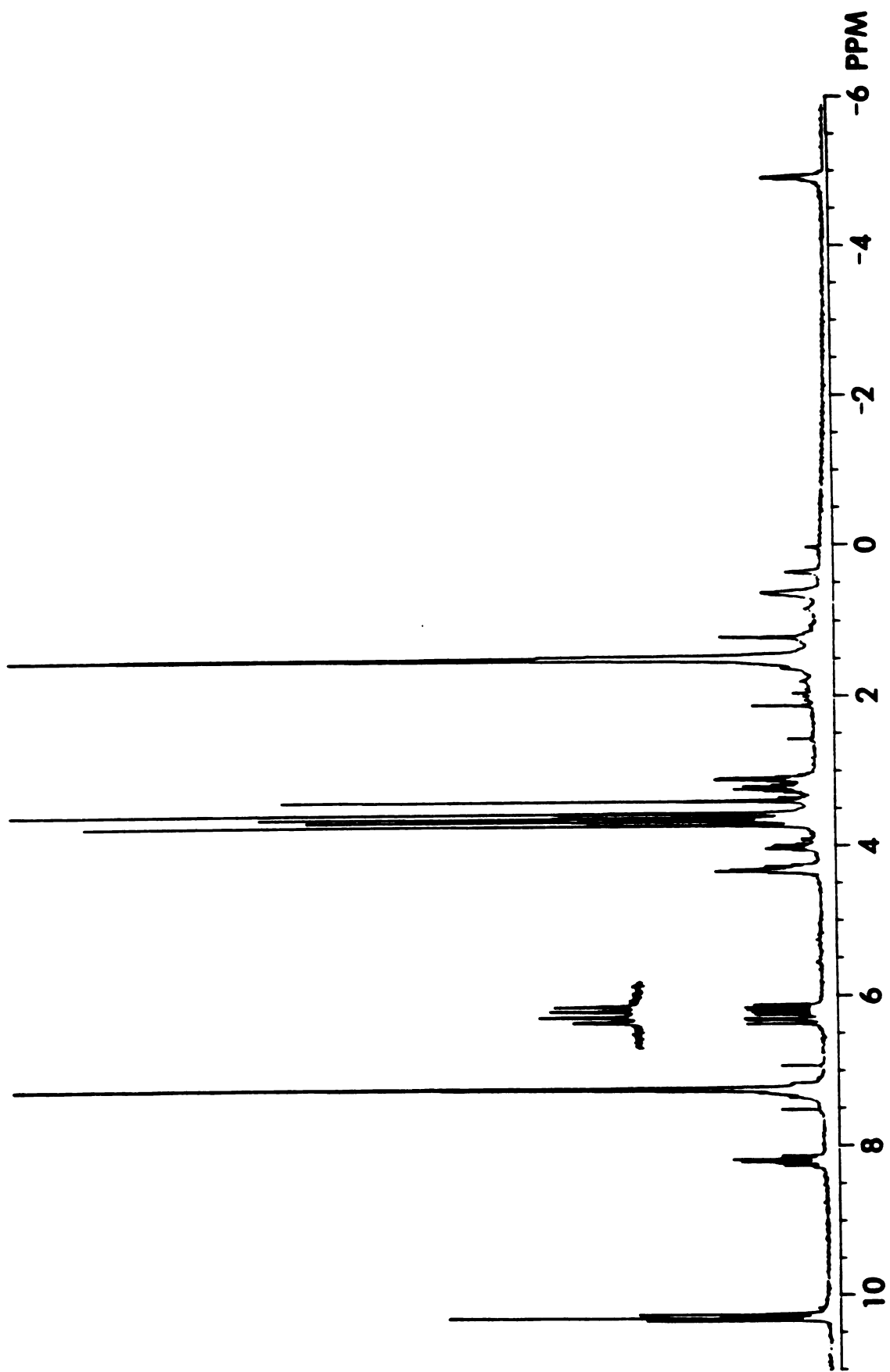
FIGURE 32

## 360 MHZ NMR SPECTRUM OF THE ZINC-COMPLEXED ETHYLENE ADDUCT

The 360 MHz NMR spectrum of the chloro-zinc-complexed dimethyl ester of the ethylene-derived abnormal pigment. The inset shows the change in the multiplet at approximately 6.1-6.4 ppm on decoupling of the protons appearing at 8.2 ppm. The peak at 7.21 ppm is due to traces of  $\text{CHCl}_3$  in the  $\text{CDCl}_3$ , that at 1.5 ppm to an impurity, and that at 1.2 ppm to a trace of water in the NMR solvent (spectrum shown on next page).

The structure of the ethylene adduct is shown below.





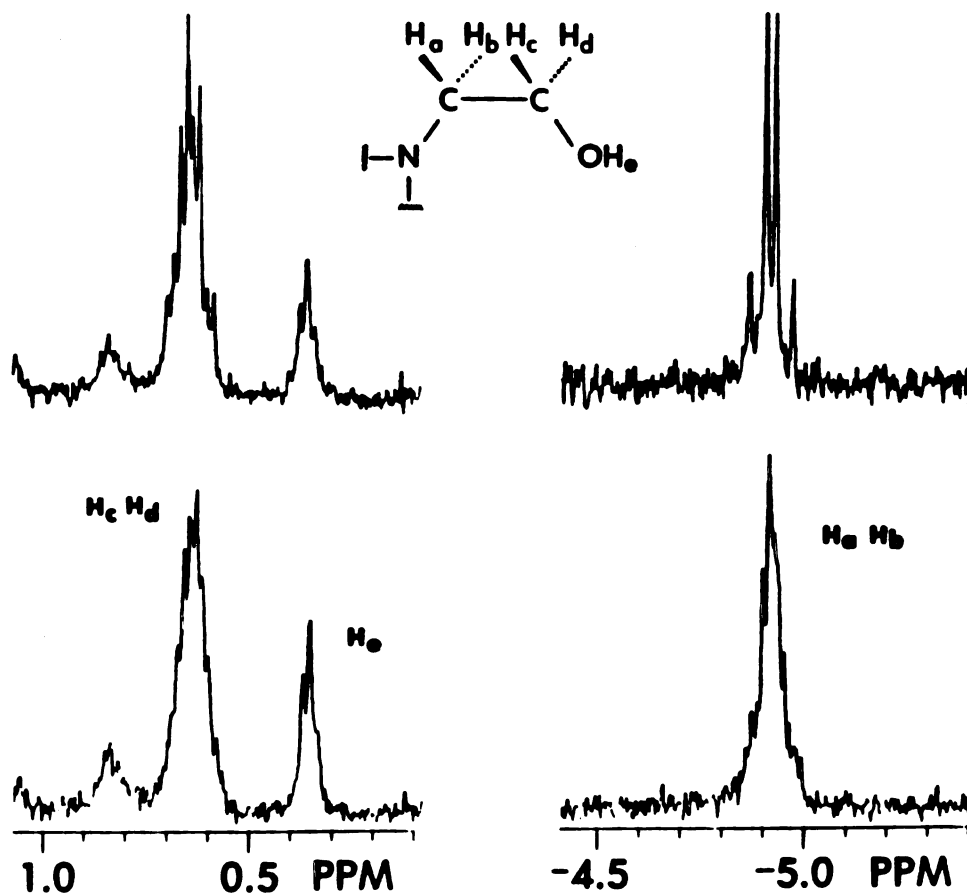
four line signal (Figure 32, inset). Other than the impurity peaks at 1.5 (column bleed) and 1.2 ppm (water), the remaining signals are attributable to the N-alkyl group. The two proton multiplet at -4.9 ppm must be due to a methylene group attached to the porphyrin pyrrole ring nitrogen. The alkylation stoichiometry dictated by the FDMS molecular ion requires the presence of three more protons, an oxygen, and a carbon. The signals arising from the three protons are found at 0.65 ppm (m, 2H) and 0.35 ppm (triplet, 1H). The triplet signal proton, which is exchangeable with  $D_2O$ , must be a hydroxyl proton. The N-alkyl group must therefore be a 2-hydroxyethyl functionality.

N-alkylation of protoporphyrin IX at a single pyrrole nitrogen removes its single symmetry element and thereby makes enantiomeric structures possible. Thus, each methylene proton present in the ethylene adduct (there are a total of 6 methylene carbons or 12 methylene protons) is prochiral and diastereotopic. Hence, any two protons sharing a common methylene carbon are non-isochronous and may have different chemical shifts. Each set of methylene protons may also be geminally coupled. The four methylene protons of the N-2-hydroxyethyl group are all diastereotopic and display different chemical shifts in the NMR spectrum (Figure 33). This relationship has been unraveled by spin decoupling experiments. Irradiation of the hydroxymethylene protons (0.65 ppm) collapses the N-methylene sig-



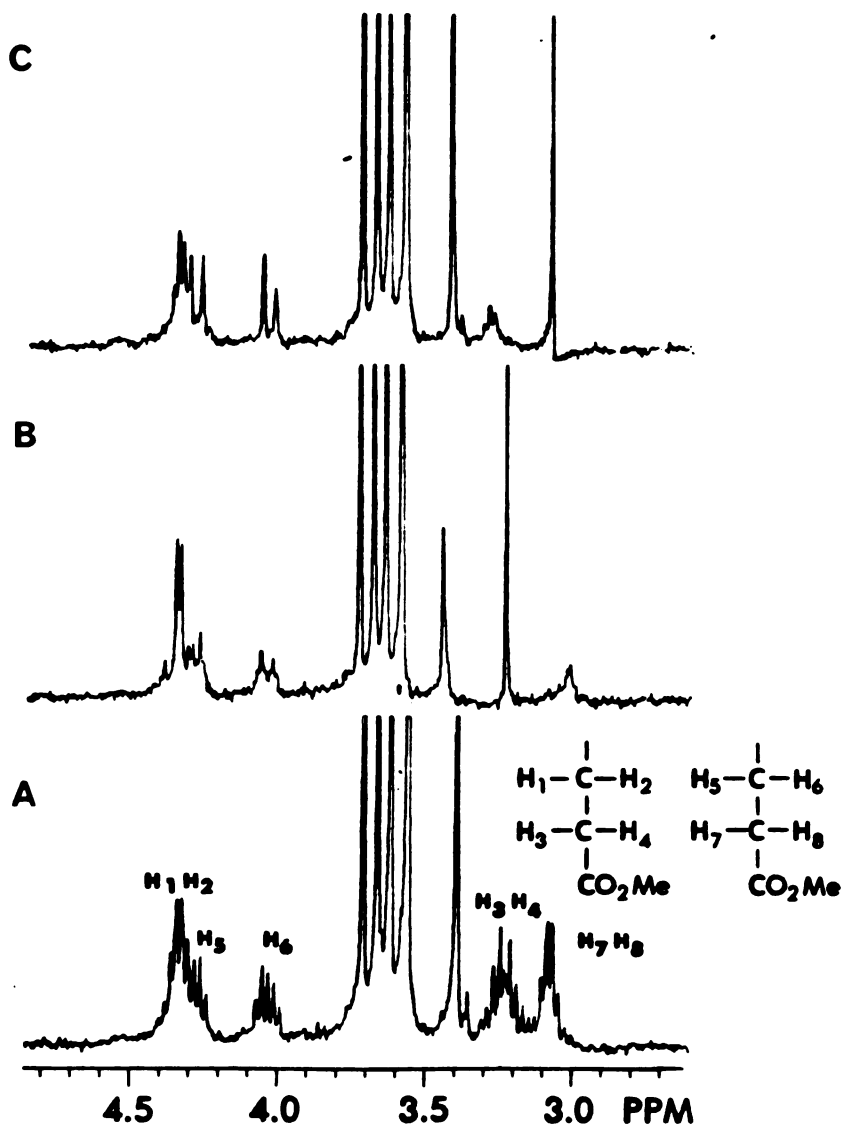
FIGURE 33

SPIN DECOUPLING OF THE  
N-2-HYDROXYETHYL PROTONS IN THE ETHYLENE ADDUCT



Amplification of the NMR signals due to the N-(2-hydroxyethyl) group in the ethylene adduct. The assignment of the protons in this functionality is given. The undecoupled proton signals are given in the bottom of each panel. The upper spectrum on the left is that obtained on decoupling of the protons at -4.9 ppm, while the upper spectrum on the right is that obtained on decoupling of the protons at 0.63 ppm

## SPIN DECOUPLING OF THE METHYLENE PROTONS IN THE ETHYLENE ADDUCT



Amplification (a) of the region of the ethylene-adduct NMR spectrum (Figure 32) in which the propionic acid sidechain protons are located, (b) the same region of the spectrum with the protons at 3.22 ppm decoupled, and (c) the same region of the spectrum with the protons at 3.07 ppm decoupled. Some line broadening is observed in the decoupled spectra due to spin tickling of the protons at 3.22 ppm on irradiation of those at 3.07 ppm, and vice versa. The propionic acid sidechain protons are shown in the diagram and their NMR signals are assigned in the undecoupled spectra.

nals at -4.9 ppm (lower right) to a four line signal (upper right). Irradiation of the N-methylene protons (lower right) simplifies the multiplet at 0.65 ppm (lower to upper left). The N-methylene protons are, therefore, part of an ABXY spin system. These two protons ( $H_a$  and  $H_b$ ) differ in chemical shift by 0.05 ppm (18 Hz at 360 MHz) and are geminally coupled ( $J_{ab}=14.5$  Hz). The additional complexity of the hydroxy-methylene signals ( $H_c$  and  $H_d$ ) is due to coupling with the hydroxyl proton. The hydroxy-methylene protons are represented by a total of 16 lines since they are part of an ABMX spin system. The multiplet at 0.65 ppm is composed of 32 lines. The multiplet at -4.9 ppm is composed of 16 lines.

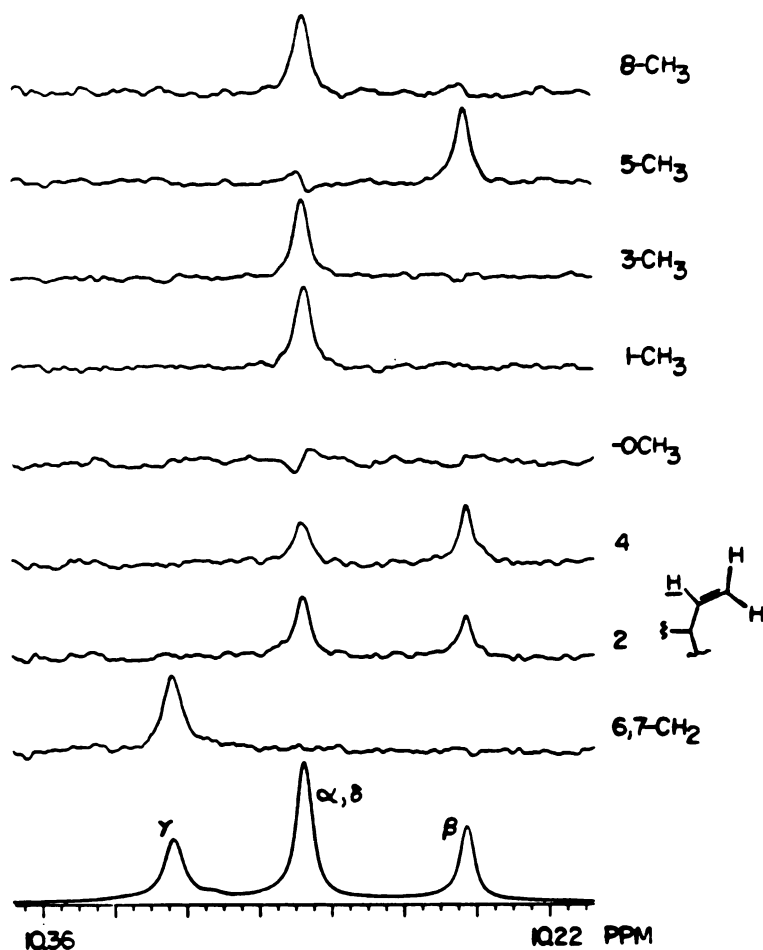
The benzylic and carboxyl methylene protons are also diastereotopic. The complexity of their signal patterns reflects this fact (Figure 34). Spin decoupling experiments provide the proton signal assignments. Irradiation of the  $H_3$  and  $H_4$  protons collapses the  $H_1$  and  $H_2$  multiplets to four lines. The spin system, ABXY, has been analyzed and the chemical shift and coupling constants extracted are as follows:  $J_{1,2}=J_{3,4}=J_{(gem)}=15$  Hz;  $\underline{\delta}_{3,4}=21$  Hz;  $J_{(vic)}=7.5$  Hz;  $\underline{\delta}_{1,2}=13$  Hz. Irradiation of  $H_7$  and  $H_8$  collapses the  $H_5$  and  $H_6$  proton signals to 4 lines:  $J_{7,8}=J_{5,6}=J_{(gem)}=15$  Hz;  $J_{(vic)}=7.5$  Hz;  $\underline{\delta}_{5,6}=77$  Hz;  $\underline{\delta}_{7,9}=13$  Hz. Thus each set of geminal protons is not only diastereotopic, but is observably so in the NMR spectrum.

### Isomer Identification

The key to isomer identification is to assign each of the peripheral methyl proton resonances, and to then determine which signal is shifted upfield from the position it would be expected to occupy if it were not on the alkylated pyrrole ring. Methyl proton signal identification is accomplished by a combination of spin lattice relaxation, spin decoupling, and nuclear Overhauser effect studies. The gamma meso proton (10.322 ppm) is identified by its short  $T_1$  (0.57 seconds; Table 8) and by the observation of an enhancement of its signal intensity upon irradiation of the benzylic methylene protons (Figure 35). One ester methyl (3.705 ppm) is identified by its long  $T_1$  (Table 8) and the other (3.555 ppm), whose signal overlaps with a ring methyl signal, by difference and integration. Further assignments are hampered by the fact that two of the remaining meso proton signals are superimposed (Figure 35). Irradiation of the protons of three separate methyl groups gives rise to an enhancement of the two superimposed meso signals. This means that one of the two meso protons giving rise to that signal is the delta meso proton. Spin decoupling experiments were conducted to isolate the 1 and 3-methyl protons from the other methyl protons. These involved sequential irradiation of each set of methyl group protons to determine which ones are coupled to internal vinyl protons. The results of these experiments are given in Figure 36 and the

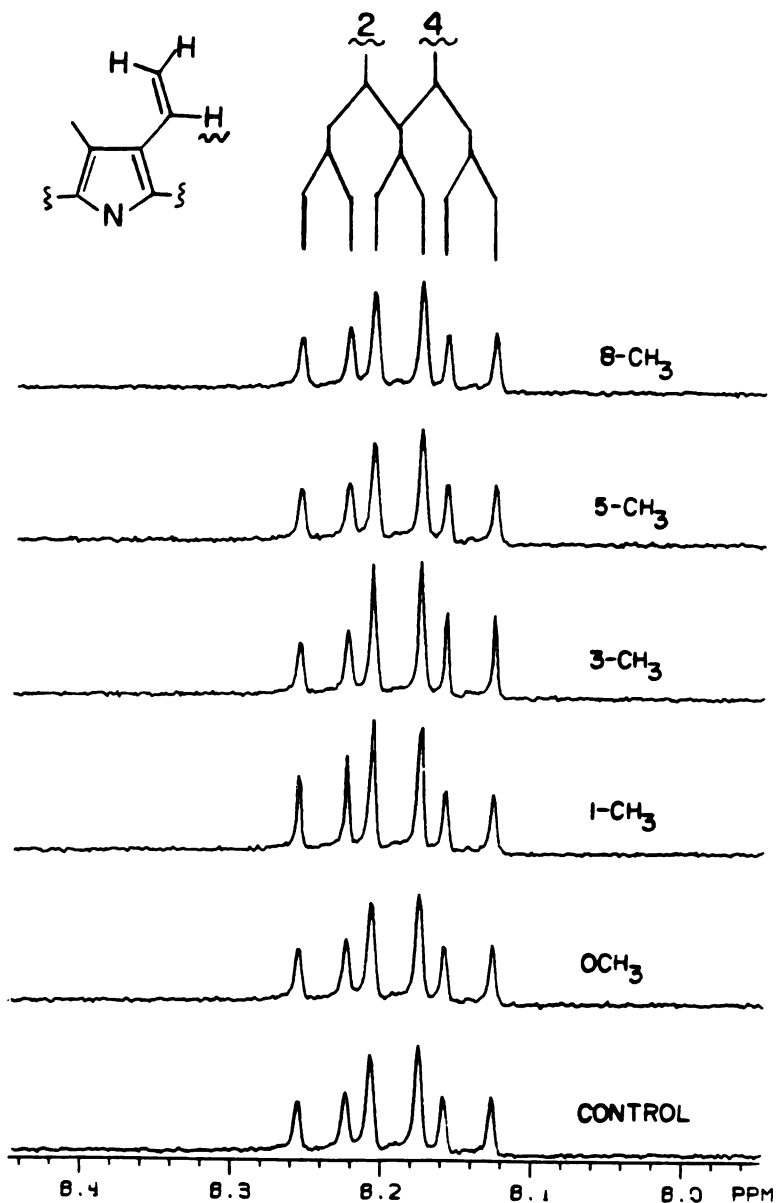
FIGURE 35

THE ETHYLENE ADDUCT:  
NOE ENHANCEMENT OF THE MESO PROTON SIGNALS



Nuclear Overhauser effect enhancement of the meso proton signals due to selective irradiation of the methylene, internal vinyl, and methyl protons (Figure 32). The identity of the irradiated protons is given on the right side of each difference spectrum. Each NOE result is given as the difference between the meso proton region in the specifically irradiated sample and the meso proton region of a control spectrum.

THE ETHYLENE ADDUCT: SHARPENING OF THE INTERNAL VINYL PROTON SIGNALS DUE TO SPIN DECOUPLING OF THE METHYL GROUP PROTONS



Sharpening of the internal vinyl proton signals of the ethylene-adduct due to specific irradiation of each set of methyl group protons (identity given on right hand side of each spectrum). The sharpening observed is due to removal of scalar coupling (0.8 Hz) between an internal vinyl proton and the methyl group protons which share a common pyrrole ring.

TABLE 8

CHEMICAL SHIFT AND RELAXATION TIME ( $T_1$ ) VALUES FOR  
THE MESO AND METHYL PROTONS OF THE ETHYLENE ADDUCT

<u>GROUP</u>	<u>CHEMICAL SHIFT (PPM)</u>	<u><math>T_1</math> (SEC)</u>
1-methyl	3.656	0.61
3-methyl	3.612	0.60
5-methyl	3.555	0.65*
8-methyl	3.388	0.61
methoxy	3.705	1.09
methoxy	3.555	0.65*
<u>alpha meso</u>	10.279	0.98
<u>beta meso</u>	10.236	0.97
<u>gamma meso</u>	10.322	0.57
<u>delta meso</u>	10.297	0.98

\* These signals were superimposed upon one another.

1 and 3-methyl proton signals are assigned (the final assignments are shown although the two could not as yet be differentiated). Nuclear Overhauser enhancement of the middle meso signal was observed when the methyl protons assigned as 1 and 3 were irradiated (Figure 35). The two proton meso signal must be due to the alpha and delta meso protons. The remaining meso proton is the beta meso (10.236 ppm). This is confirmed by the fact that an enhancement of its signal is observed when the internal vinyl protons are irradiated. Since the beta meso proton is flanked by the 5-methyl group, the dipolar coupling observed between the two (Figure 35) assigns the latter (3.555 ppm). The 8-methyl group (3.388 ppm) can be assigned by difference since it is the only methyl group not yet assigned. Selective irradiation of the two internal vinyl protons was, unfortunately, not possible, but, differential enhancements could be observed by selective placement of the decoupler frequency. Irradiation at 8.17 ppm gave a stronger enhancement of the beta than the alpha meso proton signal. Correspondingly, irradiation at 8.22 ppm gave a stronger enhancement of the alpha signal. This difference follows from the fact that the two internal vinyl protons have slightly different chemical shifts (4 line multiplets centered at 8.22 and 8.17 ppm). Thus the vinyl proton dipolar-coupled to the beta meso proton is the one centered at 8.17 ppm (4 internal vinyl proton). Isolation of the methyl group sharing the same ring as the 4 vinyl proton by spin decoupling



experiments (Figure 36) assigns the 3-methyl and, by difference, the 1-methyl proton signals. The complete meso and methyl assignments are given in Table 8.

The ethylene adduct is a single isomer of N-(2-hydroxyethyl)-protoporphyrin IX dimethyl ester. The identity of the alkylated ring can be deduced by determining which of the peripheral substituents are displaced in the porphyrin ring current. The signals found to be shifted upfield by 0.1 to 0.15 ppm from their normal position must arise from association of the corresponding protons with the alkylated ring (section 3.1). Such an upfield shift is observed for the 8-methyl proton signal (Table 8) at 3.388 ppm. The alkylated pyrrole ring must therefore be ring D. The complete structure of the ethylene adduct is given in Figure 32.

#### The Propene Adduct

Approximately 33% of the spectroscopically observable cytochrome P-450 present in phenobarbital induced rat liver microsomes is lost during a 30 minute incubation with propene (5% in air). The loss of enzyme is only observed when NADPH is provided in the incubation mixture. Hepatic green pigments accumulate in the livers of phenobarbital induced rats treated with a 40% mixture of propene in air. The zinc-complexed porphyrins, purified by thin layer chromatography on silica gel and then by chromatography on a Partisil

10-PAC column, were demetalated. The metal-free porphyrins were rechromatographed on the same column. The pigment chromatographed as a single, slightly asymmetric peak.

The visible absorption spectrum of the propene adduct displayed a pattern of absorbances characteristic of the many adducts isolated in this laboratory. A monoprotinated molecular ion at  $m/e$  649 was the only significant peak in the FDMS spectrum of the metal-free adduct. This value, 14 mass units higher than the molecular ion of the ethylene adduct, is that predicted by the alkylation stoichiometry observed in the structure of the ethylene adduct.

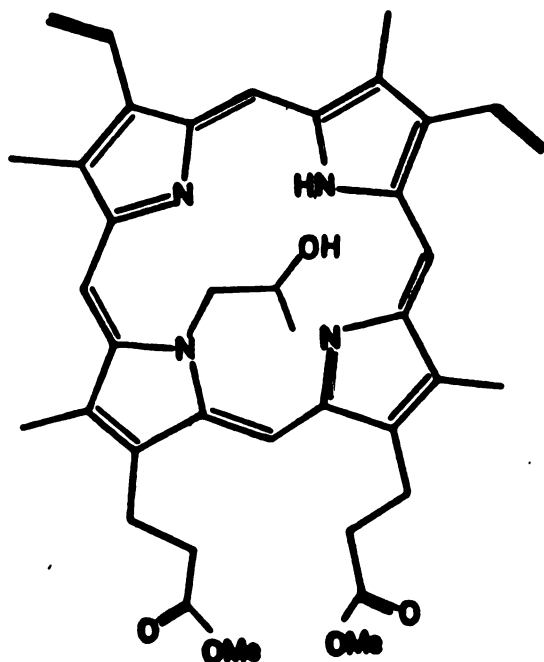
The 360 MHz NMR spectrum of the chloro-zinc complexed propene adduct is shown in Figure 37. The peripheral proton signal patterns are remarkably similar to those in the spectrum of the ethylene adduct (Figure 32). Particularly striking similarities are observed for the carboxyl and benzylic methylene proton signals. The protons giving rise to these signals are all diastereotopic and sufficiently dissimilar to be distinguished in the NMR spectrum.

A total of eight distinct porphyrins must be considered as possible products of the alkylation reaction. Each of the four pyrrole nitrogens could, in principle, bear either a 2-hydroxypropyl group or a 2-hydroxy-1-methyl-ethyl group,

## 360 MHZ NMR SPECTRUM OF THE ZINC-COMPLEXED PROPENE ADDUCT

The 360 MHz NMR spectrum of the chloro-zinc-complexed dimethyl ester of the propene-derived abnormal porphyrin. The peak at 7.21 ppm is due to traces of chloroform in the deuteriochloroform solvent, that at 1.5 ppm to an impurity, and that at 1.2 ppm to a trace of water in the NMR solvent (spectrum shown on next page).

The structure of the propene adduct is given below



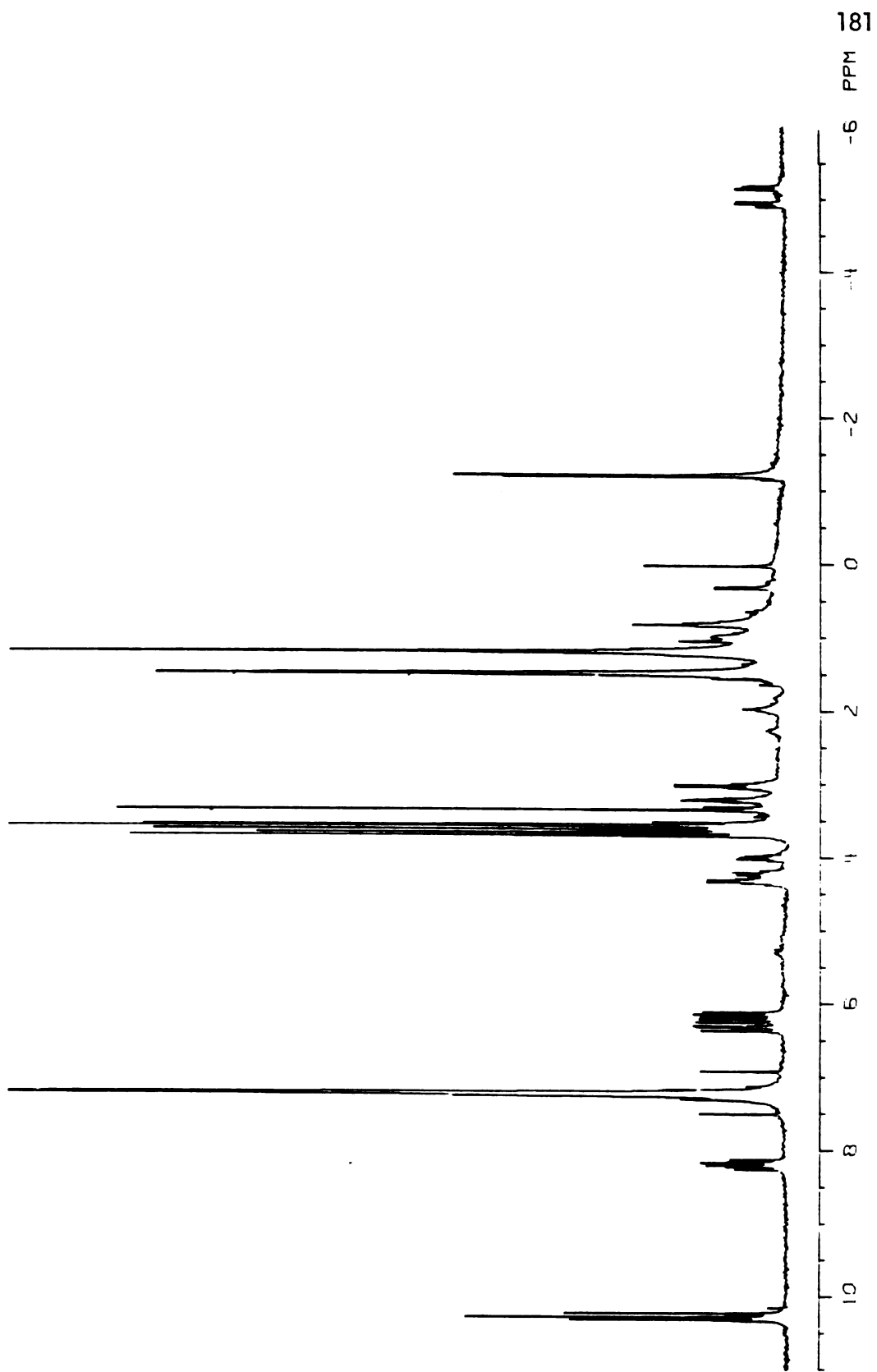
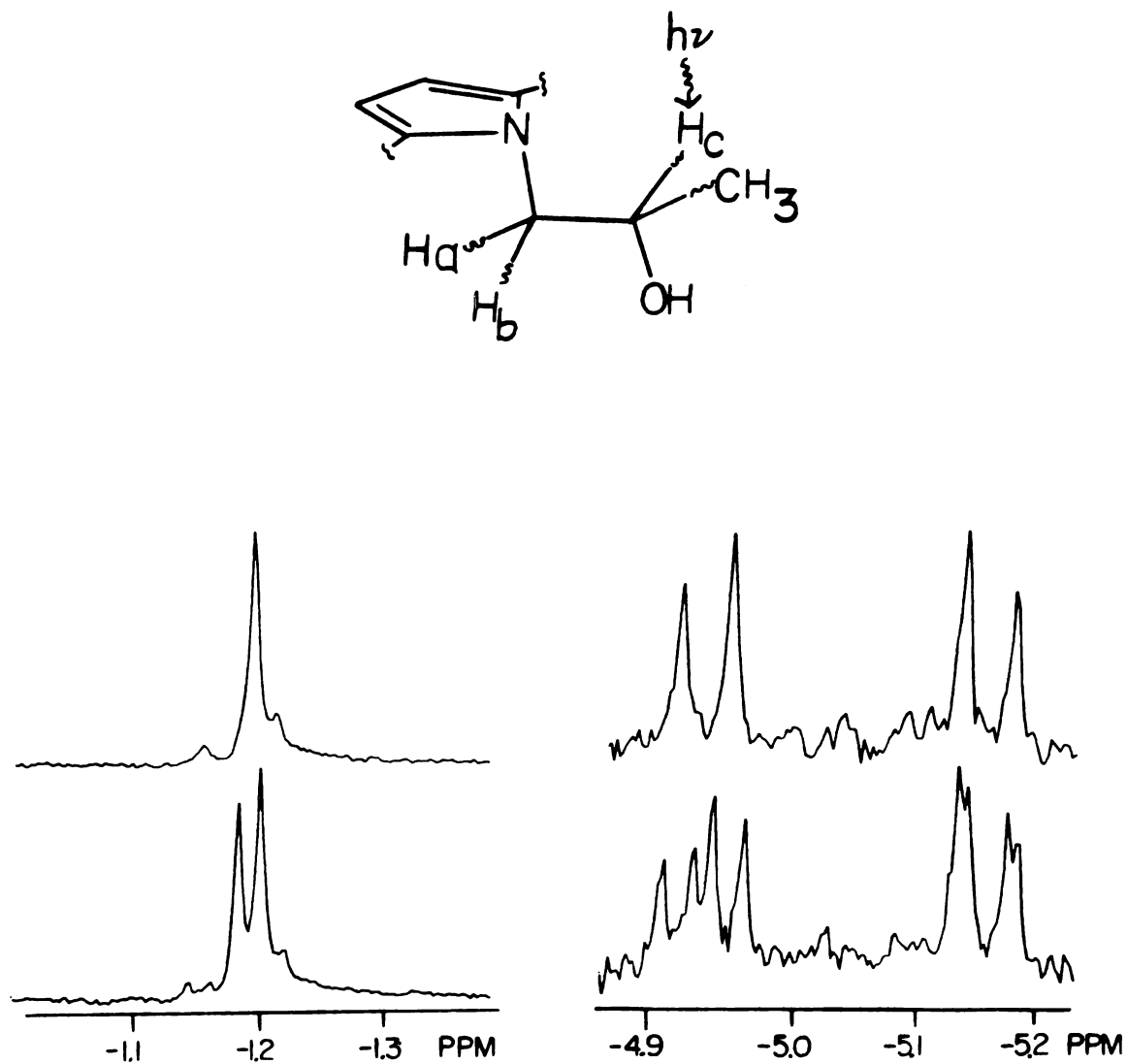


FIGURE 38

## SPIN DECOUPLING OF THE N-(2-HYDROXYPROPYL) METHINE PROTON



Expansion of the N-(2-hydroxypropyl) methyl and methylene proton signals (lower trace) and the effect of spin decoupling of the methine proton at 0.8 to 1.0 ppm. (upper trace).

depending on the identity of the alkylating acyclic precursor (a total of 48 porphyrins are possible when the potential for enantiomers and diastereomers is considered). The pattern of the NMR signals indicates that a single major porphyrin is formed although traces of at least one other porphyrin can be detected. A three proton doublet at -1.2 ppm and a two proton multiplet at -5 ppm occupy high field positions characteristic of N-alkyl group protons. The multiplet at -5 ppm must be due to protons attached to a carbon bound to a pyrrole nitrogen. Since two protons are represented by these signals, they must be part of a methylene group. Only one of the two possible hydroxypropyl arrangements is consistent with this result. The propene adduct must be, therefore, one of the four isomers of N-(2-hydroxypropyl)-protoporphyrin IX dimethyl ester.

This assignment has been confirmed by spin decoupling experiments (Figure 38). Irradiation of the three protons represented by the doublet at -1.2 ppm has no effect on the multiplet at -5 ppm. These protons are not part of the same spin system. Subtle changes were noted in the congested region at 0.8 to 1.0 ppm when either the methyl or methylene protons were irradiated. Irradiation of the protons giving rise to signals in this region caused the eight line signal at -5 ppm to collapse to a four line signal and the doublet at -1.3 ppm to collapse to a singlet. The  $ABMX_3$  spin system exposed by these decoupling experiment is exactly that

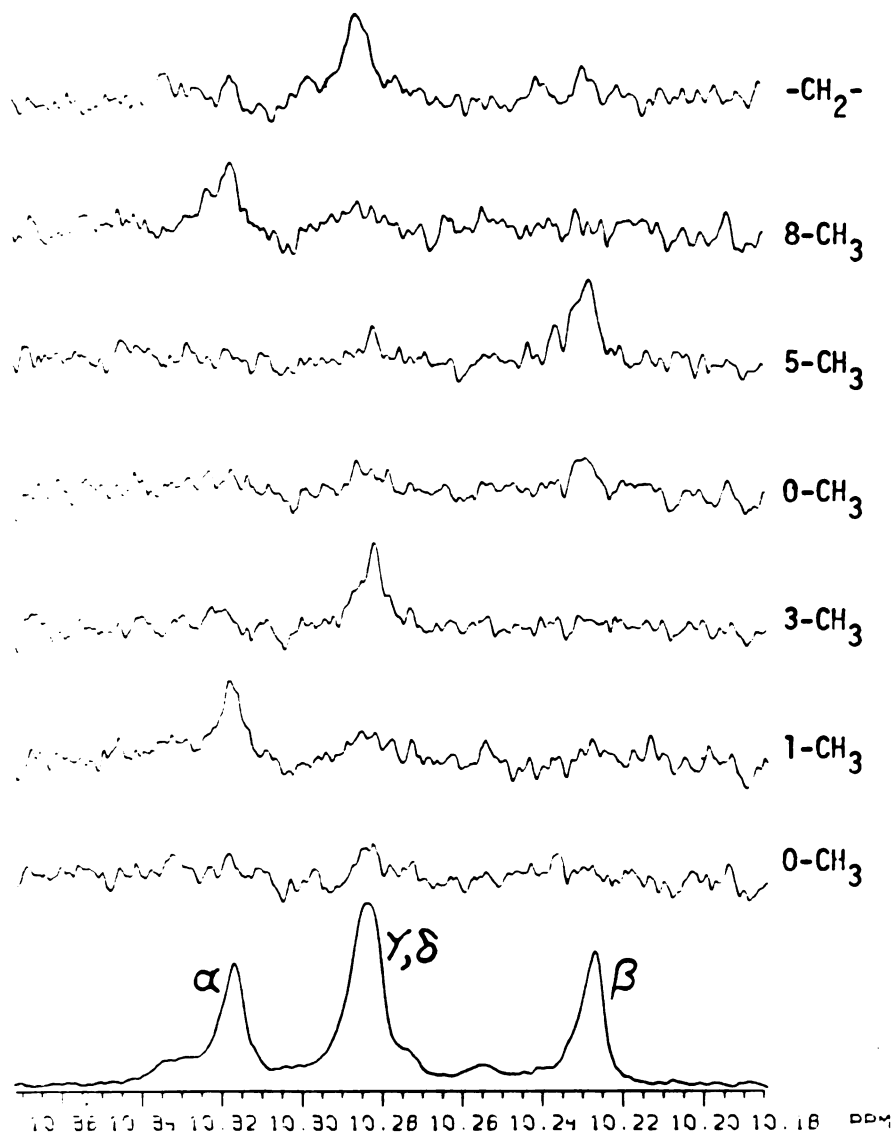
predicted by the structure. The geminal coupling constant for the methylene protons is 14 Hz. The vicinal coupling constants of  $H_a$  and  $H_b$  with  $H_c$  are different ( $J_{a,b}=7$  Hz;  $J_{b,c}=2$  Hz), indicating that rotation about the carbon-carbon bond does not occur on the NMR time scale at room temperature.

### Isomer Assignment

Irradiation of the benzylic methylene protons gives rise to a nuclear Overhauser enhancement of the two proton meso signal at 10.281 ppm (Figure 39), a result which identifies one of the two protons giving rise to that signal as the gamma meso proton. No enhancement of the meso signals was observed when the ester methyl protons assigned by  $T_1$  measurements were irradiated. Dipolar coupling was detected between two sets of methyl group protons (3.664 ppm and 3.352 ppm) and the meso proton (10.315 ppm, Figure 39). This signal must be due to the delta meso proton since it is the only meso proton flanked by two methyl groups (methyls 1 and 8). The methyl protons giving rise to the signal at 3.664 ppm were found to be scalar-coupled to an internal vinyl proton, whereas the methyl protons resonating at 3.352 ppm were not. The 1-methyl proton signal is, therefore, at 3.664 ppm and the 8-methyl proton signal is at 3.352 ppm. Scalar coupling was detected between the remaining internal vinyl proton and what must be the 3-methyl protons (3.617

FIGURE 39

THE PROPENE ADDUCT  
NOE ENHANCEMENT OF THE MESO PROTON SIGNALS



Nuclear Overhauser effect enhancement of the meso proton signals due to selective irradiation of the methylene, internal vinyl, and methyl protons (Figure 37). The identity of the irradiated protons is given on the right side of each difference spectrum. Each NOE result is given as the difference between the meso proton region in the specifically irradiated sample and the meso proton region of a control spectrum.



TABLE 9

CHEMICAL SHIFT AND RELAXATION TIME ( $T_1$ ) VALUES FOR  
THE MESO AND METHYL PROTONS OF THE PROPENE ADDUCT

<u>GROUP</u>	<u>CHEMICAL SHIFT (PPM)</u>	<u><math>T_1</math> (SEC)</u>
1-methyl	3.664	0.62
3-methyl	3.617	0.64
5-methyl	3.558	0.64
8-methyl	3.352	0.61
methoxy	3.703	1.06
methoxy	3.575	1.12
<u>alpha meso</u>	10.315	0.86
<u>beta meso</u>	10.226	0.95
<u>gamma meso</u>	10.281	0.83*
<u>delta meso</u>	10.281	0.83*

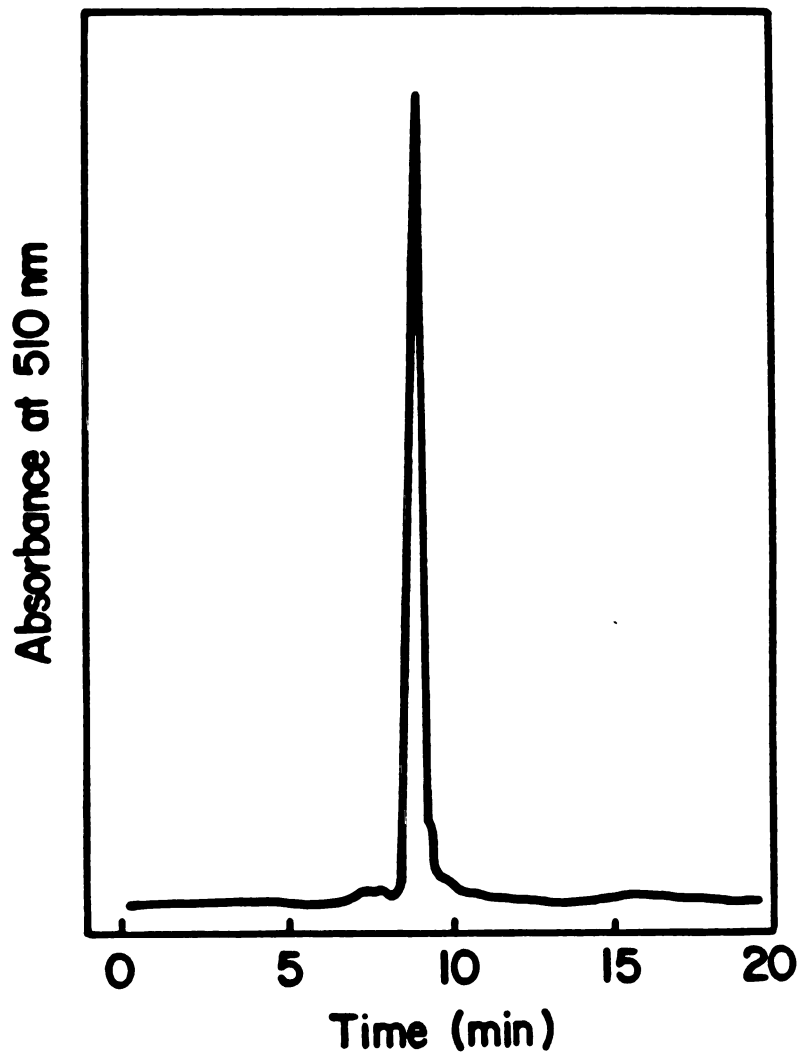
\* These signals were superimposed upon one another

ppm). The two proton meso signal at 10.281 is enhanced by irradiation of the 3-methyl protons. This meso signal is due, therefore, to the alpha and gamma meso protons. The 5-methyl proton signal at 3.558 ppm and the beta meso proton signal (10.226 ppm) are assigned by difference. The chemical shift assignments are given in Table 9. The abnormally high-field position of the 8-methyl proton resonance identifies the propene adduct as the isomer of N-(2-hydroxypropyl)-protoporphyrin IX dimethyl ester which bears the N-alkyl group on the D ring. The structure of the adduct is given in Figure 37

#### 3.4 STRUCTURE OF THE PROPYNE ADDUCT

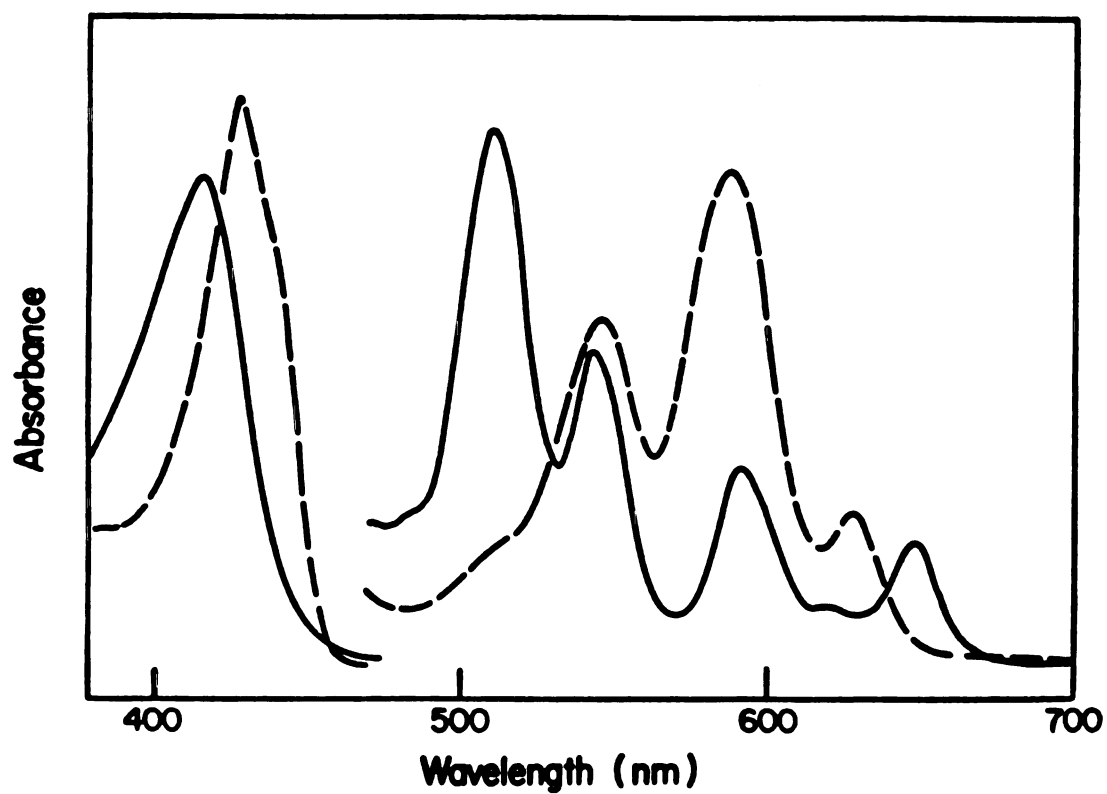
The propyne pigment was isolated from phenobarbital induced rats exposed to a 50% mixture of propyne in air for four hours. The pigment was purified by HPLC and found to chromatograph as a single peak in both the metal-free and zinc-complexed forms (Figure 40). The visible absorption spectrum of the metal-free pigment (Figure 41) exhibited the pattern of absorbances typical of the acetylene and olefin pigments isolated in this laboratory. The Soret band of the zinc-complexed pigment displayed a slight longwavelength shoulder. The molecular weight of the adduct given by FDMS studies is 646 ( $M/e(MH^+) = 647$ , Table 4).

## ANALYSIS OF THE PROPYNE ADDUCT BY HPLC



Analysis of the purified propyne adduct (metal free) by high pressure liquid chromatography on a Partisil 10-PAC column. The elution solvent is a ternary mixture consisting of 5% methanol and 95% of a 1:1 hexane/THF mixture.

ELECTRONIC ABSORPTION SPECTRA OF THE  
ZINC-COMPLEXED AND METAL-FREE PROPYNE ADDUCT



Electronic absorption spectrum of the metal-free (solid line) and zinc-complexed (dashed line) propyne adduct in chloroform. The Soret bands are attenuated ten-fold.

The NMR spectrum of the chloro-zinc-complexed pigment is given in Figure 42. In addition to the signals associated with the peripheral protons of the porphyrin ring, a three proton singlet at -0.26 ppm and a two proton singlet at -4.43 ppm are present in this spectrum. These signals must be due to an N-2-oxopropyl group (section 2.34). The two minor porphyrins detectable in this spectrum must also be N-2-oxopropyl isomers of protoporphyrin IX dimethyl ester (section 2.34).

The gamma meso proton (10.156) is assigned (a) by the observation of an enhancement of its signal in the NOE experiment when the benzylic methylene protons are irradiated (Figure 43) and (b) by its rapid  $T_1$  (0.70 seconds, Table 10). The delta meso proton (10.213 ppm), the only meso proton adjacent to two ring methyl groups (1 and 8), is assigned from the NOE experiments (Figure 43) since only this signal is enhanced by irradiation of two different methyl groups. One of the two sets of methyl protons dipolar-coupled to the delta meso proton was also found to be scalar-coupled to one of the two internal vinyl protons (Figure 43). The 1-methyl protons (3.426 ppm) are scalar-coupled to one of the two internal vinyl protons and dipolar-coupled to the delta meso proton. The remaining methyl group dipolar-coupled to the delta meso must be the 8-methyl group (3.562 ppm). The other methyl group protons scalar-coupled to an internal vinyl proton are those of the

FIGURE 42

NMR SPECTRUM OF THE CHLORO-ZINC COMPLEX  
OF THE PROPYNE PIGMENT

360 MHz NMR spectrum (next page) of the zinc complex of the propyne adduct in deuteriochloroform. The region of the spectrum between 0 and 2 ppm is not shown. The only signals in the deleted region are due to impurities and water. The baseline of the upfield region of the spectrum is displaced upwards and to the left. The meso region of the spectrum has been expanded in the inset.

STRUCTURE OF THE METAL-FREE PROPYNE ADDUCT

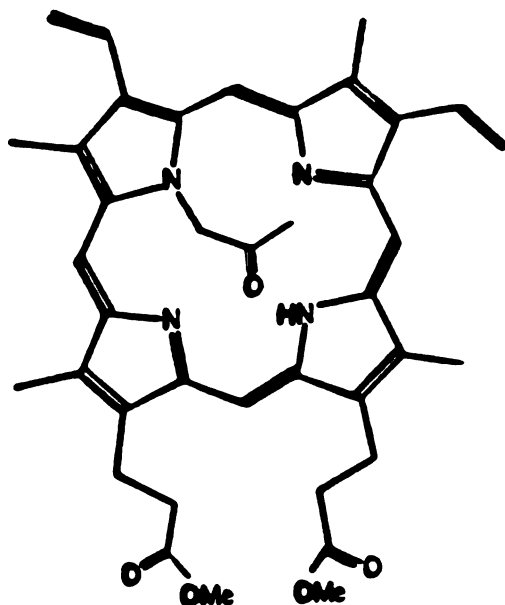
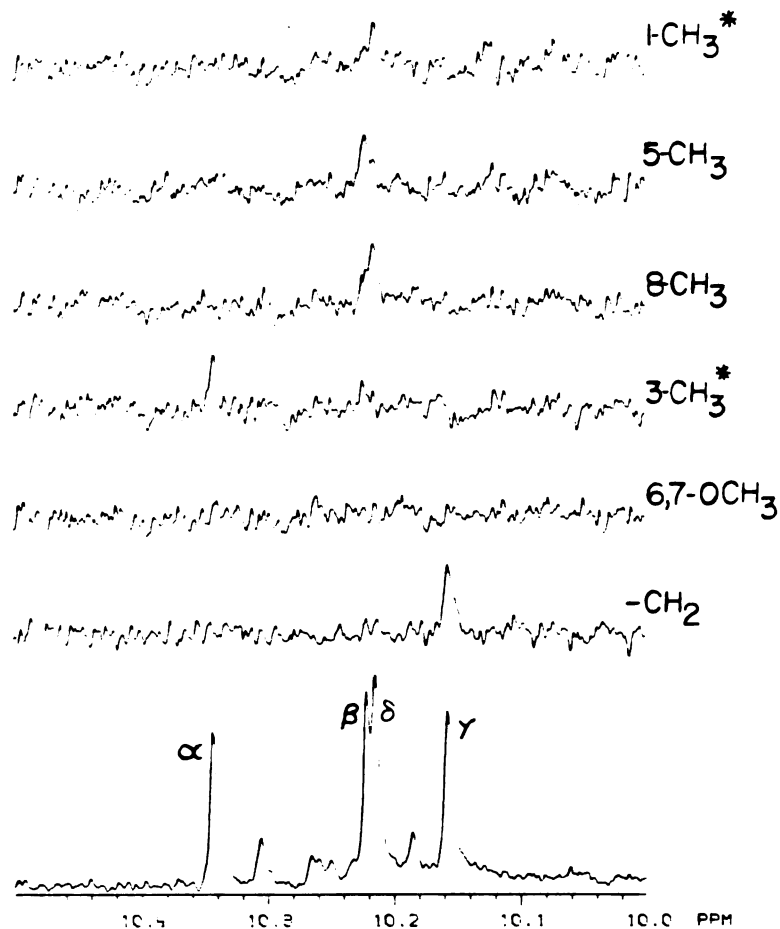




FIGURE 43

THE PROPYNE ADDUCT  
NOE ENHANCEMENT OF THE MESO PROTON SIGNALS



Nuclear Overhauser effect enhancement of the meso proton signals due to selective irradiation of the methylene and methyl protons. The identity of the irradiated protons is given on the right side of each difference spectrum. Each NOE result is given as the difference between the meso proton region in the specifically irradiated sample and the meso proton region of a control spectrum.

\* Spin coupled to an internal vinyl proton.



TABLE 10

CHEMICAL SHIFT AND RELAXATION TIME ( $T_1$ ) VALUES FOR  
THE MESO AND METHYL PROTONS OF THE PROPYNE ADDUCT

<u>GROUP</u>	<u>CHEMICAL SHIFT (PPM)</u>	<u><math>T_1</math> (SEC)</u>
1-methyl	3.426	0.69
3-methyl	3.626	0.68
5-methyl	3.536	0.68
8-methyl	3.562	0.67
methoxy	3.701	1.05
methoxy	3.697	1.24
<u>alpha meso</u>	10.341	1.04
<u>beta meso</u>	10.220	1.02
<u>gamma meso</u>	10.156	0.70
<u>delta meso</u>	10.213	0.95

3-methyl group (3.626 ppm). The meso signal enhanced upon irradiation of the 3-methyl protons is that of the alpha meso proton (10.341 ppm). The remaining meso signal in the spectrum must be that of the beta meso proton (10.220 ppm). The methyl group dipolar-coupled to the beta meso proton is the 5-methyl group (3.536 ppm). The two remaining methyl group signals are the ester methyls (3.701 and 3.697 ppm). This assignment is confirmed by the  $T_1$  data in Table 10.

The two internal vinyl protons differ in chemical shift by 0.2 ppm, whereas the benzylic methylene protons are essentially chemical shift equivalent. The methyl proton signal found at high field is due to the 1-methyl protons. The other vinyl-bearing pyrrole ring methyl proton signal (the 3-methyl, 3.626 ppm) is found at much lower field. The propyne adduct is, therefore, the isomer of N-(2-oxopropyl)-protoporphyrin IX alkylated on pyrrole ring A (see Figure 42 for structure).

## CHAPTER FOUR

### EXPERIMENTAL

#### 1.0 INSTRUMENTATION

Proton Nuclear Magnetic Resonance Studies: NMR spectra were obtained either at 80 MHz on a Varian FT-80 instrument or at 360 MHz on the Nicolet NT-360 instrument at the University of California (Davis) NMR Facility. All spectra were recorded in deuteriochloroform and chemical shifts are reported relative to the residual chloroform signal at 7.21 ppm.

Mass Spectral Studies: Electron impact spectra were obtained on a Kratos MS-25 instrument. An OV-1 column was used for GCMS studies. Field desorption spectra were recorded using a modified Kratos MS-902 instrument located at the Berkely Biomedical and Environmental Mass Spectrometry Resource, University of California at Berkely (Burlingame et al, 1978).

Electronic Absorption Studies: All porphyrin spectra were recorded in chloroform or methylene chloride solutions using 1 cm cells on a Varian-Carey 118 spectrophotometer. Microsomal cytochrome P-450 concentration studies were conducted on an Aminco DW-2 instrument.

Scintillation Counting: Radioactivity was measured on a Packard Tri-Carb Model 3375 scintillation counter in Aquasol (New England Nuclear).

High Pressure Liquid Chromatography: Porphyrin purification and isomer separations were carried out on a system comprised of twin Altex Model 110A pumps, a Hitachi Model 100-40 variable wavelength detector, a Laboratory Data Control Model 400 Solvent Programmer and Whatman Partisil 10 PAC columns (4.6x250 mm, 9.4x250 mm, or 9.4x500mm). All solvents were purchased at HPLC grade or distilled prior to use. Tetrahydrofuran was distilled from sodium under an atmosphere of nitrogen just prior to use to prevent peroxide formation.

Circular Dichroism Studies: CD spectra were recorded on a Jouan Dichrographe II using 3 cm cells.

Centrifugation: Microsomes were prepared using a Sorvall Superspeed RC2-B centrifuge (Sorvall SC34 rotor) for 10,000xg spin and a Beckman L-2 Ultracentrifuge (Type 40 rotor) for 100,000xg spins.

#### 4.1 BIOLOGICAL EXPERIMENTS

##### 4.11 PREPARATION OF LIVER MICROSOMES

Microsomes were isolated from unstarved, 200-250 gram male Sprague-Dawley rats which had been induced with phenobarbital by intraperitoneal injection for four consecutive days (sodium phenobarbital, 80 mg/kg, 80 mg/ml aqueous solution). The animals were killed on the fifth day by decapitation and their livers perfused in situ with ice-cold isotonic KCl (1.15% W/V, 50-100 ml/liver) via the inferior vena cava. The livers were carefully trimmed of attachment tissue and homogenized in isotonic KCl (3 grams wet weight liver per 10 ml KCl solution) in a Blessing glass homogenizing apparatus, first with a loose-fitting pestle (15-20 passes), and then a tight-fitting pestle (20 passes). The homogenate was spun (10,000xg, 4°C, 30 minutes) and the supernatant collected and spun (96,000xg, 1 hour, 5-8°C) to give the microsomal pellet. The microsomal pellet was resuspended in fresh isotonic KCl and spun at 96,000xg for 30 minutes. The pelleted microsomes were resuspended in a pH 7.4 buffer solution containing 0.1M sodium/potassium phosphate, 150 mM KCl, and 1.5 mM tetrasodium EDTA by gentle homogenization in a Blessing homogenizing apparatus using a tight-fitting pestle. Protein concentrations were measured by the method of Lowry et al (1951) using human serum albumin as the standard. Typical microsomal solutions contained 1.8-2.2 nanomoles of cytochrome P-450 per mg of protein. Microsomes were kept on ice whenever possible during the isolation procedure.

#### 4.12 ASSAY FOR CYTOCHROME P-450 DESTRUCTION IN VITRO

Duplicate incubation mixtures containing substrates and microsomes (1 mg microsomal protein per ml final concentration) in buffer (0.1M sodium/potassium phosphate, 150 mM KCl, 1.5 mM EDTA, pH 7.4) were preincubated, with shaking, in a water bath (120 cycles per minute, 37°C). All substrates were added as the solid or neat liquid except for the gases, propyne and propene, which were passed over the incubation mixtures in air. The experiment was initiated by the addition of a concentrated solution of NADPH (final NADPH concentration, 1mM) to one flask, and an equivalent volume of buffer to the other. Two to three ml aliquots were immediately removed and placed in test tubes immersed in ice-water. Carbon monoxide was gently passed through each solution for 20 seconds. The NADPH-free solution was split into two cuvettes (1 cm light path) and approximately 1 mg of sodium dithionite added to one of the two cuvettes. The cuvettes were placed in an Aminco DW-2 spectrophotometer and the difference spectrum from 390 to 520 nm recorded. The cuvette containing dithionite was replaced with another cuvette containing the dithionite-reduced, NADPH-containing solution and another difference spectrum recorded. At specified timepoints, usually 10, 20, and 30 minutes, this procedure was repeated. Cytochrome P-450 content was measured as the difference in absorbance at 450 and 490 nanometers (Waterman, 1978). The extinction coefficient for cyto-

chrome P-450 measured in this fashion is  $100 \text{ mM}^{-1} \text{ cm}^{-1}$ . At the beginning of each series of experiments a separate run was conducted in the presence of NADPH, but in the absence of any substrate, to insure the absence of any NADPH-dependent lipid peroxidation.

#### 4.13 ISOLATION AND PURIFICATION OF HEPATIC GREEN PIGMENTS GENERATED IN VIVO

Male Sprague-Dawley rats weighing 200 to 250 grams were induced with sodium phenobarbital for 4 days by daily interperitoneal injections (80 mg/kg, 80 mg/ml solution in water). Solid and liquid agents were administered by intraperitoneal injection as follows: norethisterone, 100 mg/kg in 0.25 ml triactonoin; other solid agents, 200 mg/kg in 0.25 ml ethanol; liquid agents 200 mg/kg neat or in 0.25 ml ethanol. Acetylene gas was administered by passage through a chamber containing the animals at a concentration of 10 to 15 percent in air. Propyne and propene were administered at a concentration of 40 to 50 percent in air. Flow rates of 200 to 800 ml per minute were used depending upon how many animals were in the chamber. Radiolabeled (9,11- $^3\text{H}$ ) norethisterone (200 mCi/mmole) was a gift from Syntex and was purified by silica gel thin layer chromatography (solvent system chloroform/acetone 2:1) immediately before use. The sterol specific activity after dilution with cold norethisterone was 0.220 mCi/mmole.

Four hours after administration of the agents (the gases were continually administered throughout the four hours), the animals were killed by decapitation and their livers perfused in situ with cold isotonic sodium chloride (50 ml/liver) via the inferior vena cava. The livers were then removed, homogenized and added to a solution of 5% V/V sulfuric acid in methanol (4-6 ml of solution per gram wet weight of liver), and left standing overnight at 4°C in the dark. From this point on all manipulations and procedures were carried out under subdued light whenever possible. The following day the solution was filtered to remove the denatured protein and added to half volumes each of chloroform and water. The two phases were separated and the aqueous phase re-extracted with a small volume of fresh chloroform. The combined chloroform fractions were washed with distilled water three times, or until neutral, and dried over anhydrous sodium sulphate. One ml of a saturated solution of zinc acetate in methanol was added, the solution filtered to remove the drying agent, and the solvent stripped to leave a brown residue. The brown residue was taken up in a minimal amount of chloroform/methanol 5:1 (4-6 ml of solution per thin layer plate) and applied to 2mm Analtech Silica Gel G thin layer plates. The equivalent of 4 livers worth of solution was applied per plate used. The plates were eluted with a chloroform/acetone 3:1 solution. The green band (red-fluorescing under 365 nm light) observed at an  $rf = 0.4$  to 0.6 was scraped and then eluted from the silica with



acetone. In some cases the pigments was not cleanly separated from the slower running dimethyl heme (brown, non-fluorescing), in which case, the sample was replated on a 1mm silica plate. The zinc-complexed pigments were further purified by high pressure liquid chromatography (HPLC) on a Whatman Partisil 4.6x250 mm column in a mobile phase of methanol/THF 4:1 delivered at a flow rate of 3 ml/min. The pigments were detected in the eluent by monitoring the absorbance at 432 nm. The retention times of the pigments in this system varied between 6 and 10 minutes. The zinc-complexed pigments were demetalated (see section 4.14 for procedure) and the metal-free porphyrins further purified by HPLC on the same column in a solvent system of hexane/THF/methanol 10:3:1 (detector set to 417 nm).

Pigments isolated from propene and propyne treated animals were chromatographed, following initial thin layer purification, as the zinc complexes on a Partisil 9.6x500 mm column using a 0-100% gradient of methanol into hexane/THF 1:1. The zinc-complexed porphyrins were collected, demetalated, and further purified on this column in a solvent system of hexane/THF/methanol 97:97:6. Chloro-zinc complexes were prepared for NMR studies by addition of a small amount of a saturated solution of zinc acetate in methanol to chloroform solutions of the purified, metal-free, porphyrins followed by a minimum of three washes of the chloroform solution with saturated sodium chloride. The chloroform

solution containing the pigment was dried by passage through a Pasteur pipet half-filled with anhydrous sodium sulphate which was retained by a glass wool plug at the taper. The solvent was removed under a stream of nitrogen and the dried sample left under high vacuum overnight to remove the remaining traces of solvents.

#### 4.14 DEMETALATION OF ZINC-COMPLEXED PIGMENTS

The zinc-complexed pigment was dissolved in 2 ml of 5% sulfuric acid in methanol in a test tube equipped with a Teflon screw top. Demetalation was almost instantaneous. Two ml of chloroform and 5 ml distilled water were added and the upper phase, after vigorous shaking with the cap in place, removed with a pipet. The chloroform phase was again washed with water, then dilute aqueous sodium bicarbonate, and finally water. The chloroform layer was then passed through a Pasteur pipet half-filled with sodium sulfate which was retained by a glass wool plug at the taper.

### 4.3 SYNTHESIS

#### 4.31 Meso-Deuterated Protoporphyrin IX Dimethyl Ester

This compound was prepared by a procedure patterned after that of Smith et al (1979). One gram of *p*-toluene sulfonic acid monohydrate was dissolved in 10 ml deuterated

water (99.8 atom D) and the water removed in vacuo. This exchange procedure was repeated twice more to give monodeuterated *p*-toluene sulfonic acid. Protoporphyrin IX dimethyl ester (200 mg, 0.34 mmole) and deuterated *p*-toluene sulfonic acid (1 gram, 5.3 mmole) were dissolved in 25 ml 1,2-dichlorobenzene (dried and distilled) and the reaction mixture stirred at 90°C under argon in the dark for 3 days. The solution was partitioned between equal volumes of dichloromethane and 5% W/V aqueous sodium bicarbonate to remove the *p*-toluene sulfonic acid. The organic layer was dried over sodium sulfate and the solvent removed under vacuum (1 mm Hg, 50°C). The brownish residue was dissolved in methanol/sulphuric acid 20:1 (100 ml) and left overnight in the dark at room temperature to re-esterify any free porphyrin carboxyl groups. An equal volume of chloroform was added and the solution washed with water three times. The organic phase was dried over sodium sulphate and the chloroform removed. The residue was chromatographed on silica (Merck silica gel 60, deactivated with water 10% W/V) in a solvent system of chloroform/methanol 5:1. The red band was collected and crystallized from methanol/chloroform to give 90 mg (45% yield) of the deuterated protoporphyrin IX dimethyl ester.

#### 4.32 N-Methyl-Protoporphyrin IX Dimethyl Ester (4 isomers)

Methyl fluorosulphonate (1.0 ml, 12 mmol) was added to 500 mg (0.83 mmole) of protoporphyrin IX dimethyl ester in 50 ml dry dichloromethane. The flask was wrapped in aluminum foil, sealed with a rubber septum, and left standing in the hood for three days at room temperature. (Note: Methyl fluorosulphonate is extremely toxic. Any solution or glassware contaminated with this reagent was handled in the hood with a minimum of three layers of gloves. The outer layer of gloves was shed before leaving the hood area. Methyl fluorosulphonate will pass through surgical gloves. All glassware and solutions were washed with KOH/methanol before being removed from the hood.)

After three days, the solution was added to 200 ml each of dichloromethane and 5% aqueous sodium bicarbonate in a separatory funnel and the mixture shaken extensively. The organic layer was washed with water and dried over sodium sulphate. The residue, after solvent removal, was chromatographed on a 4x37 cm column of silica gel (Merck Silica Gel 60, 10% w/w water deactivated) using a mobile phase of 5% methanol/chloroform. The brown, red-fluorescing, band containing the four isomers of N-methyl protoporphyrin IX dimethyl ester was eluted after unreacted protoporphyrin IX dimethyl ester. The N-methyl isomers were dissolved in a minimal volume of boiling chloroform and precipitated from solution with hexane (250 mg, 47% yield). VIS ( $\text{CHCl}_3$ )

417(116,000), 512(10,800), 546(7580), 592(5200), 652(2200);  
FDMS (m/e 604, M<sup>+</sup>); zinc complex, VIS (CHCl<sub>3</sub>) 431(124,000),  
545(7600), 594(7600), 632(2600).

The four N-methyl isomers were resolved by HPLC on a Whatman Partisil 9.4x250 mm column in a solvent system of hexane/THF/methanol 97:97:6 delivered at four ml per min. The porphyrins were detected by absorbance at 651 nm. The leading or trailing edges of each peak, as appropriate, were collected and rechromatographed under the same conditions to give the pure isomers. The zinc chloride complexes were prepared for NMR by addition of zinc acetate (2 ml saturated zinc acetate solution in methanol) to chloroform solutions of the porphyrins. The excess zinc acetate was removed by repeated water washes of the chloroform solutions, and the acetate counter-ion replaced by chloride by repeated washing with saturated aqueous sodium chloride. The chloroform solutions were dried with sodium sulphate and the solvent removed, after filtration, under a stream of nitrogen. The samples were then left in high vacuum overnight (1 mm Hg) to remove the last traces of solvent. See section 3.1 for detailed spectroscopic characterization of the four isomers.

#### 4.33 N-Ethyl Protoporphyrin IX (four isomers)

Ethyl fluorosulphonate (1ml, 6 mmoles) was added to 200 mg (0.3 mmoles) of protoporphyrin IX dimethyl ester in 50 ml dry dichloromethane and stirred in the dark for 3 days at

room temperature. The reaction mixture was added to equal volumes of dichloromethane (200 ml) and saturated aqueous sodium bicarbonate (200 ml) in a separatory funnel and shaken vigorously. The organic layer was collected, dried over sodium sulfate, and stripped of solvent. The brown residue was dissolved in 100 ml sulphuric acid/methanol 1:20 and left overnight in the dark. Equal volumes of chloroform and water (300 ml each) were added, the chloroform phase washed with water, and dried over sodium sulfate. The product obtained after solvent removal was chromatographed on a 4x30 cm column of 10% water deactivated Merck silica gel 60 in a solvent system of chloroform/methanol 20:1, yielding 130 mg of pure N-ethyl protoporphyrin IX dimethyl ester (4 isomers). VIS ( $\text{CHCl}_3$ ) 417(114,000), 512(10,200), 547(6800), 592(5,000), 650(1,900); FDMS (618,  $\text{M}^+$ ): Zinc complex VIS ( $\text{CHCl}_3$ ) 432(124,000), 545(8,000), 594(13,200), 633(2,100).

The four N-ethyl protoporphyrin IX isomers were resolved by HPLC on a 9.4x500 mm Whatman Partisil column in a solvent system of hexane/THF/methanol 12:12:1. Porphyrins were detected in the eluent by their absorbance at 650 nm. See preceding section for other experimental details. See section 3.2 for isomer assignments.

#### 4.34 1-<sup>2</sup>H-2-Biphenylacetylene

Biphenylacetylene (178 mg, 1 mmole) was dissolved in 10 ml dry THF and cooled to -78° in a nitrogen atmosphere. 1.1 equivalents of n-butyl lithium (1.6 M in hexane) was added via a syringe and the reaction brought to 0° for one hour. Excess D<sub>2</sub>O (99.8% atom D) was added and the reaction mixture partitioned between ether and water. The ether layer was dried over anhydrous magnesium sulphate and the residue, after solvent evaporation, purified by column chromatography (Lobar Lichroprep Si60, Size B, ethyl acetate/hexane 1:20, 8 ml/min). The appropriate fractions were pooled, the solvent removed, and the product crystallized from ethanol/water. Yield 125 mg; mp 85-87°; no residual acetylene proton by NMR and MS.

#### 4.35 Methyl-2-<sup>2</sup>-2-biphenylacetate from 1-<sup>2</sup>H-2-biphenylacetylene

1-<sup>2</sup>H-2-biphenylacetylene (10 mg, 0.055 mmole) and pH 7 phosphate-washed, m-chloroperbenzoic acid (12 mg, 0.069 mmole) were stirred for 24 hours at room temperature in 3 ml of methylene chloride containing 1% methanol. The unreacted peracid was decomposed with sodium bisulphite, and the reaction mixture partitioned between methylene chloride and dilute aqueous sodium bicarbonate. The organic layer was dried over anhydrous magnesium sulphate and the residue, after solvent evaporation, was purified by column

chromatography (silica gel 60, methylene chloride).

NMR(CDCl<sub>3</sub>): aromatic protons (7.25-7.75 ppm, 9H), -OCH<sub>3</sub> (3.77 ppm, 3H), methylene proton (3.67 ppm, 1H, broad due to H-D geminal coupling); GCEIMS (70 ev) m/e (relative intensity), 227 (40), 168 (100). See section 2.4 for spectra.

#### 4.36 Methyl-2-<sup>2</sup>H-2-Biphenylacetate from 1-<sup>2</sup>H-2-Biphenylacetylene by Microsomal Oxidation

Microsomes were isolated from phenobarbital-induced rats as previously outlined. Deuterated biphenylacetylene (10 mg, 0.056 mmole) and NADPH (89 mg, 0.098 mmole) were added to a 40 ml microsomal solution containing 0.1 M sodium-potassium phosphate buffer (pH 7.4), 1.5 mM EDTA, and 150 mM KCl. The reaction was allowed to proceed for 40 minutes at 37°C. The microsomal mixture was carefully acidified to pH 5 with 1 M HCl and extracted 3X with equal volumes of methylene chloride. The combined organic layer extracts were dried over anhydrous magnesium sulphate, the solvent removed, and the residue dissolved in ethereal diazomethane (1 mmole) and 2°C for 24 hours. The solvent was removed under a stream of nitrogen, and the residue purified by low pressure liquid chromatography (Lobar Lichroprep S160 Size A, ethyl acetate/hexane 1:19). Spectroscopic properties of the product were identical to above (4.35). See section 2.4 for spectra.



4.37 1-<sup>13</sup>C-1-Biphenylacetylene from Biphenyl (modified procedure from Parke et al (1979)).

Biphenyl (192 mg, 1.25 mmole) and 1-<sup>13</sup>C-acetyl chloride (100 mg, 1.1 mmole, 90% <sup>13</sup>C, Prochem) were dissolved in dry methylene chloride and added to 150 mg aluminum chloride in refluxing methylene chloride (5 ml) in an atmosphere of nitrogen. The reaction was held at reflux for 4 hours, cooled to 20°C and partitioned between water and methylene chloride. The organic layer was washed with water until the washes were neutral, dried over magnesium sulphate, and stripped of solvent. The labeled 4-acetylbiphenyl was twice recrystallized from ethanol/water. Yield 180 mg (64%), mp 117-118°C, NMR(CDCl<sub>3</sub>) aromatic (8.0-7.2 ppm 9H), methyl (2.5 ppm, 3H, J(<sup>13</sup>C-H=5Hz)).

Labeled acetylbiphenyl (100 mg, 0.51 mmole) and PCl<sub>5</sub> (600 mg, 4.2 mmole) were dissolved in 6 ml anhydrous pyridine and the reaction mixture stirred under nitrogen for 12 hours at 45°C. The solution was poured into cold 2N HCl and extracted with chloroform. The organic layer was washed with 2N HCl, then distilled water, and dried over anhydrous magnesium sulphate. The residue after solvent evaporation, was chromatographed on a column of silica gel 60 in a solvent of methylene chloride, and recrystallized from ethanol/water to give 45 mg of 1-<sup>13</sup>C-1-biphenylacetylene (42% yield, mp 86-87°C). NMR (CDCl<sub>3</sub>) 7.25-7.65 ppm (9H), 3.15 ppm (2H, J(<sup>13</sup>C-H=51 Hz). Chemical and microsomal oxi-

dation reactions were carried out as previously described for deuterated biphenylacetylene.

#### 4.4 NMR STUDIES

All NMR studies on the porphyrins were performed on a 360 MHz Nicolet NT-360 FT NMR instrument. The porphyrins were examined in deuteriochloroform (99.96% atom D) solution. The residual chloroform peak at 7.21 ppm was used as a chemical shift reference. Spin lattice relaxation time experiments were conducted on non-degassed solutions of the porphyrins using a spectral width of 2000 Hz. The center of the spectrum was adjusted such that no signal fold-over occurred into the regions of interest. Proton relaxation times were determined by the inversion recovery with alternating phases method to minimize pulse non-idealities. A minimum of 11 tau values were used. A two Hz line broadening function was applied to each FID prior to FT.  $T_1$  values were computed by a three parameter fit of the relative peak heights. Proton-proton NOE enhancements were measured using a selective, 4 second, gated, presaturation pulse and a sweep width of 2000 Hz over 16K data points. A line broadening function of 0.5 Hz was applied to each FID. Each FID was zero-filled to 32K prior to FT. Methyl group saturation required a 20 microsecond, 42 dB pulse, whereas a 25 microsecond, 48 dB pulse was required to saturate the

vinyl and methylene protons. A control spectrum was acquired at both power levels in which the decoupler frequency was set a 4.8 ppm. Each transformed spectrum was subtracted from the appropriate control to give the difference spectra given in the text. Enhancements of 7-15% were observed.

## REFERENCES

- Abritti, A. and DeMatteis, F. (1971), Chemico. Biol. Interactions 4, 291-296.
- Abdel-Aziz, M.T. and Williams, I.H. (1969), Steroids 13, 809-820.
- Agoisin, M., Morello, A., White, R., Repetto, Y., and Pedemonte, J. (1974), J. Biol. Chem. 254, 9915-9920.
- Anderson, O.P. and Lavalley, D.K. (1977), Inorg. Chem. 16, 1634-1640.
- Baron, J., Hildebrandt, A.G., Peterson, J.A., and Estabrook, R.W. (1973), Drug Metab. Dispos. 1, 129-134.
- Beckey, H.D. and Schulten, H.R. (1979), in Mass Spectrometry, Part A (Merritt, C. Jr. and McEwen, C.N., eds.) pp 145-263, Marcel-Dekker, New York.
- Bini, A., Vecchi, G., Vivoli, G., Vannini, V., and Cessi, C. (1975), Pharmacol. Res. Comm. 7, 143-149.
- Bjorkhem, I. (1977), Pharmac. Ther. A. 1, 327-348.
- Bond, E.J., and DeMatteis, F.A. (1969), Biochem. Pharmacol. 18, 2531-2549.
- Bonfils, C., Debey, P., and Magerel, P. (1979), Biochem. Biophys. Res. Comm. 88, 1301-1307.
- Bradshaw, J.J., Ziman, M.R., and Ivanetich, K.M. (1978), Biochem. Biophys. Res. Comm. 78, 317-322.
- Burlingame, A.L., Kumbara, J., and Walls, F.C. (1978), in 26th Annual Conference on Mass Spectrometry and Applied Topics held at St. Louis, Missouri, May 28-June 2, pp 184-185.
- Burlingame, A.L., Baillie, T.M., Derrick, P.J., and Chizhov, O.S. (1980), Anal. Chem. 52, 214R-258R.
- Calligaro, A. and Vannini, V. (1975), Pharmacol. Res. Comm. 1, 323-331.
- Callot, H.J., Chevriei, B., and Weiss, R. (1978), J. Am. Chem. Soc. 100, 4733.
- Callot, H.J. and Schaffer, E. (1980), Tet. Lett. 21, 1375.

- Casida, J.E. (1970), J. Agric. Food Chem. 18, 753-772.
- Catignani, G.L. and Neal, R.A. (1975), Biochem. Biophys. Res. Comm. 65, 629-636.
- Chevion, M., Peisach, J., and Blumberg, W.E. (1977), J. Biol. Chem. 252, 3637-3645.
- Ciabattoni, J., Cambell, R.A., Renner, C.A., and Concannon, P.W. (1970), J. Am. Chem. Soc. 92, 3826-3828.
- Concannon, P.W. and Ciabattoni, J. (1973), J. Am. Chem. Soc. 95, 3284-3289.
- Conney, A.H., Lu, A.Y.H., Levin, W., Somogyi, A., West, S., Jacobson, M., Ryan, D., and Kuntzman, R. (1973), Drug Metab. Dispos. 1, 199-210.
- Coon, M.J., Vermilion, J.L., Vatsis, K.P., French, J.S., Dean, W.L., and Haugen, D.A. (1977), in Drug Metabolism Concepts (Jerina, D.M., ed.) pp 46-71, American Chemical Society, Washington D.C.
- Cramer, S.P., Dawson, J.H., Hodgson, K.O., and Hager, L.P. (1978), J. Am. Chem. Soc. 100, 7282-7290.
- Dalvi, R.R., Poore, R.E., and Neal, R.A. (1974), Life Sci. 14, 1785-1796.
- Dalvi, R.R., Hunter, A.L., and Neal, R.A. (1975), Chemico-Biol. Interactions 10, 347-361.
- DeMatteis, F.A. (1971), Biochem. J. 124, 767-777.
- DeMatteis, F.A. and Seawright, A.A. (1973), Chemico-Biol. Interactions 7, 375-388.
- DeMatteis, F.A. (1974), Molec. Pharmacol. 10, 849-854.
- DeMatteis, F.A. (1978), Pharmac. Ther. Acta. 2, 693-725.
- DeMatteis, F.A. and Cantoni, L. (1979), Biochem. J. 183, 99-103.
- DeMatteis, F.A., Gibbs, A.H., and Tephly, T.R. (1980), Biochem. J. 188, 145-152.
- Derrick, P.J. (1977), in Mass Spectrometry (Johnston, R.A.W., ed.) Vol. 4, pp 132-145, The Chemical Society, Burlington House, London.
- Ebel, R.E., O'Keefe, D.H., and Peterson, J.A. (1977), Arch. Biochem. Biophys. 183, 317-327.

- El Masri, A.M., Smith, J.N., and Williams, R.T. (1958), Biochem. J. 68, 199-204.
- Estabrook, R.W., Franklin, M.R., Baron, J., Shigematsu, A., and Hildebrandt, A. (1971), in Drugs and Cell Regulation (Michich, E., ed.) pp 227-249, Academic Press, New York.
- Estabrook, R.W. and Werringloer, J. (1977), in Drug Metabolism Concepts (Jerina, D.M., ed.) pp 1-26, American Chemical Society, Washington D.C.
- Estabrook, R.W. and Werringloer, J. (1979), in The Induction of Drug Metabolism (Estabrook, R.W. and Lindenlaub, E., eds.) pp 187-199, F.K. Schattauer Verlag, Stuttgart.
- Fellig, J., Barnes, J.R., Rachlin, A.I., O'Brien, J.P., and Focella, A. (1970), J. Agric. Food Chem. 18, 78-80.
- Foster, A.B., Jarman, M., Stevens, J.D., Thomas, P., and Westwood, J.H. (1974), Chemico-Biol. Interactions 9, 327-340.
- Freundt, K.J. and Dreher, W. (1969), Arch. Pharmacol. Expt. Path. 263, 208-299.
- Frommer, U., Ullrich, V., Standiger, H., and Orrenius, S. (1972), Biochem. Biophys. Acta. 280, 487-494.
- Gelboin, H.V. (1971), in Handbook of Experimental Pharmacology; Concepts in Biochemical Pharmacology, Part 2, pp 431-451, Springer-Verlag, Berlin, New York.
- Gelboin, H.V. and Whitlock, J.P. (1979), in The Induction of Drug Metabolism (Estabrook, R.W. and Lindenlaub, E., eds.) pp 67-111, F.K. Schallauer Verlag, New York.
- Griffin, B.W. and Peterson, J.A. (1975), J. Biol. Chem. 250, 6445-6451.
- Grigg, R., King, T.J., and Shelton, G. (1970), J. Chem. Soc. Chem. Commun. p. 56.
- Groves, J.T., McClusky, G.A., White, R.E., and Coon, M.J. (1978), Biochem. Biophys. Res. Comm. 81, 154-160.
- Groves, J.T., Nemo, T.E., and Myers, R.S. (1979), J. Am. Chem. Soc. 101, 1032-1033.
- Groves, J.T. and Kruper, W.J. (1979), J. Am. Chem. Soc. 101, 7613-7615.
- Guengerich, F.P., Ballou, D.P., and Coon, M.J. (1976), Biochem. Biophys. Res. Comm. 70, 951-956.

Guroff, G., Daley, J.W., Jerina, D.M., Rensan, J., Witkop, B., and Udenfriend, S. (1967), Science 157, 1524-1530.

Gustavusson, J.A., Rondahl, I., and Bergman, J. (1979), Biochem. 18, 865-870.

Halpert, J. and Neal, R.A. (1980), Molec. Pharmacol. 17, 427-434.

Halpert, J. (1981), Biochem. Pharmacol. 30, 975-881.

Hamilton, G.A. (1964), J. Am. Chem. Soc. 86, 3391-3392.

Hamilton, G.A. (1974), in Mechanisms of Oxygen Activation (Hayaishi, O., ed.) pp 405-451, Academic Press, New York.

Hanasono, G.K. and Fisher, L.J. (1974), Drug Metab. Dispos. 2, 159-168.

Hjelmeland, L.M., Aronow, L., and Trudell, J.R. (1977), Biochem. Biophys. Res. Comm. 76, 541-549.

Ichikawa, Y. and Mason, H. (1973), in Oxidases and Related Redox Systems (King, T., Mason, H., and Morrison, M., eds.) pp 605-625, University Park Press, Baltimore.

Ishimura, Y. (1978), in Cytochrome P-450 (Sato, R. and Omura, T., eds.) pp 209-227, Kodnasha, Tokoyo and Academic, New York.

Iyanagi, T., Anan, F.K., Imai, Y., and Mason, H.S. (1978), Biochem. 17, 2224-2230.

Jackson, A.H. and Dearden, G.R. (1973), Annals of the New York Academy of Sciences 206, 151-176.

Jackson, A.H. (1979), Phil. Trans. R. Soc. London A293, 21-37.

Johnson, A.W., Ward, D., Batten, P., Hamilton, A.L., Skelton, G., and Elson, C.M. (1975), J. Chem. Soc. Perk. I 2076.

Johnson, A.W. and Ward, D. (1976), J. Chem. Soc. Perk. I 720.

Jollow, D.J., Mitchell, J.R., Zampaglione, N., and Gillette, J.R. (1974), Pharmacology 11, 151-169.

Kappus, H. and Bolt, H.M. (1976), Steroids 27, 29-45.

Kirmse, W. (1971), in Carbene Chemistry, 2nd edition, pp 209-261, Academic Press, New York.

- Klingenberg, M. (1958), Arch. Biochem. Biophys. 75, 376-386.
- Kuntzman, R., Levin, W., Schilling, G., and Alvares, A. (1969), in Microsomes and Drug Oxidations (Gillette, J.R., Conney, A.H., Cosmides, G.J., Estabrook, R.W., Fouts, J.R., and Mannering, G.J., eds.) pp 349-363, Academic Press, New York.
- Kunze, K.L., Wheeler, C., Beilan, H.S., and Ortiz de Montelano, P.R. (1981), Fed. Proc. 40, 708.
- Lange, M. and Mansuy, D. (1981), Tet. Lett. 22, 2561-2564.
- Latos-Grayzyski, Cheng, R., LaMar, G.N., and Balch, A.L. (1981), J. Am. Chem. Soc. 103, 4270-4272.
- Lavallee, D.K. and Anderson, O.P. (1977), J. Am. Chem. Soc. 99, 1404-1409.
- Lavallee, D.K., Kopelove, A.B., and Anderson, O.P. (1978), J. Am. Chem. Soc. 100, 3025-3033.
- Levin, W., Jacobson, M., and Kuntzman, R. (1972a), Arch. Biochem. Biophys. 148, 262-269.
- Levin, W., Sernatinger, E., Jacobson, M., and Kuntzman, R. (1972b), Science 176, 1341-1343.
- Levin, W., Sernatinger, E., Jacobson, M., and Kuntzman, R. (1973), Drug Metab. Dispos. 1, 275-285.
- Low, L.K. and Castagnoli, N. (1980), in Burger's Medicinal Chemistry, 4th edition, Part 1, pp 107-226, John Wiley and Sons, New York.
- Lowry, O.H., Rosebrough, N.J., Farr, A.L., and Randall, R.J. (1951), J. Biol. Chem. 193, 265-275.
- Lowry, T.H. and Richardson, K.S. (1976), in Mechanism and Theory in Organic Chemistry, pp 263-265, Harper and Row, New York.
- Lu, A.Y.H. and West, S.B. (1980), Pharmacol. Rev. 31, 277-295.
- Mackinnon, A.M. and Simon, F.R. (1975), Biochem. Pharmacol. 24, 748-749.
- Mackinnon, A.M., Sutherland, E., and Simon, F.R. (1978), Biochem. Pharmacol. 27, 29-35.
- Mason, H.S. (1957), Adv. Enzymology 19, 79-233.



Masters, B.S.S. (1980), in Enzymatic Basis of Detoxification (Jakoby, W.B., ed.) Vol. 1, pp 183-200, Academic Press, New York.

Maynert, E.W., Foreman, R.L., and Watabe, T. (1970), J. Biol. Chem. 245, 5234-5238.

McDonald, R.N. and Schwab, P.A. (1964), J. Am. Chem. Soc. 86, 4865-4871.

McLaughlin, G.M. (1974), J. Chem. Soc. Perk. Trans. 2, 136-140.

McMahon, R.E., Sullivan, H.R., Craig, J.E., and Pereira, W.E. (1969), Arch. Biochem. Biophys. 132, 575-577.

McMahon, R.E. (1958), J. Am. Chem. Soc. 80, 411-414.

Miller, J.A. and Miller, E.C. (1977), in Biological Reactive Intermediates (Jollow, D., Kocsis, J., Synder, R., and Vainio, H., eds.) pp 6-24, Plenum Press, New York.

Mitoma, C., Dehn, R.L., and Tanabe, M. (1971), Biochem. Biophys. Acta. 237, 21-27.

Moore, P.D., Koreeda, M., Wislocki, P.G., Levin, W., Conney, A.H., Yagi, H., and Jerina, D.M. (1977), in Drug Metabolism Concepts (Jerina, D.M., ed.) pp 127-154, American Chemical Society, New York.

Murata, T., Eto, S., Fuchigami, S. (1964), Chem. Pharm. Bull. 12, 624-625.

Myrant, N.B. and Mitropoulos, K.A. (1977), J. Lipid Res. 18, 135-153.

Neal, R.A., Katamaki, T., Hunter, A.L., and Catignani, G. (1976), Hoppe-Seyler's Z. Physiol. Chem. 357, 1044.

Neal, R.A., Kamataki, T., Lin, M., Ptashne, K.A., Dalvi, R., and Poore, R.Y. (1977), in Biological Reactive Intermediates (Jollow, D.J., Koesis, J.J., Synder, R., and Vainio, H., eds.) pp 320-332, Plenum Press, New York.

Nebert, D.W., Eisen, H.J., Negishi, M., Lang, M., Hjelme-land, L., and Okey, A. (1981), Ann. Rev. Pharmacol. Toxicol. 21, 431-462.

Nerland, D.E., Iba, M.M., and Mannering, G.J. (1980), Molec. Pharmacol. 19, 162-167.

Neumeyer, J.I. and Incho, H.H. (1969), U.S. Patent 3,485,916.

- Northrop, D. (1975), Biochem. 14, 2644-2651.
- O'Brien, P.J. (1978), Pharmac. Ther. A. 2, 517-536.
- Omura, T. (1978) in Cytochrome P-450 (Sato, R. and Omura, T., eds.) pp 138- 163, Kodansha, Tokyo and Academic, New York.
- Omura, T. (1979), in The Induction of Drug Metabolism (Estabrook, R.W. and Lindenlaub, E., eds.) pp 161-175, F.K. Schattauer Verlag, New York.
- Omura, T. and Sato, R. (1964), J. Biol. Chem. 239, 2370-2378.
- Orrenius, S., Das, M., and Gnesselius (1969), in Microsomes and Drug Oxidations (Gillette, J.R., Conney, A.H., Cosmides, G.J., Estabrook, R.W., Fouts, J.R., and Mannering, G.J., eds.) pp 251-277, Academic Press, New York.
- Ortiz de Montellano, P.R., Mico, B.A., and Yost, G.S. (1978), Biochem. Biophys. Res. Comm. 83, 132-137.
- Ortiz de Montellano, P.R., Yost, G.S., Mico, B.A., Dinizo, S.E., Correia, M.A., and Kambara, H. (1979a), Arch. Biochem. Biophys. 197, 524-533.
- Ortiz de Montellano, P.R., Kunze, K.L., Yost, G.S., and Mico, B.A. (1979b), Proc. Nat. Acad. Sci. 76, 746-749.
- Ortiz de Montellano, P.R. and Mico, B.A. (1980b), Molec. Pharmacol. 18, 128-135.
- Ortiz de Montellano, P.R., Kunze, K.L., and Mico, B.A. (1980c), Molec. Pharmacol. 18, 602-605.
- Ortiz de Montellano, P.R. and Kunze, K.L. (1980d), Biochem. Biophys. Res. Comm. 94, 443-449.
- Ortiz de Montellano, P.R. and Kunze, K.L. (1980e), J. Biol. Chem. 255, 5578-5585.
- Ortiz de Montellano, P.R. and Kunze, K.L. (1980f), J. Am. Chem. Soc. 102, 7373-7375.
- Ortiz de Montellano, P.R., Kunze, K.L., Cole, S.B., and Marks, G. (1980g), Biochem. Biophys. Res. Comm. 97, 1436-1442.
- Ortiz de Montellano, P.R., Beilan, H.S., Kunze, K.L., and Mico, B.A. (1981a), J. Biol. Chem. 256, 4395-4399.
- Ortiz de Montellano, P.R. and Kunze, K.L. (1981b), Archives

Biochem. Biophys. 209, 710-712.

Ortiz de Montellano, P.R. and Mico, B.A. (1981c), Archiv. Biochem. Biophys. 206, 43-50.

Ortiz de Montellano, P.R., Beilan, H.B., and Kunze, K.L. (1981d), Proc. Nat. Acad. Sci. 78, 1490-1494.

Ortiz de Montellano, P.R., Beilan H.S., and Kunze, K.L. (1981e), J. Biol. Chem. 256, 6708-6713.

Ortiz de Montellano, P.R., Mico, B.A., Mathews, J.M., Kunze, K.L., Miwa, G.T., and Lu, A.Y.H. (1981f), Arch. Biochem. Biophys. 210, 717-728.

Ortiz de Montellano, P.R. and Kunze, K.L. (1981g), Biochem. in press.

Ortiz de Montellano, P.R., Mico, B.A., Beilan, H.B., Kunze, K.L. (1981h), in Molecular Basis of Drug Action (Singer, T. and Ondarza, R., eds.) pp 151-166, Elsevier, New York.

Palmer, K.H., Feierabend, J.F., Bagget, B., and Wall, M.E. (1969), J. Phcol. Exp. Ther. 167, 217-222.

Parke, D.V. (1979), in The Induction of Drug Metabolism (Estabrook, R.W. and Lindenlaub, E., eds.) pp 101-111, F.K. Schattauer Verlag, New York.

Pessayne, D., Wandscheer, J.C., Descatoire, V., Artigou, J.Y., and Benhamou, J.P. (1979), Toxic. Appl. Pharmacol. 49, 505-515.

Peterson, J.A., Ebel, R.E., O'Keefe, D.H., Matsubara, I., and Estabrook, R.W. (1976), J. Biol. Chem. 251, 4010-4016.

Philson, S.B., Debrunner, P.G., Schmidt, P., and Gunsalas, I.C. (1979), J. Biol. Chem. 254, 10173-10179.

Rao, K.S. and Recknagel, R.O. (1968), Exp. Mol. Path. 9, 271-278.

Rahimitula, A.D. and O'Brien, P.J. (1974), Biochem. Biophys. Res. Comm. 60, 440-447.

Recknagel, R.O. and Ghoshal, A.K. (1966), Lab. Investig. 15, 132-146.

Reilly, P.E. and Ivey, D.E. (1978), Fed. Eur. Biochem. Soc. Lett. 97, 141-143.

Russel, R. and Rowland, F. (1970), J. Am. Chem. Soc. 92, 7508-7510.

- Reynolds, E.S. (1967), J. Phcol. Expt. Therap. 155, 1117-1125.
- Ryan, D.E., Thomas, P.E., Korzeniowski, D., and Levin, W. (1978), J. Biol. Chem. 254, 1365-1374.
- Sacher, R.M., Metcalf, R.L., and Fukuto, T.R. (1968), J. Agric. Food Chem. 16, 779-786.
- Sanders, J.K.M., Watweton, J.C., and Denniss, I.S. (1978), J. Chem. Soc. Perk. Trans. 1, 1150-1157.
- Sato, R. (1978), in Cytochrome P-450 (Sato, R. and Omura, T., eds.) pp 23-27, Kodansha, Tokyo, and Academic Press, New York.
- Schulten, H.R. (1979), Int. J. Mass Spec. Ion Phys. 32, 79.
- Schwartz, S. and Ikedo, K. (1955), in Ciba Foundation Symposia on Porphyrin Biosynthesis and Metabolism (Wolstenholme, G. and Millar, E., eds.) pp 129-155, Churchill, London.
- Shirota, F.N., DeMaster, E.G., and Nagasawa, H.T. (1979), J. Med. Chem. 22, 463-464.
- Sisenwine, S.F., Kimmel, H.B., Liu, A.L., and Ruelius, H.W. (1973), Acta Endocrinol. 73, 91-104.
- Sisenwine, S.F., Kimmel, H.B., Liu, A.L., and Ruelius, H.W. (1974), Drug Metab. Dispos. 2, 65-70.
- Sisenwine, S.F., Kimmel, H.B., Liu, A.L., and Ruelius, H.W. (1979), Drug Metab. Dispos. 7, 1-6.
- Skrinjaric-Spoljar, M., Matthews, H.B., Engel, J.L., and Casida, J.E. (1971), Biochem. Pharmacol. 20, 1607-1618.
- Sligar, S.G. and Gunsalus, I.C. (1979), Biochem. 18, 2290-2295.
- Sliyai, S.G., Cinti, S.L., Gibson, G.G., and Schenkman, J.B. (1979), Biochem. Biophys. Res. Comm. 90, 925-972.
- Smith, K.M., Langry, K.C., and De Ropp, J.S. (1979), J. Chem. Soc. Chem. Commun. 1001-1003.
- Smuckler, E.A., Arreniuns, E., and Hultin, T. (1967), Biochem. J. 103, 55-64.
- Stille, J.K. and Whitehurst, D.D. (1964), J. Am. Chem. Soc. 86, 4871-4876.
- Straus, P.P., Gosavi, R.K., Denes, A.S., and Csizmadia, I.G.

- (1976), J. Am. Chem. Soc. 98, 4784-4786.
- Sullivan, H.R., Roffey, P., and McMahon, R.E. (1979), Drug Metab. Dispos. 7, 76-80.
- Tanaka, K. and Yoshimine, M. (1980), J. Am. Chem. Soc. 102, 7655-6662.
- Tephly, T.R., Gibbs, A.H., and DeMatteis, F. (1974), Biochem. J. 180, 241-244.
- Tomioka, H., Okuno, H., Kondo, S., and Izawa, Y. (1980), J. Am. Chem. Soc. 102, 7123-7125.
- Trager, W.F. (1977), in Drug Metabolism Concepts (Jerina, D.J., ed.) pp 81-98, American Chemical Society, Washington D.C.
- Trager, W.F. (1980), in Concepts in Drug Metabolism, Part A (Jenner, P. and Testa, B., eds.) pp 177-209, Marcel-Dekker, New York.
- Thompson, J.A. and Holtzman, J.L. (1974), Drug Metab. Dispos. 2, 577-582.
- Uehleke, H., Hellmer, K.H., and Tabaielli, S. (1973), Xenobiotica 3, 1-11.
- Unsold, A. and DeMatteis, F. (1976), in Proceedings of the International Porphyrin Meeting, Freiburg, May 1975.
- Wada, O., Yano, Y., Urata, G., and Nukuo, K. (1968), Biochem. Pharmacol. 17, 595-603.
- Wade, A., Symons, A.M., Martin, L., and Parke, D.V. (1979), Biochem. J. 184, 509-517.
- Wade, A., Symons, A.M., Martin, L., and Parke, D.V. (1980), Biochem. J. 188, 867-872.
- Walsh, C. (1979), in Enzymatic Reaction Mechanisms, pp 474-477, W.H. Freeman Company, San Francisco.
- Warner, M. and Neims, A.H. (1979), Drug Metab. Dispos. 7, 188-193.
- Watabe, T. and Akamatsu, K. (1974), Biochem. Pharmacol. 23, 1845-1851.
- White, I.N.H. and Muller-Eberhard, U. (1977), Biochem. J. 166, 57-64.
- White, I.N.H. (1979), Biochem. J. 174, 853-861.

White, I.N.H. (1980), Biochem. Pharmacol. 29, 3253-3255.

White, R.E. and Coon, M.J. (1980), Ann. Rev. Biochem. 49, 315-356.

White, R.E., Sligar, S.G., and Coon, M.J. (1980), J. Biol. Chem. 255, 11108-11111.

Williams, J.G. and Williams, K.I.H. (1975), Steroids 26, 707-720.

Wislocki, P.G., Miwa, G.T., and Lu, A.Y.H. (1980), in Enzymatic Basis of Detoxication (Jakoby, W.B., ed.) Vol 1, pp 135-182, Academic Press, New York.

With, T.K. (1976), in Porphyryns in Human Diseases (Doss, M., ed.) pp 481- 485, Karyer, Switzerland.

Zeller, K. (1977), Ang. Chem. Int. Ed. 16, 781-782.



